
Moshpit SGD: Communication-Efficient Decentralized Training on Heterogeneous Unreliable Devices

Max Ryabinin^{*12} Eduard Gorbunov^{*13} Vsevolod Plokhotnyuk² Gennady Pekhimenko⁴⁵

Abstract

Training deep neural networks on large datasets can often be accelerated by using multiple compute nodes. This approach, known as distributed training, can utilize hundreds of computers via specialized message-passing protocols such as Ring All-Reduce. However, running these protocols at scale requires reliable high-speed networking that is only available in dedicated clusters. In contrast, many real-world applications, such as federated learning and cloud-based distributed training, operate on unreliable devices with unstable network bandwidth. As a result, these applications are restricted to using parameter servers or gossip-based averaging protocols. In this work, we lift that restriction by proposing Moshpit All-Reduce — an iterative averaging protocol that exponentially converges to the global average. We demonstrate the efficiency of our protocol for distributed optimization with strong theoretical guarantees. The experiments show $1.3\times$ speedup for ResNet-50 training on ImageNet compared to competitive gossip-based strategies and $1.5\times$ speedup when training ALBERT-large from scratch using preemptible compute nodes.

1. Introduction

Many recent influential discoveries in deep learning were enabled by the trend of scaling model and dataset size. Over the last decade, computer vision has grown from training models with 60 million parameters (Krizhevsky et al., 2012) on 1.3 million images (Deng et al., 2009) to 15 times more parameters (Kolesnikov et al., 2020) and 200 times more training data (Sun et al., 2017). In natural language processing, the state-of-the-art language models (Brown

et al., 2020) with 175 billion parameters are trained on over 570GB of text data, and even this amount does not saturate the model quality (Kaplan et al., 2020). Training these large models can take years even with a top-of-the-line GPU server (Li, 2020). As a result, researchers and practitioners often have to run distributed training with multiple machines (Mattson et al., 2020).

The dominant approach to distributed deep learning is data-parallel training (Valiant, 1990), where each worker processes a fraction of the training batch and then exchanges its gradients with peers. If done naively, the gradient exchange can overload the network as the number of workers increases. To combat this issue, modern distributed training algorithms take advantage of communication-efficient protocols, such as all-reduce (Patarasuk & Yuan, 2009). These protocols allow workers to collectively compute the global average gradient with a constant communication overhead, regardless of the total number of peers. However, this efficiency makes the protocols more fragile: if any single participant fails or takes too long to process its batch, all other nodes will be stalled.

Therefore, scaling all-reduce protocols beyond a couple of servers requires specialized infrastructure with dedicated ultra-high bandwidth networking (Mattson et al., 2020). This kind of infrastructure is notoriously expensive compared to regular GPU servers or preemptible cloud VMs (see Appendix A). Hence, it is tempting to consider distributed training with cheap unreliable instances as a cost-efficient alternative. A similar scenario arises in federated learning (McMahan et al., 2017), where one must run distributed training with heterogeneous devices due to privacy concerns.

In both scenarios, participants use a shared network, where both latency and bandwidth can vary drastically due to interference from other users (Persico et al., 2015). Furthermore, compute nodes are also subject to failure (or preemption) caused by factors beyond the protocol’s control.

Running large-scale distributed training in these circumstances requires fault- and latency-tolerant algorithms (Lian et al., 2017; Assran et al., 2019b). Most of these algorithms replace all-reduce averaging with **gossip**: each participant periodically downloads the latest parameters from his neigh-

^{*}Equal contribution ¹Yandex, Russia ²National Research University Higher School of Economics, Russia ³Moscow Institute of Physics and Technology, Russia ⁴University of Toronto, Canada ⁵Vector Institute, Canada. Correspondence to: Max Ryabinin <mryabinin0@gmail.com>.

bors in a sparsely connected communication graph and averages the results. The updates gradually propagate through the graph over multiple rounds of averaging. However, the communication required to perform gossip grows linearly with the number of neighbors. Hence, when scaling to hundreds of peers, decentralized SGD has to keep the communication graph sparse, slowing down the convergence.

In this work, we propose an alternative approach. Instead of relying on a predefined communication graph, participants dynamically organize themselves into groups using a fully decentralized matchmaking algorithm which we call **Moshpit All-Reduce**. This strategy allows us to use communication-efficient all-reduce protocols that significantly reduce the network load compared to gossip-based averaging, while still being able to operate in unreliable hardware and network conditions.

Our contributions can be summarized as follows:

- We propose **Moshpit All-Reduce** — a novel decentralized averaging protocol for large-scale training with unreliable communication-constrained devices. According to our analysis, this method has exponential convergence independent of network topology.
- Armed with this averaging protocol, we develop **Moshpit SGD** for distributed optimization. We derive convergence rates for this algorithm and establish its equivalence to Centralized (Local) SGD in terms of iteration complexity under realistic assumptions.
- Our experiments demonstrate that Moshpit All-Reduce is significantly more efficient under network latency. In particular, we train ResNet-50 on ImageNet to 75% accuracy 1.3 times faster than existing decentralized training algorithms and train ALBERT-large from scratch 1.5 times faster on preemptible cloud VMs.
- We release the reference implementation of Moshpit All-Reduce and the code for all experiments online.¹

2. Related Work

2.1. Data parallel training

The most popular way to accelerate neural network training with multiple devices is data-parallel training (Valiant, 1990; Goyal et al., 2017; You et al., 2020). On each optimization step, this strategy splits the training batch among participants. Each participant then runs forward and backward passes to obtain gradients of the objective function on their part of the training batch. After that, we can aggregate the gradients from workers and perform an optimization step. There are two main strategies for this aggregation.

Historically, the first solution to gradient aggregation was

to use Parameter Server (PS) (Li, 2014): a separate process or a dedicated server that keeps track of model parameters and optimizer statistics. After each round, the PS accumulates the gradients from each worker and updates the model parameters using SGD or any other optimizer, such as Adam (Kingma & Ba, 2015). Finally, the server distributes the updated model parameters to workers.

This strategy is robust and easy to implement, but it requires the server to regularly download full model gradients from every single worker. As a result, the parameter server can quickly become a bottleneck for large-scale training (Alqah-tani & Demirbas, 2019). Since the original PS, researchers have proposed several modifications that reduce the communication load: accumulating multiple batches (Zinkevich et al., 2010), compression (Lin et al., 2018; Koloskova et al., 2019), server sharding (Dean et al., 2012; Jiang et al., 2020). A more detailed overview is given in Appendix B.

In turn, many practical distributed training systems have instead switched to averaging with All-Reduce (Goyal et al., 2017; Mikami et al., 2019; Shoeybi et al., 2019; You et al., 2020). This name refers to a collection of protocols originally developed for HPC applications. Workers can follow these protocols to collectively compute the average² gradient more efficiently than with a central server.

2.2. Communication-efficient All-Reduce

There are several all-reduce protocols optimized for different network topologies. The simplest one is known as Butterfly All-Reduce (Patarasuk & Yuan, 2009). Each of N participants splits its local vector into N chunks. Then, i -th worker aggregates i -th chunk of data from all peers and sends back the averaged chunk.

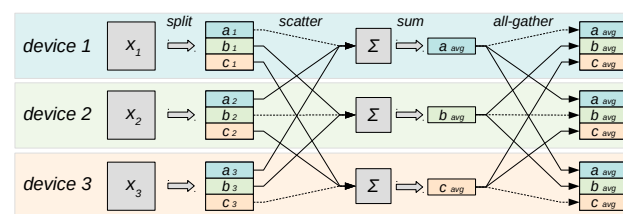


Figure 1. A schematic illustration of Butterfly All-Reduce.

As long as the vector size s is greater than N , this protocol uses $\mathcal{O}(s \times \frac{N-1}{N})$ total bandwidth on each worker. However, it requires all-to-all communication, which is not always practical for the HPC infrastructure. Real-world systems typically use Ring or Tree All-Reduce, where each worker only communicates with a small subset of its peers.

These protocols enable highly efficient and scalable averag-

²All-Reduce works with any commutative associative operation, such as min, max, or product. We use mean as an example.

¹github.com/yandex-research/moshpit-sgd

ing with $\mathcal{O}(1)$ or $\mathcal{O}(\log N)$ total communication per worker, but they also share a common drawback: they cannot tolerate node failures or network instability. If any single participant fails to execute its part or takes long to respond, this paralyzes all other workers.

2.3. Distributed training in unstable conditions

Some distributed training applications must deal with unstable network bandwidth and/or unreliable workers. This issue is most prevalent in federated learning (McMahan et al., 2017; Segal et al., 2017; Bonawitz et al., 2019). When dealing with privacy-sensitive data distributed across multiple actors, such as hospital servers (Sheller et al., 2020; Li et al., 2019a) or mobile phones (Hard et al., 2018; Yang et al., 2018), one must train the model using whichever hardware and network available to those actors.

Another important motivational factor is cost: HPC-grade infrastructure can be prohibitively expensive, pushing researchers and practitioners towards commodity servers or preemptible cloud VMs that are significantly cheaper (see Appendix A). Another solution is to use volunteer computing (Kijssipongse et al., 2018; Ryabinin & Gusev, 2020) with abundant, but even less reliable, compute resources.

Training under these conditions requires specialized distributed strategies. At a small scale, one can deploy one or a few reliable parameter servers to aggregate the updates from workers. This strategy can tolerate individual node failures (Harlap et al., 2017), but scales poorly due to the same reasons we discussed in Section 2.1.

2.4. Decentralized training

If there are too many participants for PS, it can be advantageous to use decentralized SGD via **gossip-based** averaging (Boyd et al., 2006; Tsitsiklis, 1984; Lian et al., 2017). In this scenario, participants form a sparse graph: each worker periodically downloads parameters from its neighbors and mixes them with local parameters.

In essence, gossip-based averaging removes the communication bottlenecks of PS at the cost of using different local parameters on each peer. That said, gossip-based optimization algorithms can match, and sometimes even outperform, their centralized counterparts in terms of training speed (Scaman et al., 2017; 2018; 2019; Lian et al., 2017; Assran et al., 2019a). However, the convergence properties of gossip averaging and gossip-based optimization methods significantly depend on the communication graph through the spectral properties of the mixing matrix (Xiao & Boyd, 2004; Scaman et al., 2019) or the Laplacian matrix of the network (Merris, 1994; Uribe et al., 2020).

Consequently, as the number of peers increases, gossip-based averaging has to either increase the number of neigh-

bors (hence more communication) or accept slower convergence speed. Because of this, gossip is less communication-efficient than all-reduce algorithms reviewed in Section 2.2. However, gossip-based algorithms are more robust to the changes, which makes them applicable to time-varying networks (Nedić & Olshevsky, 2014; 2016; Nedić et al., 2018; Rogozin & Gasnikov, 2019) and federated learning (Ram et al., 2009; Yan et al., 2012; Yuan et al., 2016).

2.5. Distributed Hash Tables

In this work, we set out to improve distributed averaging with a dynamic matchmaking protocol. Without a central server, this protocol relies on decentralized data structures to organize peers. The main data structure we use is the Distributed Hash Table, or DHT. On a high level, DHT is a distributed fault-tolerant “dictionary” that can be accessed by every participant. Each key-value pair is stored on a subset of peers determined by the hash function of the key.

Each participant has a unique identifier (ID) sampled uniformly from the hash function output range. When storing a $(key, value)$ pair, one must find k peers whose IDs are nearest to $\text{hash}(key)$ according to a chosen metric. After that, the participant requests each of those peers to store $(key, value)$. When retrieving a value for a key, one should compute $\text{hash}(key)$, search for peers with IDs nearest to that hash value and request the value from those peers.

Specific DHT versions, such as Chord (Balakrishnan et al., 2003) or Kademlia (Maymounkov & Mazieres, 2002), employ different hash types and algorithms for finding nearest peers. For instance, Kademlia DHT sorts peers based on the XOR distance function: $d(x, y) = \text{int}(x \oplus y)$.

In DHT, each participant is directly aware of only a small subset of peers. When storing or retrieving a key, the participant requests additional peers from its neighbors in a semi-greedy search, minimizing the XOR distance until it finds k nearest peers. In Kademlia, nodes form a special navigable graph structure that lets them find nearest peers in at most $\mathcal{O}(k + \log N)$ requests to other peers, where N is the total number of participants. Due to their scalability and fault-tolerance, DHTs found numerous applications including BitTorrent, Ethereum, I2P and even deep learning with Mixtures-of-Experts (Ryabinin & Gusev, 2020).

3. Method

Large-scale training with unreliable participants requires a protocol that is both communication-efficient and fault-tolerant. Unfortunately, existing methods can only provide one of these two properties. To better address our conditions, we propose Moshpit All-Reduce — a fully decentralized averaging protocol that combines the efficiency of all-reduce and the fault tolerance of gossip-based averaging.

The rest of this section is organized as follows:

- Section 3.1 describes the protocol, demonstrates its correctness and communication efficiency;
- Section 3.2 provides the analysis of the proposed protocol and proves exponential convergence rate for averaging and linear convergence rate for optimization;
- Section 3.3 contains implementation details for training with heterogeneous compute nodes;

3.1. Moshpit Averaging

The core idea of Moshpit All-Reduce is that workers perform averaging in small independent groups. That way, a single failed participant would only affect his current group. In turn, the composition of each group should be chosen dynamically to converge in the least number of steps. Ideally, if there are 16 peers with local parameters θ , we can average them in 2 rounds, as demonstrated in Figure 2.

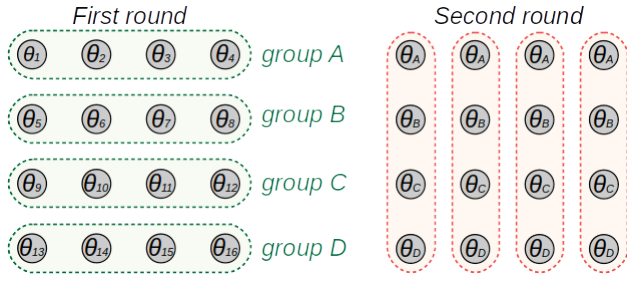


Figure 2. Averaging 16 peers in 2 rounds. Each group performs Butterfly All-Reduce; groups of the same color average in parallel. To produce this behavior in a decentralized system, we use Distributed Hash Tables. On each averaging round:

- Each worker computes his group key C_i ;
- Workers add their network addresses to the DHT key corresponding to C_i ;
- Each worker can now fetch a full list of peers that have the same C_i and run All-Reduce with those peers;

Unfortunately, the averaging structure from Figure 2 is impossible to maintain when participants are constantly joining, leaving, and failing. However, we can achieve equivalent results without global structure using a simple rule: *if two peers were in the same group in round t , they must choose different groups in round $t+1$.*

A natural way to enforce this rule is to take advantage of the chunk indices from Butterfly All-Reduce (see Figure 1). Recall that each worker accumulates a *unique* chunk of parameters defined by an index c_i . By setting $C_i := c_i$, we can guarantee that any workers that were in the same group at a round t will have different group indices in round $t+1$.

This averaging scheme can be generalized to more than two dimensions in order to fit a larger number of peers or reduce the group size. For a d -dimensional hypercube, nodes

should find groups of peers that they have not communicated with during $d-1$ previous rounds. To that end, we define C_i as tuples containing chunk indices from $d-1$ previous rounds:

$$C_i^t := (c_i^{t-d+1}, c_i^{t-d+2}, \dots, c_i^t), \quad (1)$$

where t denotes the communication round.

The above intuition can be formalized with Algorithm 1. Here, N peers form a virtual d -dimensional grid with M peers per row and average their parameters θ_i over T rounds.

Algorithm 1 Moshpit All-Reduce for peer i

```

Input:  $\theta_i, N, d, M, T, i$ 
 $\theta_i^0 := \theta_i$ 
 $C_i^0 := \text{get\_initial\_index}(i)$ 
for  $t \in 1 \dots T$  do
   $\text{DHT}[C_i^{t-1}, t].\text{add}(\text{address}_i)$ 
  /* wait for peers to assemble */
   $\text{peers}_t := \text{DHT.get}([C_i^{t-1}, t])$ 
   $\theta_i^t, c_i^t := \text{AllReduce}(\theta_i^{t-1}, \text{peers}_t)$ 
   $C_i^t := (C_i^{t-1}[1:], c_i^t)$  // same as eq. (1)
end for
Return  $\theta_i^T$ 

```

Here, $\text{DHT}[\cdot]$ is a shortcut for using the DHT to add or retrieve values for a given key. In turn, AllReduce denotes running all-reduce to compute the average θ in a given group of peers. The get_initial_index function takes the peer index i and returns $d-1$ integers in range $[0, M)$ such as the size of initial groups does not exceed M . That way, the groups formed on all subsequent rounds will also have at most M participants. One possible strategy is:

$$\text{get_initial_index}(i) = \begin{pmatrix} i \bmod M \\ [i/M] \bmod M \\ \vdots \\ [i/M^{d-1}] \bmod M \end{pmatrix} \quad (2)$$

If $N=M^d$ and there are no node/network failures, Algorithm 1 is equivalent to Torus All-Reduce (Sack & Gropp, 2015), achieving the exact average after d rounds of communication (see Appendix C.1). However, our typical use case is far from this perfect scenario; for example, some groups can have less than M members. Furthermore, there is a chance that any peer will fail during all-reduce, causing its groupmates to skip a full round of averaging. Still, Moshpit All-Reduce is applicable even in these conditions:

Theorem 3.1 (Correctness). *If all workers have a non-zero probability of successfully running a communication round and the order of peers_t is random, then all local vectors θ_i^t converge to the global average with probability 1*

$$\forall i, \left\| \theta_i^t - \frac{1}{N} \sum_i \theta_i^0 \right\|_2 \xrightarrow[t \rightarrow \infty]{} 0. \quad (3)$$

Sketch of the proof. Running all-reduce with any subset of peers will preserve the invariant $\frac{1}{N} \sum_i \theta_i^t = \frac{1}{N} \sum_i \theta_i^{t-1}$ and reduce the “error” of local estimates θ_i^t . The full proof is deferred to Appendix C.2. \square

Complexity. The matchmaking protocol is implemented over Kademia DHT (Maymounkov & Mazieres, 2002), meaning that each read and write operation requires at most $\mathcal{O}(\log N)$ requests and $\mathcal{O}(M)$ bandwidth to load `peerst`.

After the matchmaking is over, each group runs a single all-reduce round to compute the average. In principle, Moshpit Averaging can use any general-purpose all-reduce protocol. We opted for a butterfly-like version (Figure 1), as it is simpler than Ring All-Reduce while still being communication-efficient. The communication complexity of this algorithm is $\mathcal{O}(\max(s, M) \times \frac{M-1}{M})$, where s is the size of vector θ .

Thus, the total time complexity of Algorithm 1 becomes:

$$\mathcal{O}\left(T \times \left[\log_2 N + M + \max(s, M) \times \frac{M-1}{M}\right]\right) \quad (4)$$

This is in stark contrast to gossip, where the total bandwidth per node grows linearly with the number of neighbors.

3.2. Convergence analysis

3.2.1. MIXING PROPERTIES OF MOSHPIT AVERAGING

As stated in the previous section, Moshpit All-Reduce computes the exact average when $N = M^d$. However, this property cannot be guaranteed in practice. Therefore, additional analysis is needed to establish how quickly the result of Moshpit Averaging approximates the actual average of N vectors stored on peers.

In the following theorem, we provide such analysis for a simplified version of Moshpit Averaging. One can find the full proof in Appendix C.3.

Theorem 3.2. *Consider a modification of Moshpit All-Reduce that works as follows: at each iteration $k \geq 1$, 1) peers are randomly split in r disjoint groups of sizes M_1^k, \dots, M_r^k in such a way that $\sum_{i=1}^r M_i^k = N$ and $M_i^k \geq 1$ for all $i = 1, \dots, r$ and 2) peers from each group compute their group average via All-Reduce. Let $\theta_1, \dots, \theta_N$ be the input vectors of this procedure and $\theta_1^T, \dots, \theta_N^T$ be the outputs after T iterations. Then,*

$$\mathbb{E} \left[\frac{1}{N} \sum_{i=1}^N \|\theta_i^T - \bar{\theta}\|^2 \right] = \left(\frac{r-1}{N} + \frac{r}{N^2} \right)^T \frac{1}{N} \sum_{i=1}^N \|\theta_i - \bar{\theta}\|^2, \quad (5)$$

where $\bar{\theta} = \frac{1}{N} \sum_{i=1}^N \theta_i$.

In particular, this result implies that even if workers are randomly split into pairs at each iteration, the simplified version of Moshpit Averaging makes the average distortion

Algorithm 2 Moshpit SGD

```

1: Input: starting point  $\theta^0$ , learning rate  $\gamma > 0$ , commu-
   nication period  $\tau \geq 1$ 
2: for  $k = 0, 1, \dots$  do
3:   for each peer  $i \in P_{k+1}$  in parallel do
4:     Compute the stochastic gradient  $g_i^k$  at the current
     point  $\theta_i^k$ 
5:     if  $k + 1 \pmod{\tau} = 0$  then
6:        $\theta_i^{k+1} = \left[ \text{MoshpitAvg}_{\mathcal{E}_{j \in P_{k+1}}}(\theta_j^k - \gamma g_j^k) \right]_i$ 
7:     else
8:        $\theta_i^{k+1} = \theta_i^k - \gamma g_i^k$ 
9:     end if
10:  end for
11: end for

```

(the left-hand side of Equation 5) less than ε in expectation after $\mathcal{O}(\log(1/\varepsilon))$ iterations. That is, this algorithm finds ε -accurate average on each node with the rate that *does not* depend on the spectral properties of the communication graph. Since Moshpit Averaging prevents two peers from participating in the same groups during successive iterations, the actual algorithm should find ε -accurate averages on participating peers even faster than Equation 5 predicts. Moreover, in Appendix C.3 we explain how this result can be generalized to the case when $\{M_i^k\}_{i=1}^N$ and r depends on k or even is random. In Appendix C.4, we also provide the guarantees measuring how fast Algorithm 1 reduces the variance when averaging random vectors.

3.2.2. MOSHPIT SGD

We consider a classical distributed optimization problem

$$\min_{\theta \in \mathbb{R}^n} \left\{ f(\theta) = \frac{1}{N} \sum_{i=1}^N f_i(\theta) \right\}, \quad (6)$$

where N is the number of workers and worker i has access only to the function f_i .

We propose a new algorithm called Moshpit SGD to solve this problem (see Algorithm 2). In this algorithm, workers perform independent local SGD steps and periodically synchronize their parameters θ_i^k with other peers using Moshpit All-Reduce. Moreover, we define the indices of participating nodes at iteration k as P_{k+1} ($P_0 = \{1, \dots, N\}$) allowing peers to vanish.

First of all, we list the key assumptions that we use in the convergence analysis of Moshpit SGD.

Assumption 3.1 (Bounded variance). *We assume that for all $k \geq 0$ and $i = 1, \dots, N$ stochastic gradients g_i^k satisfy $\mathbb{E}[g_i^k | \theta_i^k] = \nabla f_i(\theta_i^k)$ and*

$$\mathbb{E}[\|g_i^k - \nabla f_i(\theta_i^k)\|^2 | \theta_i^k] \leq \sigma^2. \quad (7)$$

This assumption is classical in the stochastic optimization

literature (Nemirovski et al., 2009; Ghadimi & Lan, 2013). We notice that our analysis can be generalized to the settings when the stochastic gradients satisfy less restrictive assumptions such as expected smoothness (Gower et al., 2019) or have more sophisticated structure similar to (Karimireddy et al., 2020) using the theoretical framework from Gorbunov et al. (2020a).

The following assumption controls the averaging properties and the effect of the peers' vanishing.

Assumption 3.2 (Averaging quality & peers' vanishing). *We assume that the vanishing of peers does not change the global average of the iterates of Moshpit SGD too much, i.e., $P_{k+1} \subseteq P_k$ and $|P_k| \geq N_{\min}$ for all $k \geq 0$, $|P_{a\tau}| \leq 2|P_{a(\tau+1)}|$ for all non-negative integers $a \geq 0$, and there exist such $\tilde{\theta} \in \mathbb{R}^n$ and a sequence of non-negative numbers $\{\Delta_{pv}^k\}_{k \geq 0}$ that for all $k \geq 0$*

$$\mathbb{E} \left[\langle \theta^{k+1} - \hat{\theta}^{k+1}, \theta^{k+1} + \hat{\theta}^{k+1} - 2\tilde{\theta} \rangle \right] \leq \Delta_{pv}^k, \quad (8)$$

if f is convex, and

$$\mathbb{E} \left[\langle \nabla f(\theta^k), \theta^{k+1} - \hat{\theta}^{k+1} \rangle + L \|\hat{\theta}^{k+1} - \theta^{k+1}\|^2 \right] \leq \Delta_{pv}^k, \quad (9)$$

if f is non-convex and L -smooth (see Def. D.1), where $N_k = |P_k|$, $\theta^{k+1} = \frac{1}{N_{k+1}} \sum_{i \in P_{k+1}} \theta_i^{k+1}$, and $\hat{\theta}^{k+1} = \frac{1}{N_k} \sum_{i \in P_k} (\theta_i^k - \gamma g_i^k)$ for $k \geq 0$. Moreover, we assume that for some $\delta_{aq} \geq 0$ and for all non-negative integers $a \geq 0$

$$\mathbb{E} \left[\frac{1}{N_{a\tau}} \sum_{i \in P_{a\tau}} \|\theta_i^{a\tau} - \theta^{a\tau}\|^2 \right] \leq \gamma^2 \delta_{aq}^2. \quad (10)$$

If $P_k = P_{k+1} = \{1, \dots, N\}$ for all $k \geq 0$, i.e., peers do not vanish, then $\theta^k = \hat{\theta}^k$ and properties (8, 9) hold with $\Delta_{pv}^k \equiv 0$ for all $k \geq 0$. Moreover, according to the mixing properties of Moshpit Averaging established in Theorem 3.2, inequality 10 holds after $\mathcal{O}(\log(1/\gamma^2 \delta_{aq}^2))$ iterations of Algorithm 1. Therefore, the assumption above is natural and well-motivated.

Under these assumptions, we derive the convergence rates both for convex and non-convex problems. The full statements and complete proofs are deferred to Appendix D.

Theorem 3.3 (Convex case). *Let $f_1 = \dots = f_N = f$, function f be μ -strongly convex (Def. D.2) and L -smooth (see Def. D.1), and Assumptions 3.1 and 3.2 hold with $\Delta_{pv}^k = \delta_{pv,1} \gamma \mu \mathbb{E}[\|\theta^k - \theta^*\|^2] + \gamma^2 \delta_{pv,2}^2$ and $\tilde{\theta} = \theta^*$, where $\theta^* \in \arg\min_{\theta \in \mathbb{R}^n} f(\theta)$ and $\delta_{pv,1} \in [0, 1]$, $\delta_{pv,2} \geq 0$. Then there exists a choice of γ such that $\mathbb{E} \left[f(\bar{\theta}^K) - f(\theta^*) \right] \leq \varepsilon$ after K iterations of Moshpit SGD, where K equals*

$$\tilde{\mathcal{O}} \left(\frac{L}{(1 - \delta_{pv,1})\mu} + \frac{\delta_{pv,2}^2 + \sigma^2 / N_{\min}}{(1 - \delta_{pv,1})\mu\varepsilon} + \sqrt{\frac{L((\tau - 1)\sigma^2 + \delta_{aq}^2)}{(1 - \delta_{pv,1})^2 \mu^2 \varepsilon}} \right)$$

when $\mu > 0$, and

$$\mathcal{O} \left(\frac{LR_0^2}{\varepsilon} + \frac{R_0^2(\delta_{pv,2}^2 + \sigma^2 / N_{\min})}{\varepsilon^2} + \frac{R_0^2 \sqrt{L((\tau - 1)\sigma^2 + \delta_{aq}^2)}}{\varepsilon^{3/2}} \right)$$

when $\mu = 0$, where $\bar{\theta}^K = \frac{1}{W_K} \sum_{k=0}^K \frac{1}{N_k} \sum_{i \in P_k} w_k \theta_i^k$, $w_k = (1 - \gamma\mu)^{-(k+1)}$, $W_K = \sum_{k=0}^K w_k$, $R_0 = \|\theta^0 - \theta^*\|$ and $\tilde{\mathcal{O}}(\cdot)$ hides constant and $\log(1/\varepsilon)$ factors.

That is, if $\delta_{pv,1} \leq 1/2$, $N_{\min} = \Omega(N)$, $\delta_{pv,2}^2 = \mathcal{O}(\sigma^2 / N_{\min})$, and $\delta_{aq}^2 = \mathcal{O}((\tau - 1)\sigma)$, then Moshpit SGD has the same iteration complexity as Local-SGD in the homogeneous case (Khaled et al., 2020; Woodworth et al., 2020b). However, the averaging steps of Moshpit SGD are much faster than those of the parameter-server architecture when the number of peers is large. Also, unlike the state-of-the-art convergence guarantees for Decentralized Local-SGD (Koloskova et al., 2020b), our bounds do not depend on the spectral properties of the communication graph.

Theorem 3.4 (Non-convex case). *Let $f_1 = \dots = f_N = f$, function f be L -smooth and bounded from below by f_* , and Assumptions 3.1 and 3.2 hold with $\Delta_{pv}^k = \delta_{pv,1} \gamma \mathbb{E}[\|\nabla f(\theta^k)\|^2] + L\gamma^2 \delta_{pv,2}^2$, $\delta_{pv,1} \in [0, 1/2]$, $\delta_{pv,2} \geq 0$. Then there exists such choice of γ that $\mathbb{E}[\|\nabla f(\theta_{rand}^K)\|^2] \leq \varepsilon^2$ after K iterations of Moshpit SGD, where K equals*

$$\mathcal{O} \left(\frac{L\Delta_0}{(1 - 2\delta_{pv,1})^2 \varepsilon^2} \left[1 + \tau \sqrt{1 - 2\delta_{pv,1}} + \frac{\delta_{pv,2}^2 + \sigma^2 / N_{\min}}{\varepsilon^2} + \frac{\sqrt{(1 - 2\delta_{pv,1})(\delta_{aq}^2 + (\tau - 1)\sigma^2)}}{\varepsilon} \right] \right),$$

$\Delta_0 = f(\theta^0) - f(\theta^*)$ and θ_{rand}^K is chosen uniformly at random from $\{\theta^0, \theta^1, \dots, \theta^{K-1}\}$ defined in As. 3.2.

Again, if $\delta_{pv,1} \leq 1/3$, $N_{\min} = \Omega(N)$, $\delta_{pv,2}^2 = \mathcal{O}(\sigma^2 / N_{\min})$, and $\delta_{aq}^2 = \mathcal{O}((\tau - 1)\sigma)$, then the above theorem recovers the state-of-the-art results in the non-convex case for Local-SGD (Li et al., 2019b; Koloskova et al., 2020b).

3.3. Implementation details

Training on heterogeneous unreliable hardware also poses a number of engineering challenges that we need to address.

Bandwidth variation. When participants have unequal network bandwidth, standard all-reduce protocols can be inefficient. For instance, consider a group of size 4 where one peer has 1000Mb/s bandwidth and others have 100Mb/s. For this group, aggregating all parameters on the first peer is faster than running Butterfly All-Reduce.

In order to minimize averaging time for arbitrary group compositions, Moshpit All-Reduce splits parameters into

uneven chunks based on the bandwidth of each peer. Groupmates obtain optimal chunk sizes as a solution of the linear program minimizing the total runtime. We describe the corresponding optimization problem in Appendix E.

Training with dynamic number of peers. Many practical setups with unreliable devices allow peers to join or leave at any time, which can produce undesirable side-effects. For instance, consider a participant that joins the “swarm” midway through the training process. If this participant starts with the initial model parameters, it can undo some of the progress made by other peers.

To circumvent this issue, we require each new participant to download the latest parameters from a random up-to-date peer discovered through DHT. The same technique is used to synchronize the optimizer statistics and the learning rate schedule. This protocol is also triggered if a peer becomes desynchronized with others, e.g., after a network freeze.

4. Experiments

In this section, we first check the theoretical properties of Moshpit All-Reduce in a controlled setup (Section 4.1). Then, we compare Moshpit SGD with other distributed methods on practical tasks of image classification and masked language model pretraining (Sections 4.2 and 4.3).

4.1. Decentralized averaging

We aim to verify the convergence and fault tolerance properties proven in Section 3.2. To achieve this, we initialize vectors of 512–1024 peers with standard Gaussian noise and run Moshpit Averaging for up to 18 steps. We report the average squared difference between the worker parameters and the true average parameters for a 32×32 grid with varying density and failure rate. We simulate failures by randomly shutting down peers with probability p . Failed peers return in the next round of averaging.

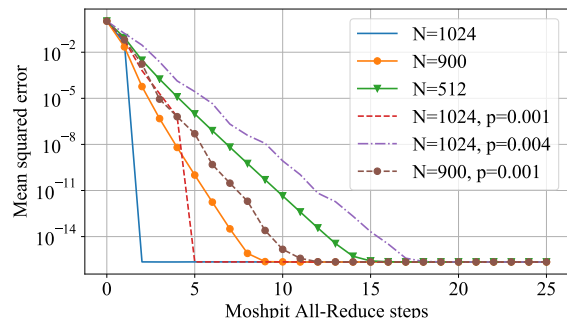


Figure 3. Averaging error for Moshpit All-Reduce.

The results in Figure 3 outperform the theoretical estimate (Theorem 3.2) in all but one scenario: when $N=1024$, the algorithm finds the exact average (within 32-bit precision) in 2 steps. We also verified that despite worker failures, the global average vector remains constant. We report additional grid configurations in Appendix G.

4.2. ImageNet training

Here, we evaluate the performance of Moshpit SGD in distributed training. More specifically, we train ResNet-50 (He et al., 2015) on the ILSVRC (Deng et al., 2009) dataset, following the training protocol of Goyal et al. (2017). Trainers use SGD with Nesterov momentum with a batch size of 256 and 32-bit precision regardless of the GPU type³. We evaluate the following training strategies:

- **All-Reduce SGD (AR-SGD)** — traditional distributed training with all-reduce gradient averaging;
- **Asynchronous Decentralized Parallel SGD (AD-PSGD)** — parallel SGD that runs gossip communication in a cycle: each worker averages parameters with 2 neighbors. Communication rounds are performed in background while the algorithm trains;
- **Stochastic Gradient Push (SGP)** — a more advanced algorithm with an exponential communication graph and push-based communication (Assran et al., 2019b).
- **Moshpit SGD** — similar to SGP, but we perform 1 round of Moshpit Averaging instead of PushSum.

We report top-1 validation accuracy as a function of training time in two experimental setups:

- **Homogeneous:** 16 servers, each with a single Tesla V100-PCIe GPU, 6 CPU cores, and 64GB RAM.
- **Heterogeneous:** a total of 81 GPUs (V100, 1080Ti, and P40) across 64 servers and workstations.⁴

All servers and workstations communicate over the network with 1Gb/s Ethernet (non-dedicated symmetric bandwidth). The machines are located in two data centers and one office within 300 km of one another. The communication latency is 1–6ms depending on the location. To simulate shared usage, at the beginning of each communication round we inject additional latency sampled from the exponential distribution (Sukhov et al., 2016) with the mean of 100ms.

For Moshpit SGD, we use a two-dimensional “grid” with 4 and 8 groups for homogeneous and heterogeneous setups respectively. For AD-PSGD, we attempt to compensate for slow convergence by training for 60 more epochs without changing the learning rate schedule. Finally, we only report AR-SGD in the first setup, as it is unsuitable for heterogeneous hardware.

The results in Figure 4 (Left) demonstrate that the two most efficient strategies for our setting are Moshpit SGD and SGP. In the **homogeneous** setup, Moshpit is only slightly more efficient than SGP, likely due to higher communication efficiency of all-reduce. This advantage increases to over 30%

³For GPUs that cannot fit this batch size into memory, we accumulate gradients over 2 minibatches of 128 examples.

⁴We provide a detailed configuration in Appendix F.

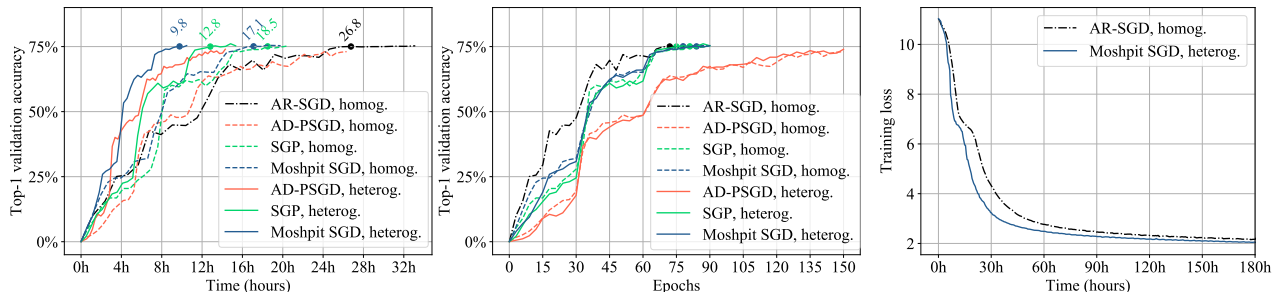


Figure 4. (Left, Middle) ResNet-50 top-1 validation accuracy for ImageNet as a function of training time (left) and epochs (middle). (Right) Full training objective (MLM + SOP) of ALBERT-large on BookCorpus as a function of training time.

for the **heterogeneous** setup with 64 servers. In turn, AR-SGD demonstrates the best performance per iteration, but its training time is by far the longest due to network latency ($1.5\times$ of Moshpit SGD). Finally, AD-PSGD predictably shows the best throughput (time per epoch), but achieves lower training accuracy even after training for 150 epochs. We also report results for smaller setups in Appendix H.

4.3. Masked Language Model training

Finally, we evaluate Moshpit All-Reduce training performance in the wild with preemptible cloud instances. For this experiment, we perform one of the most resource-demanding tasks in modern deep learning — unsupervised pretraining of Transformers (Devlin et al., 2019; Liu et al., 2019; Radford et al., 2019; Brown et al., 2020). We opt for the ALBERT model (Lan et al., 2020) to make better use of communication-constrained devices. This model has fewer trainable parameters due to layer-wise weight sharing.

Specifically, we train ALBERT-large (18M parameters) on the BookCorpus (Zhu et al., 2015) dataset, following the training setup from the original paper. We minimize the masked language modeling loss (MLM) along with the sentence order prediction loss (SOP) using the LAMB optimizer (You et al., 2020) with a global batch size of 4096 and sequence length 512. We measure convergence in terms of full training loss (Lin et al., 2020a; Fedus et al., 2021). Similarly to Section 4.2, we use two training setups:

- **Homogeneous:** a single cloud instance with 8 Tesla V100-PCIe GPUs and 56 vCPUs;
- **Heterogeneous:** a total of 66 preemptible GPUs, 32 of which are cloud T4, and the remaining 34 are various devices rented on a public marketplace.

Despite the fact that the latter setup has almost $3\times$ more raw compute⁵, its hourly rent costs less than the homogeneous setup due to relying on preemptible instances⁶. This instance type is much cheaper than regular cloud instances, but it can be interrupted at any time. As a side-effect, the participants in **heterogeneous** setup are also spread across 3 continents with uneven network bandwidth, ranging from

100Mb/s to 1500Mb/s per worker. These limitations make it impractical to deploy conventional all-reduce protocols. By contrast, the fully decentralized nature of Moshpit SGD allows it to operate on unreliable nodes.

In this setup, the participants accumulate gradients over multiple local batches and use DHT to track the global batch size. Once the swarm collectively accumulates gradients over 4096 training samples, it runs 2 rounds of Moshpit All-Reduce with $M=8$ and $d=2$. Unfortunately, training with simple parameter averaging does not converge, likely due to diverging LAMB statistics. To mitigate this issue, workers recover “pseudo-gradients” (Reddi et al., 2021; Chen et al., 2020) after averaging to update the optimizer statistics.

Figure 4 (right) demonstrates that Moshpit SGD with a fully preemptible fleet of machines trains 1.5 times faster than the traditional data-parallel setup. The final loss achieved by two training strategies is the same within the margin of error. A closer investigation reveals that this speedup is entirely explained by the reduced iteration time. An interesting observation is that the iteration time of Moshpit SGD varies between 10–22 seconds, while AR-SGD consistently spends 25s per step. This can be explained by natural variation in the preemptible fleet size: there were 30–66 active participants depending on availability.

5. Conclusion

In this work, we propose Moshpit All-Reduce — a decentralized averaging protocol intended for distributed optimization. It has favorable theoretical properties when compared to gossip-based approaches and achieves considerable distributed training speedups for image classification and masked language modeling.

Our approach was primarily designed for cloud-based training and federated learning, as well as for distributed training on unreliable instances; future work might explore additional settings, such as collaborative training of neural networks. Another perspective research direction is to study the combination of the proposed protocol with other techniques that aim for communication efficiency in distributed optimization, for example, gradient compression.

⁵Based on official performance benchmarks (NVIDIA).

⁶Please refer to Appendix F for full experimental setups.

Acknowledgements

Eduard Gorbunov was supported by Russian Foundation for Basic Research (Theorem 3.3, project No. 19-31-51001) and by Russian Science Foundation (Theorem 3.4, project No. 21-71-30005). We would like to thank Anastasia Koloskova, Liudmila Prokhorenkova and Anton Osokin for helpful feedback and discussions. Finally, we would like to thank Dmitry Afanasiev, Vladimir Aliev and Anand Jayarajan for their suggestions on the technical aspects of our study. The computational resources for the experiments were provided by the Amazon Research Awards program and Yandex.

References

- Agarwal, A. and Duchi, J. C. Distributed delayed stochastic optimization. In *Proceedings of the 24th International Conference on Neural Information Processing Systems*, pp. 873–881, 2011.
- Aldous, D. and Fill, J. A. Reversible markov chains and random walks on graphs, 2002. unfinished monograph, recompiled 2014, 2002.
- Alistarh, D., Grubic, D., Li, J. Z., Tomioka, R., and Vojnovic, M. Qsgd: communication-efficient sgd via gradient quantization and encoding. In *Proceedings of the 31st International Conference on Neural Information Processing Systems*, pp. 1707–1718, 2017.
- Alqahtani, S. and Demirbas, M. Performance analysis and comparison of distributed machine learning systems. 07 2019.
- Andersen, E. D. and Andersen, K. D. The mosek interior point optimizer for linear programming: An implementation of the homogeneous algorithm. In *Applied Optimization*, pp. 197–232. Springer US, 2000. doi: 10.1007/978-1-4757-3216-0_8. URL https://doi.org/10.1007%2F978-1-4757-3216-0_8.
- Arjevani, Y. and Shamir, O. Communication complexity of distributed convex learning and optimization. *Advances in neural information processing systems*, 28:1756–1764, 2015.
- Arjevani, Y., Shamir, O., and Srebro, N. A tight convergence analysis for stochastic gradient descent with delayed updates. In *Algorithmic Learning Theory*, pp. 111–132. PMLR, 2020.
- Assran, M., Loizou, N., Ballas, N., and Rabbat, M. Stochastic gradient push for distributed deep learning. In *International Conference on Machine Learning*, pp. 344–353. PMLR, 2019a.
- Assran, M., Loizou, N., Ballas, N., and Rabbat, M. Stochastic gradient push for distributed deep learning. In Chaudhuri, K. and Salakhutdinov, R. (eds.), *Proceedings of the 36th International Conference on Machine Learning*, volume 97 of *Proceedings of Machine Learning Research*, pp. 344–353. PMLR, 09–15 Jun 2019b. URL <http://proceedings.mlr.press/v97/assran19a.html>.
- Assran, M., Aytekin, A., Feysmahdavian, H. R., Johansson, M., and Rabbat, M. G. Advances in asynchronous parallel and distributed optimization. *Proceedings of the IEEE*, 108(11):2013–2031, 2020.
- Balakrishnan, H., Kaashoek, M. F., Karger, D., Morris, R., and Stoica, I. Looking up data in p2p systems. *Communications of the ACM*, 46(2):43–48, 2003.
- Basu, D., Data, D., Karakus, C., and Diggavi, S. Qsparse-local-SGD: Distributed SGD with quantization, sparsification and local computations. In *Advances in Neural Information Processing Systems*, pp. 14668–14679, 2019.
- Beznosikov, A., Horváth, S., Richtárik, P., and Safaryan, M. On biased compression for distributed learning. *arXiv preprint arXiv:2002.12410*, 2020.
- Bonawitz, K. A., Eichner, H., Grieskamp, W., Huba, D., Ingerman, A., Ivanov, V., Kiddon, C. M., Konečný, J., Mazzocchi, S., McMahan, B., Overveldt, T. V., Petrou, D., Ramage, D., and Roselander, J. Towards federated learning at scale: System design. In *SysML 2019*, 2019. URL <https://arxiv.org/abs/1902.01046>. To appear.
- Boyd, S., Ghosh, A., Prabhakar, B., and Shah, D. Randomized gossip algorithms. *IEEE transactions on information theory*, 52(6):2508–2530, 2006.
- Brown, T. B., Mann, B., Ryder, N., Subbiah, M., Kaplan, J., Dhariwal, P., Neelakantan, A., Shyam, P., Sastry, G., Askell, A., et al. Language models are few-shot learners. *arXiv preprint arXiv:2005.14165*, 2020.
- Chen, X., Li, X., and Li, P. Toward communication efficient adaptive gradient method. In *Proceedings of the 2020 ACM-IMS on Foundations of Data Science Conference*, FODS ’20, pp. 119–128, New York, NY, USA, 2020. Association for Computing Machinery. ISBN 9781450381031. doi: 10.1145/3412815.3416891. URL <https://doi.org/10.1145/3412815.3416891>.
- Das, R., Hashemi, A., Sanghavi, S., and Dhillon, I. S. Improved convergence rates for non-convex federated learning with compression. *arXiv preprint arXiv:2012.04061*, 2020.

- Dean, J., Corrado, G., Monga, R., Chen, K., Devin, M., Mao, M., Ranzato, M. a., Senior, A., Tucker, P., Yang, K., Le, Q., and Ng, A. Large scale distributed deep networks. In Pereira, F., Burges, C. J. C., Bottou, L., and Weinberger, K. Q. (eds.), *Advances in Neural Information Processing Systems*, volume 25, pp. 1223–1231. Curran Associates, Inc., 2012. URL <https://proceedings.neurips.cc/paper/2012/file/6aca97005c68f1206823815f66102863-Paper.pdf>.
- Deng, J., Dong, W., Socher, R., Li, L.-J., Li, K., and Fei-Fei, L. ImageNet: A Large-Scale Hierarchical Image Database. In *CVPR09*, 2009.
- Devlin, J., Chang, M.-W., Lee, K., and Toutanova, K. Bert: Pre-training of deep bidirectional transformers for language understanding. In *NAACL-HLT*, 2019.
- Fallah, A., Gurbuzbalaban, M., Ozdaglar, A., Simsekli, U., and Zhu, L. Robust distributed accelerated stochastic gradient methods for multi-agent networks. *arXiv preprint arXiv:1910.08701*, 2019.
- Fedus, W., Zoph, B., and Shazeer, N. Switch transformers: Scaling to trillion parameter models with simple and efficient sparsity, 2021.
- Feyzmahdavian, H. R., Aytekin, A., and Johansson, M. An asynchronous mini-batch algorithm for regularized stochastic optimization. *IEEE Transactions on Automatic Control*, 61(12):3740–3754, 2016.
- Ghadimi, S. and Lan, G. Stochastic first-and zeroth-order methods for nonconvex stochastic programming. *SIAM Journal on Optimization*, 23(4):2341–2368, 2013.
- Gorbunov, E., Hanzely, F., and Richtárik, P. Local sgd: Unified theory and new efficient methods. *arXiv preprint arXiv:2011.02828*, 2020a.
- Gorbunov, E., Kovalev, D., Makarenko, D., and Richtárik, P. Linearly converging error compensated sgd. *Advances in Neural Information Processing Systems*, 33, 2020b.
- Gower, R. M., Loizou, N., Qian, X., Sailanbayev, A., Shulgin, E., and Richtárik, P. Sgd: General analysis and improved rates. In *International Conference on Machine Learning*, pp. 5200–5209. PMLR, 2019.
- Goyal, P., Dollár, P., Girshick, R., Noordhuis, P., Wesolowski, L., Kyrola, A., Tulloch, A., Jia, Y., and He, K. Accurate, large minibatch sgd: Training imagenet in 1 hour, 2017.
- Haddadpour, F., Kamani, M. M., Mokhtari, A., and Mahdavi, M. Federated learning with compression: Unified analysis and sharp guarantees. *arXiv preprint arXiv:2007.01154*, 2020.
- Hard, A., Kiddon, C. M., Ramage, D., Beaufays, F., Eichner, H., Rao, K., Mathews, R., and Augenstein, S. Federated learning for mobile keyboard prediction, 2018. URL <https://arxiv.org/abs/1811.03604>.
- Harlap, A., Tumanov, A., Chung, A., Ganger, G. R., and Gibbons, P. B. Proteus: Agile ml elasticity through tiered reliability in dynamic resource markets. In *Proceedings of the Twelfth European Conference on Computer Systems*, EuroSys '17, pp. 589–604, New York, NY, USA, 2017. Association for Computing Machinery. ISBN 9781450349383. doi: 10.1145/3064176.3064182. URL <https://doi.org/10.1145/3064176.3064182>.
- He, K., Zhang, X., Ren, S., and Sun, J. Deep residual learning for image recognition. *2016 IEEE Conference on Computer Vision and Pattern Recognition (CVPR)*, pp. 770–778, 2015.
- Horvath, S., Ho, C.-Y., Horvath, L., Sahu, A. N., Canini, M., and Richtárik, P. Natural compression for distributed deep learning. *arXiv preprint arXiv:1905.10988*, 2019.
- Horváth, S., Kovalev, D., Mishchenko, K., Stich, S., and Richtárik, P. Stochastic distributed learning with gradient quantization and variance reduction. *arXiv preprint arXiv:1904.05115*, 2019.
- Jayarajan, A., Wei, J., Gibson, G., Fedorova, A., and Pekhimenko, G. Priority-based parameter propagation for distributed dnn training. In Talwalkar, A., Smith, V., and Zaharia, M. (eds.), *Proceedings of Machine Learning and Systems*, volume 1, pp. 132–145, 2019. URL <https://proceedings.mlsys.org/paper/2019/file/d09bf41544a3365a46c9077ebb5e35c3-Paper.pdf>.
- Jiang, Y., Zhu, Y., Lan, C., Yi, B., Cui, Y., and Guo, C. A unified architecture for accelerating distributed DNN training in heterogeneous gpu/cpu clusters. In *14th USENIX Symposium on Operating Systems Design and Implementation (OSDI 20)*, pp. 463–479. USENIX Association, November 2020. ISBN 978-1-939133-19-9. URL <https://www.usenix.org/conference/osdi20/presentation/jiang>.
- Kairouz, P., McMahan, H. B., Avent, B., Bellet, A., Bennis, M., Bhagoji, A. N., Bonawitz, K., Charles, Z., Cormode, G., Cummings, R., et al. Advances and open problems in federated learning. *arXiv preprint arXiv:1912.04977*, 2019.
- Kaplan, J., McCandlish, S., Henighan, T., Brown, T. B., Chess, B., Child, R., Gray, S., Radford, A., Wu, J., and Amodei, D. Scaling laws for neural language models, 2020.

- Kaplan, S. Application of programs with maximin objective functions to problems of optimal resource allocation. *Operations Research*, 22(4):802–807, 1974.
- Karimireddy, S. P., Rebjock, Q., Stich, S., and Jaggi, M. Error feedback fixes signsgd and other gradient compression schemes. In *International Conference on Machine Learning*, pp. 3252–3261. PMLR, 2019.
- Karimireddy, S. P., Kale, S., Mohri, M., Reddi, S., Stich, S., and Suresh, A. T. Scaffold: Stochastic controlled averaging for federated learning. In *International Conference on Machine Learning*, pp. 5132–5143. PMLR, 2020.
- Khaled, A., Mishchenko, K., and Richtárik, P. Tighter theory for local sgd on identical and heterogeneous data. In *International Conference on Artificial Intelligence and Statistics*, pp. 4519–4529. PMLR, 2020.
- Kijsipongse, E., Piyatumrong, A., and U-ruekolan, S. A hybrid gpu cluster and volunteer computing platform for scalable deep learning. *The Journal of Supercomputing*, 04 2018. doi: 10.1007/s11227-018-2375-9.
- Kingma, D. P. and Ba, J. Adam: A method for stochastic optimization. In *3rd International Conference on Learning Representations, ICLR 2015*, 2015.
- Kolesnikov, A., Beyer, L., Zhai, X., Puigcerver, J., Yung, J., Gelly, S., and Houlsby, N. Big transfer (bit): General visual representation learning. In *ECCV*, 2020.
- Koloskova, A., Stich, S., and Jaggi, M. Decentralized stochastic optimization and gossip algorithms with compressed communication. In Chaudhuri, K. and Salakhutdinov, R. (eds.), *Proceedings of the 36th International Conference on Machine Learning*, volume 97 of *Proceedings of Machine Learning Research*, pp. 3478–3487. PMLR, 09–15 Jun 2019. URL <http://proceedings.mlr.press/v97/koloskova19a.html>.
- Koloskova, A., Lin, T., Stich, S. U., and Jaggi, M. Decentralized deep learning with arbitrary communication compression. In *International Conference on Learning Representations*, 2020a. URL <https://openreview.net/forum?id=SkGcKkrKvH>.
- Koloskova, A., Loizou, N., Boreiri, S., Jaggi, M., and Stich, S. A unified theory of decentralized sgd with changing topology and local updates. In *International Conference on Machine Learning*, pp. 5381–5393. PMLR, 2020b.
- Konečný, J., McMahan, H. B., Yu, F. X., Richtárik, P., Suresh, A. T., and Bacon, D. Federated learning: Strategies for improving communication efficiency. *arXiv preprint arXiv:1610.05492*, 2016.
- Kovalev, D., Koloskova, A., Jaggi, M., Richtárik, P., and Stich, S. U. A linearly convergent algorithm for decentralized optimization: Sending less bits for free! *arXiv preprint arXiv:2011.01697*, 2020a.
- Kovalev, D., Salim, A., and Richtárik, P. Optimal and practical algorithms for smooth and strongly convex decentralized optimization. *Advances in Neural Information Processing Systems*, 33, 2020b.
- Krizhevsky, A., Sutskever, I., and Hinton, G. E. Imagenet classification with deep convolutional neural networks. In Pereira, F., Burges, C. J. C., Bottou, L., and Weinberger, K. Q. (eds.), *Advances in Neural Information Processing Systems 25*, pp. 1097–1105. Curran Associates, Inc., 2012. URL <http://papers.nips.cc/paper/4824-imagenet-classification-with-deep-convolutional-neural-networks.pdf>.
- Lan, Z.-Z., Chen, M., Goodman, S., Gimpel, K., Sharma, P., and Soricut, R. Albert: A lite bert for self-supervised learning of language representations. In *International Conference on Learning Representations*, 2020.
- Leblond, R., Pedregosa, F., and Lacoste-Julien, S. Asaga: asynchronous parallel saga. In *Artificial Intelligence and Statistics*, pp. 46–54. PMLR, 2017.
- Li, C. Demystifying gpt-3 language model: A technical overview, 2020. "<https://lambdalabs.com/blog/demystifying-gpt-3>".
- Li, M. Scaling distributed machine learning with the parameter server. In *Proceedings of the 2014 International Conference on Big Data Science and Computing*, Big-DataScience '14, New York, NY, USA, 2014. Association for Computing Machinery. ISBN 9781450328913. doi: 10.1145/2640087.2644155. URL <https://doi.org/10.1145/2640087.2644155>.
- Li, W., Milletari, F., Xu, D., Rieke, N., Hancox, J., Zhu, W., Baust, M., Cheng, Y., Ourselin, S., Cardoso, M., and Feng, A. *Privacy-Preserving Federated Brain Tumor Segmentation*, pp. 133–141. Lecture Notes in Computer Science (including subseries Lecture Notes in Artificial Intelligence and Lecture Notes in Bioinformatics). SPRINGER, January 2019a. ISBN 9783030326913. doi: 10.1007/978-3-030-32692-0_16. 10th International Workshop on Machine Learning in Medical Imaging, MLMI 2019 held in conjunction with the 22nd International Conference on Medical Image Computing and Computer-Assisted Intervention, MICCAI 2019 ; Conference date: 13-10-2019 Through 13-10-2019.
- Li, X., Yang, W., Wang, S., and Zhang, Z. Communication efficient decentralized training with multiple local updates. *arXiv preprint arXiv:1910.09126*, 5, 2019b.

- Li, Z. and Richtárik, P. A unified analysis of stochastic gradient methods for nonconvex federated optimization. *arXiv preprint arXiv:2006.07013*, 2020.
- Li, Z., Kovalev, D., Qian, X., and Richtarik, P. Acceleration for compressed gradient descent in distributed and federated optimization. In *International Conference on Machine Learning*, pp. 5895–5904. PMLR, 2020.
- Lian, X., Zhang, C., Zhang, H., Hsieh, C.-J., Zhang, W., and Liu, J. Can decentralized algorithms outperform centralized algorithms? a case study for decentralized parallel stochastic gradient descent. In *Advances in Neural Information Processing Systems*, pp. 5330–5340, 2017.
- Lin, J., Li, X., and Pekhimenko, G. Multi-node bert-pretraining: Cost-efficient approach, 2020a.
- Lin, T., Stich, S. U., Patel, K. K., and Jaggi, M. Don’t use large mini-batches, use local SGD. *ICLR*, pp. arXiv:1808.07217, 2020b. URL <https://arxiv.org/abs/1808.07217>.
- Lin, Y., Han, S., Mao, H., Wang, Y., and Dally, B. Deep gradient compression: Reducing the communication bandwidth for distributed training. In *International Conference on Learning Representations*, 2018. URL <https://openreview.net/forum?id=SkhQHMW0W>.
- Liu, Y., Ott, M., Goyal, N., Du, J., Joshi, M., Chen, D., Levy, O., Lewis, M., Zettlemoyer, L., and Stoyanov, V. Roberta: A robustly optimized bert pretraining approach. *ArXiv*, abs/1907.11692, 2019.
- Mattson, P., Cheng, C., Coleman, C., Diamos, G., Micikevicius, P., Patterson, D., Tang, H., Wei, G.-Y., Bailis, P., Bittorf, V., Brooks, D., Chen, D., Dutta, D., Gupta, U., Hazelwood, K., Hock, A., Huang, X., Jia, B., Kang, D., Kanter, D., Kumar, N., Liao, J., Ma, G., Narayanan, D., Oguntebi, T., Pekhimenko, G., Pentecost, L., Reddi, V. J., Robie, T., John, T. S., Wu, C.-J., Xu, L., Young, C., and Zaharia, M. MLPerf Training Benchmark. In *Proceedings of the 3rd Conference on Machine Learning and Systems (MLSys’20)*, 2020.
- Maymounkov, P. and Mazieres, D. Kademia: A peer-to-peer information system based on the xor metric. In *International Workshop on Peer-to-Peer Systems*, pp. 53–65. Springer, 2002.
- McMahan, B., Moore, E., Ramage, D., Hampson, S., and y Arcas, B. A. Communication-efficient learning of deep networks from decentralized data. In *Artificial Intelligence and Statistics*, pp. 1273–1282, 2017.
- Merris, R. Laplacian matrices of graphs: a survey. *Linear algebra and its applications*, 197:143–176, 1994.
- Mikami, H., Suganuma, H., U-chupala, P., Tanaka, Y., and Kageyama, Y. Massively distributed sgd: Imagenet/resnet-50 training in a flash, 2019.
- Mishchenko, K., Iutzeler, F., Malick, J., and Amini, M.-R. A delay-tolerant proximal-gradient algorithm for distributed learning. In *International Conference on Machine Learning*, pp. 3587–3595. PMLR, 2018.
- Mishchenko, K., Gorbunov, E., Takáč, M., and Richtárik, P. Distributed learning with compressed gradient differences. *arXiv preprint arXiv:1901.09269*, 2019.
- Nedić, A. and Olshevsky, A. Distributed optimization over time-varying directed graphs. *IEEE Transactions on Automatic Control*, 60(3):601–615, 2014.
- Nedić, A. and Olshevsky, A. Stochastic gradient-push for strongly convex functions on time-varying directed graphs. *IEEE Transactions on Automatic Control*, 61(12):3936–3947, 2016.
- Nedić, A., Olshevsky, A., and Rabbat, M. G. Network topology and communication-computation tradeoffs in decentralized optimization. *Proceedings of the IEEE*, 106(5):953–976, 2018.
- Nemirovski, A., Juditsky, A., Lan, G., and Shapiro, A. Robust stochastic approximation approach to stochastic programming. *SIAM Journal on optimization*, 19(4):1574–1609, 2009.
- NVIDIA. Nvidia data center deep learning product performance. ”<https://developer.nvidia.com/deep-learning-performance-training-inference>”, accessed at 2021.02.03.
- Patarasuk, P. and Yuan, X. Bandwidth optimal all-reduce algorithms for clusters of workstations. *J. Parallel Distrib. Comput.*, 69(2):117–124, February 2009. ISSN 0743-7315. doi: 10.1016/j.jpdc.2008.09.002. URL <https://doi.org/10.1016/j.jpdc.2008.09.002>.
- Peng, Z., Xu, Y., Yan, M., and Yin, W. Arock: an algorithmic framework for asynchronous parallel coordinate updates. *SIAM Journal on Scientific Computing*, 38(5):A2851–A2879, 2016.
- Persico, V., Marchetta, P., Botta, A., and Pescapé, A. On network throughput variability in microsoft azure cloud. In *2015 IEEE Global Communications Conference (GLOBECOM)*, pp. 1–6, 2015. doi: 10.1109/GLOCOM.2015.7416997.
- Persico, V., Marchetta, P., Botta, A., and Pescapè, A. Measuring network throughput in the cloud: The case of amazon ec2. *Computer Networks*, 93:408 – 422, 2015. ISSN 1389-1286. doi:

- <https://doi.org/10.1016/j.comnet.2015.09.037>. URL <http://www.sciencedirect.com/science/article/pii/S138912861500362X>. Cloud Networking and Communications II.
- Philippenko, C. and Dieuleveut, A. Artemis: tight convergence guarantees for bidirectional compression in federated learning. *arXiv preprint arXiv:2006.14591*, 2020.
- Qian, X., Richtárik, P., and Zhang, T. Error compensated distributed sgd can be accelerated. *arXiv preprint arXiv:2010.00091*, 2020.
- Radford, A., Wu, J., Child, R., Luan, D., Amodei, D., and Sutskever, I. Language models are unsupervised multitask learners. 2019.
- Rajpurkar, P., Zhang, J., Lopyrev, K., and Liang, P. Squad: 100, 000+ questions for machine comprehension of text. In *EMNLP*, 2016.
- Ram, S. S., Nedić, A., and Veeravalli, V. V. Asynchronous gossip algorithms for stochastic optimization. In *Proceedings of the 48th IEEE Conference on Decision and Control (CDC) held jointly with 2009 28th Chinese Control Conference*, pp. 3581–3586. IEEE, 2009.
- Recht, B., Re, C., Wright, S., and Niu, F. Hogwild: A lock-free approach to parallelizing stochastic gradient descent. In *Advances in neural information processing systems*, pp. 693–701, 2011.
- Reddi, S. J., Charles, Z., Zaheer, M., Garrett, Z., Rush, K., Konečný, J., Kumar, S., and McMahan, H. B. Adaptive federated optimization. In *International Conference on Learning Representations*, 2021. URL <https://openreview.net/forum?id=LkFG31B13U5>.
- Reisizadeh, A., Mokhtari, A., Hassani, H., and Pedarsani, R. An exact quantized decentralized gradient descent algorithm. *IEEE Transactions on Signal Processing*, 67(19):4934–4947, 2019.
- Rogozin, A. and Gasnikov, A. Projected gradient method for decentralized optimization over time-varying networks. *arXiv preprint arXiv:1911.08527*, 2019.
- Ryabinin, M. and Gusev, A. Towards crowdsourced training of large neural networks using decentralized mixture-of-experts. In *Advances in Neural Information Processing Systems*, 2020.
- Sack, P. and Gropp, W. Collective algorithms for multiported torus networks. *ACM Trans. Parallel Comput.*, 1(2), February 2015. ISSN 2329-4949. doi: 10.1145/2686882. URL <https://doi.org/10.1145/2686882>.
- Scaman, K., Bach, F., Bubeck, S., Lee, Y. T., and Massoulié, L. Optimal algorithms for smooth and strongly convex distributed optimization in networks. In *International Conference on Machine Learning*, pp. 3027–3036, 2017.
- Scaman, K., Bach, F., Bubeck, S., Massoulié, L., and Lee, Y. T. Optimal algorithms for non-smooth distributed optimization in networks. In *Advances in Neural Information Processing Systems*, pp. 2740–2749, 2018.
- Scaman, K., Bach, F., Bubeck, S., Lee, Y., and Massoulié, L. Optimal convergence rates for convex distributed optimization in networks. *Journal of Machine Learning Research*, 20:1–31, 2019.
- Segal, A., Marcedone, A., Kreuter, B., Ramage, D., McMahan, H. B., Seth, K., Bonawitz, K. A., Patel, S., and Ivanov, V. Practical secure aggregation for privacy-preserving machine learning. In *CCS*, 2017. URL <https://eprint.iacr.org/2017/281.pdf>.
- Seide, F., Fu, H., Droppo, J., Li, G., and Yu, D. 1-bit stochastic gradient descent and its application to data-parallel distributed training of speech dnns. In *Fifteenth Annual Conference of the International Speech Communication Association*, 2014.
- Sheller, M. J., Edwards, B., Reina, G. A., Martin, J., Pati, S., Kotrotsou, A., Milchenko, M., Xu, W., Marcus, D., Colen, R. R., and Bakas, S. Federated learning in medicine: facilitating multi-institutional collaborations without sharing patient data. *Scientific Reports*, 10(1):12598, Jul 2020. ISSN 2045-2322. doi: 10.1038/s41598-020-69250-1. URL <https://doi.org/10.1038/s41598-020-69250-1>.
- Shoeybi, M., Patwary, M., Puri, R., LeGresley, P., Casper, J., and Catanzaro, B. Megatron-lm: Training multi-billion parameter language models using gpu model parallelism. *arXiv preprint arXiv:1909.08053*, 2019.
- Stich, S. U. Local SGD converges fast and communicates little. *International Conference on Learning Representations (ICLR)*, pp. arXiv:1805.09767, 2019. URL <https://arxiv.org/abs/1805.09767>.
- Stich, S. U., Cordonnier, J.-B., and Jaggi, M. Sparsified sgd with memory. In *Proceedings of the 32nd International Conference on Neural Information Processing Systems*, pp. 4452–4463, 2018.
- Sukhov, A. M., Astrakhantseva, M., Pervitsky, A., Boldyrev, S., and Bukatov, A. Generating a function for network delay. *Journal of High Speed Networks*, 22(4):321–333, 2016.

- Sun, C., Shrivastava, A., Singh, S., and Gupta, A. Revisiting unreasonable effectiveness of data in deep learning era. In *ICCV*, 2017. URL <https://arxiv.org/abs/1707.02968>.
- Suresh, A. T., Felix, X. Y., Kumar, S., and McMahan, H. B. Distributed mean estimation with limited communication. In *International Conference on Machine Learning*, pp. 3329–3337. PMLR, 2017.
- Tsitsiklis, J. N. Problems in decentralized decision making and computation. Technical report, Massachusetts Inst of Tech Cambridge Lab for Information and Decision Systems, 1984.
- Uribe, C. A., Lee, S., Gasnikov, A., and Nedić, A. A dual approach for optimal algorithms in distributed optimization over networks. *Optimization Methods and Software*, pp. 1–40, 2020.
- Valiant, L. G. A bridging model for parallel computation. *Communications of the ACM*, 33(8):103–111, 1990.
- Verbraeken, J., Wolting, M., Katzy, J., Kloppenburg, J., Verbelen, T., and Rellermeyer, J. S. A survey on distributed machine learning. *ACM Comput. Surv.*, 53(2), March 2020. ISSN 0360-0300. doi: 10.1145/3377454. URL <https://doi.org/10.1145/3377454>.
- Wen, W., Xu, C., Yan, F., Wu, C., Wang, Y., Chen, Y., and Li, H. Terngrad: ternary gradients to reduce communication in distributed deep learning. In *Proceedings of the 31st International Conference on Neural Information Processing Systems*, pp. 1508–1518, 2017.
- Woodworth, B., Patel, K. K., and Srebro, N. Minibatch vs local sgd for heterogeneous distributed learning. *arXiv preprint arXiv:2006.04735*, 2020a.
- Woodworth, B., Patel, K. K., Stich, S., Dai, Z., Bullins, B., McMahan, B., Shamir, O., and Srebro, N. Is local sgd better than minibatch sgd? In *International Conference on Machine Learning*, pp. 10334–10343. PMLR, 2020b.
- Xiao, L. and Boyd, S. Fast linear iterations for distributed averaging. *Systems & Control Letters*, 53(1):65–78, 2004.
- Xu, J., Tian, Y., Sun, Y., and Scutari, G. Distributed algorithms for composite optimization: Unified and tight convergence analysis. *arXiv preprint arXiv:2002.11534*, 2020.
- Yan, F., Sundaram, S., Vishwanathan, S., and Qi, Y. Distributed autonomous online learning: Regrets and intrinsic privacy-preserving properties. *IEEE Transactions on Knowledge and Data Engineering*, 25(11):2483–2493, 2012.
- Yang, T., Andrew, G., Eichner, H., Sun, H., Li, W., Kong, N., Ramage, D., and Beaufays, F. Applied federated learning: Improving google keyboard query suggestions, 2018. URL <https://arxiv.org/abs/1812.02903>.
- You, Y., Li, J., Reddi, S., Hseu, J., Kumar, S., Bhojanapalli, S., Song, X., Demmel, J., Keutzer, K., and Hsieh, C.-J. Large batch optimization for deep learning: Training bert in 76 minutes. In *International Conference on Learning Representations*, 2020. URL <https://openreview.net/forum?id=Syx4wnEtvH>.
- Yuan, H. and Ma, T. Federated accelerated stochastic gradient descent. *Advances in Neural Information Processing Systems*, 33, 2020.
- Yuan, H., Zaheer, M., and Reddi, S. Federated composite optimization. *arXiv preprint arXiv:2011.08474*, 2020.
- Yuan, K., Ling, Q., and Yin, W. On the convergence of decentralized gradient descent. *SIAM Journal on Optimization*, 26(3):1835–1854, 2016.
- Zhao, S.-Y. and Li, W.-J. Fast asynchronous parallel stochastic gradient descent: A lock-free approach with convergence guarantee. In *Proceedings of the AAAI Conference on Artificial Intelligence*, volume 30, 2016.
- Zhu, Y., Kiros, R., Zemel, R., Salakhutdinov, R., Urtasun, R., Torralba, A., and Fidler, S. Aligning books and movies: Towards story-like visual explanations by watching movies and reading books. In *Proceedings of the IEEE international conference on computer vision*, pp. 19–27, 2015.
- Zinkevich, M., Weimer, M., Li, L., and Smola, A. Parallelized stochastic gradient descent. In Lafferty, J., Williams, C., Shawe-Taylor, J., Zemel, R., and Culotta, A. (eds.), *Advances in Neural Information Processing Systems*, volume 23, pp. 2595–2603. Curran Associates, Inc., 2010. URL <https://proceedings.neurips.cc/paper/2010/file/abea47ba24142ed16b7d8fbf2c740e0d-Paper.pdf>.

Supplementary Materials

A. GPU instance costs

This section provides a brief cost analysis of typical deep learning compute resources both in the cloud and on-premises. For brevity, we limit this analysis to the popular GPUs available at the time of submission. Note that the exact costs will depend on a variety of factors such as the cloud provider, the region, electricity costs, and market fluctuations. Therefore, we warn the reader to consider this analysis only as a rough estimate.

Specifically, we estimate the compute costs for the occasional usage scenario: running a single set of experiments over several weeks or conducting infrequent experiments. This scenario covers most research scientists and small organizations. The most straightforward way to provision a GPU server in such a scenario is to rent it from a cloud provider (e.g., GCP or AWS) or a public marketplace (e.g., Vast.ai or Golem).

While the exact server specifications vary from one provider to another, there are two broad categories of GPU machines: regular and preemptible. Regular instance types typically offer 1–8 GPUs per node with tight uptime guarantees (typically 99.99%) and a high-bandwidth network (tens of Gb/s). In turn, preemptible instances provide the same resource type at a significant discount with the condition that the machine can be terminated at any time after short notice.

To account for individual variations, we report the average rent price over three popular cloud providers. We consider three popular instance types: two high-end instances with 8 Tesla V100 or A100 GPUs and a low-end instance with a single Tesla T4 GPU. We also describe several low-end servers and workstations available on a public marketplace. Unlike cloud VMs, these instances are hosted on non-curated hardware with less uptime guarantees (typically 95% – 99.9%), slower network and significant variation in performance. However, marketplace instances are the cheapest in terms of cost per TFLOPS. To quantify this, we report the average over three most affordable instances that fit the chosen minimum requirements.

As a point of comparison, we also measure each system’s training performance for BERT-Large (Devlin et al., 2019) fine-tuning on SQuAD v1.1 (Rajpurkar et al., 2016) in PyTorch with mixed precision. We follow the official benchmarking protocol by NVIDIA and reuse the official performance results for V100, A100, and T4 instances. The only exception is GTX 1080Ti, where we use full 32-bit precision because that device does not support efficient half-precision operations.

GPU	Minimum system specifications			Average cost, \$/hour		BERT-Large training samples/s
	CPU cores	CPU type	RAM, GB	Regular	Preemptible	
Cloud instances						
8× V100	64	Intel Xeon Broadwell	480	23.47	7.13	354
8× A100	96	AMD Epyc ROME	960	30.65	10.18	755
1× T4	4	Intel Xeon Cascade Lake	16	0.46	0.18	18
Marketplace instances						
6× 3090	32	AMD Epyc Rome	480	5.04	4.17	154
4× 2080Ti	16	Intel Xeon Haswell	240	0.96	0.84	83.4
1× RTX 1080Ti	8	Intel Xeon Haswell	16	0.22	0.16	12

Table 1. Cloud and marketplace GPU instance pricing for short-term usage.

Table 1 shows two main tendencies. First, preemptible *cloud* instances are, on average, three times cheaper than their non-preemptible counterparts⁷. Second, the high-end HPC-grade servers that offer the highest raw performance are less cost-effective than lower-tier servers and marketplace instances. In theory, one could match the raw floating-point performance of a 8×V100 instance at a fraction of its cost using multiple lower-tier workstations, such as 4× RTX 2080Ti, with a smaller total cost. However, in practice, running distributed training with these workstations is challenging due to their unreliability and slow network connection.

Note that this analysis does not represent the cloud costs for sustained GPU usage. If an organization plans to constantly use

⁷The cost can be up to 11× cheaper for some instance types, e.g. Azure V100 instances in the central US region at the time of writing.

GPU resources over a period of multiple years, they can reduce the costs by deploying their own compute infrastructure or relying on the sustained usage discounts reaching up to 60–70%. Thus, the long-term compute costs are much harder to analyze and depend on a number of additional factors, such as local electricity prices for on-premise infrastructure. However, this scenario offers similar trade-offs: HPC-grade infrastructure offers greater interconnectivity, but requires expensive network interface cards, high-end switches and a more complex setup process.

B. Additional Related Work

In this section, we review some of the papers relevant to our work, but omitted from the main part due to space constraints.

B.1. Decentralized training

In this subsection, we give additional details about the dependence of gossip-based optimization methods on the spectral properties on the communication graph through the spectral properties of the mixing matrix (Xiao & Boyd, 2004; Scaman et al., 2019) or the Laplacian matrix (Merris, 1994; Uribe et al., 2020) of the network. That is, gossip finds approximate average on nodes with accuracy ε after $\mathcal{O}((1 - \lambda_2(\mathbf{M}))^{-1} \log(\varepsilon^{-1}))$ iterations, where \mathbf{M} is the mixing matrix and $\lambda_2(\mathbf{M})$ is the second largest eigenvalue of \mathbf{M} when sorted by absolute value. The quantity $\eta = 1 - \lambda_2(\mathbf{M})$ is called the spectral gap of the mixing matrix \mathbf{M} , and η^{-1} is typically a polynomial of the total number of nodes N when the maximal degree of the node is $\mathcal{O}(1)$. For example, for uniformly averaging \mathbf{M} one can show that $\eta^{-1} = \mathcal{O}(N^2)$ for the ring topology (node degree 2), $\eta^{-1} = \mathcal{O}(N)$ for the two-dimensional torus topology (node degree 2), and $\eta^{-1} = \mathcal{O}(1)$ for the fully connected graph (node degree $N - 1$); one can find more examples in Aldous & Fill (2002). Similarly, the communication complexity of decentralized optimization methods often has multiplicative dependence on either $\mathcal{O}(\eta^{-1})$ (see Xu et al., 2020 and references therein) or $\mathcal{O}(\eta^{-1/2})$ (Scaman et al., 2019; Uribe et al., 2020; Fallah et al., 2019; Kovalev et al., 2020b), which is not improvable for gossip-based methods (Arjevani & Shamir, 2015; Scaman et al., 2017).

Contrary to this, Moshpit All-Reduce does not depend on a fixed communication graph and the properties of its mixing matrix. However, it depends on the number of averaging groups and the total number of peers (see Theorem 3.2), which can be viewed as properties of a time-varying random communication graph. Fortunately, this dependence is often much better than in gossip: as we mentioned in the main part of the paper, even if workers are randomly split into pairs at each iteration, the simplified version of Moshpit All-Reduce makes the average distortion (the left-hand side of Equation 5) at least 2 times smaller after each round on average.

B.2. Compressed communication

Another popular approach to addressing the communication bottleneck is communication compression (Seide et al., 2014; Alistarh et al., 2017; Suresh et al., 2017): before sending any information (e.g., iterates, gradients, Hessians or more sophisticated data) over the network, peers compress this information by applying some (possibly random) transformation. As the result, peers send fewer bits for each communication round, but the total number of communication rounds needed to achieve the predefined accuracy of the solution increases. However, communication compression is very useful in the situations when the reduction in communication costs of one round is more important than the increase in the number of these rounds (Horvath et al., 2019).

There are two distinct groups of works on distributed training with compressed communication: ones that focus on unbiased compression operators (e.g., Rand-K, ℓ_p -quantization) and ones studying algorithms with biased compressors (e.g., Top-K); see a detailed summary of popular compression operators in Beznosikov et al. (2020). Quantized SGD (QSGD) (Alistarh et al., 2017) and TernGrad (Wen et al., 2017) were among the first compression methods with convergence guarantees. Next, the convergence analysis of these methods was generalized and tightened in the (strongly) convex case in Mishchenko et al. (2019). Moreover, Mishchenko et al. (2019) proposed a modification of QSGD called DIANA: this algorithm is based on the quantization of gradients’ differences, which helps it achieve linear convergence in the strongly convex case when peers compute full gradients. Next, DIANA was generalized to arbitrary unbiased compression in Horváth et al. (2019), where authors also developed and analyzed the variance-reduced version of DIANA. After that, several further modifications, such as Accelerated DIANA (Li et al., 2020) and DIANA with bidirectional compression (Gorbunov et al., 2020b; Philippenko & Dieuleveut, 2020), were proposed. Finally, we refer the reader to Li & Richtárik (2020); Haddadpour et al. (2020); Das et al. (2020) for state-of-the-art results for distributed methods with unbiased compression in the non-convex case.

However, naïve application of biased compression operators can lead to significantly worse performance in practice.

For instance, as it was shown recently in [Beznosikov et al. \(2020\)](#), parallel SGD with Top-1 compression can diverge exponentially fast. Therefore, biased compressors are used jointly with so-called error-compensation ([Seide et al., 2014](#)). The first analysis of Error-Compensated SGD (EC-SGD) was proposed in [Stich et al. \(2018\)](#); [Karimireddy et al. \(2019\)](#) which then was generalized and tightened in [Beznosikov et al. \(2020\)](#). Next, several further improvements, such as an accelerated version of EC-SGD ([Qian et al., 2020](#)) and linearly converging EC-SGD ([Gorbunov et al., 2020b](#)), were recently proposed. However, current theory does not show any superiority of distributed methods with biased compressors to the ones with unbiased compression operators. In addition, one can combine decentralized communication with compression. Such combinations with unbiased compression operators were studied in [Reisizadeh et al. \(2019\)](#); [Kovalev et al. \(2020a\)](#) and with biased operators in [Koloskova et al. \(2019; 2020a\)](#). In this paper, we do not study the interaction of different compression methods and Moshpit Averaging, leaving this promising direction to future work.

B.3. Multiple local steps

Alternatively, to reduce the impact of the communication bottleneck, it is possible to perform several local optimization steps on each peer between the communication rounds. This approach is based on the idea that the increased computational load of peers will decrease the number of communication rounds required to obtain the optimal parameters; it is frequently used in federated learning ([Konečný et al., 2016](#); [Kairouz et al., 2019](#)). In particular, one of the most popular methods with multiple local steps is called Local-SGD or Federated Averaging ([Konečný et al., 2016](#); [Stich, 2019](#)). The first results on its convergence were given in [Stich \(2019\)](#); [Lin et al. \(2020b\)](#), and later they were tightened and generalized both for homogeneous ([Khaled et al., 2020](#); [Woodworth et al., 2020b](#)) and heterogeneous cases ([Khaled et al., 2020](#); [Woodworth et al., 2020a](#)). Recently, further modifications of Local-SGD were proposed and analyzed: these modifications include acceleration ([Yuan & Ma, 2020](#)), variance reduction ([Gorbunov et al., 2020a](#)), communication compression ([Basu et al., 2019](#); [Haddadpour et al., 2020](#); [Das et al., 2020](#)), decentralization ([Li et al., 2019b](#); [Koloskova et al., 2020b](#)), adaptive and proximal methods ([Reddi et al., 2021](#); [Yuan et al., 2020](#)), and resistance to client drift ([Karimireddy et al., 2020](#)). Moshpit SGD can perform multiple local gradient steps before synchronization by design, as shown in Algorithm 2.

B.4. Asynchronous methods

In the previous subsections, we mostly discussed synchronous distributed methods, since they are more widespread and better studied than asynchronous ones. Mainly, this is because asynchronous methods are more difficult to implement, debug and analyze under general assumptions. However, such methods can be more efficient in terms of using computational resources, which leads to faster wall-clock convergence ([Assran et al., 2020](#)). In recent years, several asynchronous stochastic methods ([Recht et al., 2011](#); [Zhao & Li, 2016](#); [Leblond et al., 2017](#)), methods with no shared memory ([Peng et al., 2016](#); [Mishchenko et al., 2018](#)), and methods with delayed updates ([Agarwal & Duchi, 2011](#); [Feysmahdavian et al., 2016](#); [Arjevani et al., 2020](#); [Gorbunov et al., 2020b](#)) were proposed and analyzed. One can find more details in a recent survey of asynchronous distributed methods ([Assran et al., 2020](#)). Moshpit SGD belongs to this family of asynchronous approaches as well, because the averaging steps happen in smaller groups and can be interleaved with local parameter updates.

C. Proofs of Mixing Properties of Moshpit All-Reduce

Here we formally state the theorems about mixing properties of Moshpit Averaging along with their proofs.

Notation. Throughout the following sections, we use the standard notation from the literature on stochastic optimization. That is, for any n -dimensional vectors $x = (x_1, \dots, x_n)^\top, y = (y_1, \dots, y_n)^\top \in \mathbb{R}^n$ we use $\langle x, y \rangle$ to denote the standard inner product: $\langle x, y \rangle = x_1 y_1 + \dots + x_n y_n$. Next, we use $\|x\|$ to denote the ℓ_2 -norm of x ($\|x\| = \sqrt{\langle x, x \rangle}$), $\mathbb{E}[\xi]$ to denote an expectation of a random variable ξ , $\mathbb{E}[\xi \mid \eta]$ is used for the conditional expectation of ξ given η , and $\mathbb{P}\{E\}$ denotes the probability of an event E .

C.1. Computing exact average in a full grid

As discussed in Section 3.1, Moshpit All-Reduce obtains the exact average of parameter vectors from N peers arranged in a grid with d coordinates and M positions per coordinate when $N \equiv M^d$. That is, when the grid is full and each step averages M parameter values along a single grid coordinate without repetitions, the algorithm needs only d steps to compute the actual average across all nodes. In this section, we give a proof of this fact.

First, let us formally define the setting and the averaging steps of Moshpit All-Reduce in this specific case. Let $\theta_{i_1 i_2 \dots i_d}$ be

the parameter vector of the worker with coordinates i_1, i_2, \dots, i_d ; each coordinate i_k takes values from 1 to M , because the hypercube of peers is completely full (thus, due to the pigeonhole principle, there are no unoccupied coordinates). Next, arrange the coordinates of these vector according to the order of averaging iterations: namely, at iteration 1

$$\bar{\theta}_{i_1 i_2 \dots i_d}^1 = \frac{1}{M} \sum_{j_1=1}^M \theta_{j_1 i_2 \dots i_d}, \quad i_1 \in \{1, \dots, M\}, \quad (11)$$

which means that for the first iteration, we take the average across the first axis $\bar{\theta}^1$ and replicate it across all M resulting vectors regardless of their index i_1 . The next averaging steps can be expressed similarly with a simple recurrence relation:

$$\bar{\theta}_{i_1 i_2 \dots i_d}^t = \frac{1}{M} \sum_{j_t=1}^M \bar{\theta}_{i_1 \dots i_{t-1} j_t i_{t+1} \dots i_d}^{t-1}. \quad (12)$$

Given this formal definition, we can now state and prove the exact averaging result:

Theorem C.1 (Exact average in a full d -dimensional hypercube after d steps). *Assume that M^d peers are arranged in a d -dimensional hypercube with M positions in each dimension. Also, assume that each peer fully participates in every averaging step and M -sized groups for each averaging iteration are determined based on the hypercube coordinates. Then, if Moshpit All-Reduce is ran in the above setup for d iterations without repeating groups (i.e. averaging across each dimension exactly once), its result for each participant is the average value of θ across all M^d peers.*

Proof. We can directly obtain the expression for the average by expanding the recurrence and rearranging the sums:

$$\begin{aligned} \bar{\theta}_{i_1 i_2 \dots i_d}^d &= \frac{1}{M} \sum_{j_d=1}^M \bar{\theta}_{i_1 \dots i_{d-1} j_d}^{d-1} = \frac{1}{M} \sum_{j_d=1}^M \left(\frac{1}{M} \sum_{j_{d-1}=1}^M \bar{\theta}_{i_1 i_2 \dots j_{d-1} j_d}^{d-2} \right) = \dots \\ &= \frac{1}{M} \underbrace{\left(\sum_{j_d=1}^M \left(\frac{1}{M} \sum_{j_{d-1}=1}^M \dots \sum_{j_2=1}^M \left(\frac{1}{M} \sum_{j_1=1}^M \theta_{j_1 \dots j_d} \right) \right) \right)}_{d \text{ summations}} = \frac{1}{M^d} \sum_{j_d=1}^M \sum_{j_{d-1}=1}^M \dots \sum_{j_2=1}^M \sum_{j_1=1}^M \theta_{j_1 \dots j_d} = \\ &= \frac{1}{M^d} \sum_{j_1, \dots, j_d=1}^M \theta_{j_1 \dots j_d}. \end{aligned}$$

But this is exactly the global average of all θ , since there are M^d participants and each vector is represented in the sum because of summation over all possible indices. \square

Notice that for a given grid of peers, if some of its indices do not have corresponding parameter vectors, Equation (12) may result in different average vectors on different workers due to different numbers of peers along a coordinate for different indices. For example, running two iterations of Moshpit Averaging with $d = 2$, $M = 2$ and three parameter vectors θ_{11} , θ_{21} , θ_{22} results in $\frac{\theta_{11} + \theta_{21}}{2}$ on the first worker and $\frac{\theta_{11} + \theta_{21}}{4} + \theta_{22}$ on other workers, so neither of the values is equal to the global average. However, the variance of the averaged vectors does decrease, which is formally proven in Section C.3.

C.2. Proof of Theorem 3.1

Below we provide the complete proof of Theorem 3.1. For the readers' convenience, we restate the theorem.

Theorem C.2 (Theorem 3.1). *If all workers have non-zero probability of successfully running a communication round in Moshpit Averaging and the order of peers s_t is random, then all local vectors θ_i^t converge to the global average with probability 1:*

$$\forall i = 1, \dots, N \quad \left\| \theta_i^t - \frac{1}{N} \sum_{i=1}^N \theta_i^0 \right\|^2 \xrightarrow[t \rightarrow \infty]{} 0. \quad (13)$$

Proof of Theorem 3.1. First of all, we notice that (13) is equivalent to

$$\forall i = 1, \dots, N, \forall j = 1, \dots, n \quad \left(\theta_i^t(j) - \frac{1}{N} \sum_{i=1}^N \theta_i^0(j) \right)^2 \xrightarrow{t \rightarrow \infty} 0, \quad (14)$$

where $\theta_i^t(j)$ denotes j -th component of θ_i^t . Consider an arbitrary component $j \in \{1, \dots, n\}$ and the sequence of intervals $\{I_{j,t}\}_{t \geq 0}$ where $I_{j,t} = \text{conv}\{\theta_1^t(j), \theta_2^t(j), \dots, \theta_N^t(j)\}$. Then, $\{I_{j,t}\}_{t \geq 0}$ is a sequence of nested intervals ($I_{j,t+1} \subseteq I_{j,t} \forall t \geq 0$), since averaging in groups does not expand the convex hull of $\{\theta_1^t, \theta_2^t, \dots, \theta_N^t\}$. For convenience, we specify the bounds of the intervals: $I_{j,t} = [a_{j,t}, b_{j,t}]$. Using the Cantor's intersection theorem, we conclude that

$$\bigcap_{t=0}^{\infty} I_{j,t} = I_j = [a_j, b_j],$$

where $\bar{\theta}(j) = \frac{1}{N} \sum_{i=1}^N \theta_i^0(j) \in [a_j, b_j]$. If $[a_j, b_j] = \{\bar{\theta}(j)\}$ with probability 1, then (14) holds with probability 1 as well. Suppose the opposite: there exist such $j \in \{1, \dots, n\}$, $[a, b]$ and $\delta, \Delta > 0$ that $\bar{\theta}(j) \in [a, b]$, $b - a = \Delta$ and

$$\mathbb{P} \left\{ \underbrace{[a, b] \subseteq \bigcap_{t=0}^{\infty} I_{j,t}}_E \right\} = \delta > 0 \quad \text{and} \quad \forall \varepsilon > 0 \mathbb{P} \left\{ \underbrace{[a - \varepsilon, b + \varepsilon] \subseteq \bigcap_{t=0}^{\infty} I_{j,t}}_{E_\varepsilon} \right\} < \delta.$$

This implies that for all $\varepsilon > 0$ there exists such $T_\varepsilon > 0$ that

$$\mathbb{P} \left\{ \underbrace{\forall t \geq T_\varepsilon \quad a_{j,t} \in [a - \varepsilon, a], b_{j,t} \in [b, b + \varepsilon]}_{E'_\varepsilon} \right\} = \delta_\varepsilon > 0.$$

Consider $\varepsilon = \frac{\Delta}{(2N+100)^{2N}}$ and assume that the event E'_ε holds. Next, we introduce new notation: $J_{\text{left}}^t = \{i \in \{1, \dots, n\} \mid \theta_i^t(j) \in [a - \varepsilon, a]\}$ and $J_{\text{right}}^t = \{i \in \{1, \dots, n\} \mid \theta_i^t(j) \in [b, b + \varepsilon]\}$. Since E'_ε holds the sets J_{left}^t and J_{right}^t are non-empty for all $t \geq T_\varepsilon$ with probability $\delta_\varepsilon > 0$:

$$\mathbb{P} \left\{ \forall t \geq T_\varepsilon \quad J_{\text{left}}^t \neq \emptyset \text{ and } J_{\text{right}}^t \neq \emptyset \right\} = \delta_\varepsilon > 0. \quad (15)$$

We notice that every pair of workers i_1, i_2 has a non-zero probability of taking part in the averaging inside the common group at each iteration since all workers have a non-zero probability of successfully running a communication round and the order of peers_t is random. This implies that every pair of workers i_1, i_2 with probability 1 take part in the averaging inside the common group infinitely many times when t goes to the infinity.

Next, we choose some $t_0 \geq T_\varepsilon$. Let $J_{\text{left}}^{t_0} = \{i_{l,1}, \dots, i_{l,q_l}\}$ and $J_{\text{right}}^{t_0} = \{i_{r,1}, \dots, i_{r,q_r}\}$. Consider the event $E'_{\varepsilon,0} \subseteq E'_\varepsilon$ such that in $E'_{\varepsilon,0}$ peer $i_{l,1}$ computes an average in the group containing any peer from $J_{\text{right}}^{t_0}$ at some iteration $t_1 > t_0$. Our observations above imply that $\mathbb{P}\{E'_{\varepsilon,0}\} = \mathbb{P}\{E'_\varepsilon\} = \delta_\varepsilon > 0$. Then, $\theta_{i_{l,1}}^{t_1}(j) \geq \frac{N-1}{N}(a - \varepsilon) + \frac{1}{N}b = a - \varepsilon + \frac{1}{N}(\Delta + \varepsilon) = a - \frac{\Delta}{(2N+100)^{2N}} + \frac{1}{N} \left(\Delta + \frac{\Delta}{(2N+100)^{2N}} \right) > a + \frac{\Delta}{2N}$, i.e., $\theta_{i_{l,1}}^{t_1}(j) \in (a, b]$ meaning that $i_{l,1} \notin J_{\text{left}}^{t_1}$. The last part of the proof shows that for any $t \geq t_1$, the peer $i_{l,1}$ will never be the part of J_{left}^t and after a finite number of iterations $J_{\text{left}}^t = \emptyset$ with probability $\delta_\varepsilon > 0$ when $E'_{\varepsilon,0}$ holds, implying the contradiction with (15).

To show that, we consider the following set of peers: $\widehat{J}_{\text{left}}^{t_1} = \{i \in \{1, \dots, n\} \mid \exists t \geq t_1 : \theta_i^t(j) \in [a - \varepsilon, a + \frac{\Delta}{2N}]\}$. Next, we consider the event $E'_{\varepsilon,1} \subseteq E'_{\varepsilon,0}$ such that in $E'_{\varepsilon,1}$ peer $i_{l,1}$ computes an average in the group containing some peer $i_{l,avg,1}$ from $\widehat{J}_{\text{left}}^{t_1}$ at some iteration $t_2 > t_1$ (and t_2 is the first such moment after t_1). Again, our observations imply $\mathbb{P}\{E'_{\varepsilon,1}\} = \mathbb{P}\{E'_{\varepsilon,0}\} = \delta_\varepsilon > 0$. Then, $\theta_{i_{l,1}}^{t_2}(j) = \theta_{i_{l,avg,1}}^{t_2}(j) > \frac{N-1}{N}(a - \varepsilon) + \frac{1}{N} \left(a + \frac{\Delta}{2N} \right) = a + \frac{\Delta}{2N^2} - \frac{(N-1)\Delta}{N(2N+100)^{2N}} > a + \frac{\Delta}{4N^2}$. After that, we consider the event $E'_{\varepsilon,2} \subseteq E'_{\varepsilon,1}$ such that in $E'_{\varepsilon,2}$ peer $i_{l,1}$ or $i_{l,avg,1}$ computes an average in the group containing a peer $i_{l,avg,2} \neq i_{l,avg,1}$ from $\widehat{J}_{\text{left}}^{t_1}$ at an iteration $t_3 > t_2$ (and t_3 is the first such moment after t_2). Then, $\theta_{i_{l,1}}^{t_3}(j), \theta_{i_{l,avg,1}}^{t_3}(j)$ and $\theta_{i_{l,avg,2}}^{t_3}(j)$ are greater than $\frac{N-1}{N}(a - \varepsilon) + \frac{1}{N} \left(a + \frac{\Delta}{4N^2} \right) = a + \frac{\Delta}{4N^3} - \frac{(N-1)\Delta}{N(2N+100)^{2N}} > a + \frac{\Delta}{8N^3}$.

Therefore, after at least $N - 1$ of such averaging iterations, with probability δ_ε all $\theta_i^t(j)$ will be greater than $a + \frac{\Delta}{(2N)^N} > a$ while E'_ε holds. This contradicts (15). Therefore,

$$\bigcap_{t=0}^{\infty} I_{j,t} = \{\bar{\theta}(j)\}$$

with probability 1, which concludes the proof. \square

C.3. Proof of Theorem 3.2

In this section, we provide the complete proof of Theorem 3.2. For convenience, we restate the theorem below.

Theorem C.3 (Theorem 3.2, averaging convergence rate). *Consider the modification of Moshpit All-Reduce that works as follows: at each iteration $k \geq 1$) peers are randomly split into r disjoint groups of sizes M_1^k, \dots, M_r^k in such a way that $\sum_{i=1}^r M_i^k = N$ and $M_i^k \geq 1 \forall i = 1, \dots, r$ and 2) peers from each group compute their group average via All-Reduce. Let $\theta_1, \dots, \theta_N$ be the input vectors of this procedure and $\theta_1^T, \dots, \theta_N^T$ be the outputs after T iterations. Then,*

$$\mathbb{E} \left[\frac{1}{N} \sum_{i=1}^N \|\theta_i^T - \bar{\theta}\|^2 \right] = \left(\frac{r-1}{N} + \frac{r}{N^2} \right)^T \cdot \frac{1}{N} \sum_{i=1}^N \|\theta_i - \bar{\theta}\|^2, \quad (16)$$

where $\bar{\theta} = \frac{1}{N} \sum_{i=1}^N \theta_i$.

Proof. First of all, let us clarify the procedure of random splitting of peers in r groups. We assume that at iteration k of the modified algorithm we generate a random permutation $\pi^k = (\pi_1^k, \dots, \pi_N^k)$ of $1, \dots, N$. Next, $J_1^k = \{\pi_1^k, \dots, \pi_{M_1^k}^k\}$ form the indices of the first group of workers, $J_2^k = \{\pi_{M_1^k+1}^k, \dots, \pi_{M_1^k+M_2^k}^k\}$ are the indices of the second group, and $J_r^k = \{\pi_{M_1^k+M_2^k+\dots+M_{r-1}^k+1}^k, \dots, \pi_N^k\}$ are the indices of group r . In other words, we generate a random permutation and take contiguous subgroups of indices corresponding to predefined group sizes M_i^k , starting from the first group.

By definition, we have $\bigsqcup_{i=1}^r J_i^k = \{1, 2, \dots, N\}$, where \bigsqcup defines the disjoint union operator. Moreover, notice that group sizes M_1^k, \dots, M_r^k can depend on k and even be random: for our analysis, it is sufficient that the randomness defining the permutation is independent from M_1^k, \dots, M_r^k . Next, vectors $\theta_1^k, \dots, \theta_N^k$ are obtained by the following formula:

$$\forall j = 1, \dots, N, \quad \theta_j^k = \frac{1}{M_i^k} \sum_{t \in J_i^k} \theta_t^{k-1}, \quad \text{where } J_i^k \text{ is the group for which } j \in J_i^k.$$

Using this, we show that the average of vectors $\{\theta_i^k\}_{i=1}^N$ remains the same throughout the iterations of Moshpit All-Reduce:

$$\frac{1}{N} \sum_{j=1}^N \theta_j^k = \frac{1}{N} \sum_{i=1}^r M_i^k \cdot \frac{1}{M_i^k} \sum_{t \in J_i^k} \theta_t^{k-1} = \frac{1}{N} \sum_{i=1}^r \sum_{t \in J_i^k} \theta_t^{k-1} = \frac{1}{N} \sum_{j=1}^N \theta_j^{k-1}.$$

Therefore, the quantity $\frac{1}{N} \sum_{j=1}^N \|\theta_j^k - \bar{\theta}\|^2$ (average distortion) measures the quality of averaging. For this quantity, we can derive the following expression:

$$\begin{aligned} \frac{1}{N} \sum_{j=1}^N \|\theta_j^k - \bar{\theta}\|^2 &= \frac{1}{N} \sum_{i=1}^r M_i^k \left\| \frac{1}{M_i^k} \sum_{t \in J_i^k} \theta_t^{k-1} - \bar{\theta} \right\|^2 \\ &= \frac{1}{N} \sum_{i=1}^r \frac{1}{M_i^k} \left(\sum_{t \in J_i^k} \|\theta_t^{k-1} - \bar{\theta}\|^2 + 2 \sum_{t, l \in J_i^k, t < l} \langle \theta_t^{k-1} - \bar{\theta}, \theta_l^{k-1} - \bar{\theta} \rangle \right). \end{aligned}$$

Taking the expectation $\mathbb{E}_{\pi^k}[\cdot]$ with respect to the randomness coming from the choice of π^k we get

$$\mathbb{E}_{\pi^k} \left[\frac{1}{N} \sum_{j=1}^N \|\theta_j^k - \bar{\theta}\|^2 \right] = \frac{1}{N} \sum_{i=1}^r \frac{1}{M_i^k} \left(\mathbb{E}_{\pi^k} \left[\sum_{t \in J_i^k} \|\theta_t^{k-1} - \bar{\theta}\|^2 \right] + 2 \mathbb{E}_{\pi^k} \left[\sum_{t, l \in J_i^k, t < l} \langle \theta_t^{k-1} - \bar{\theta}, \theta_l^{k-1} - \bar{\theta} \rangle \right] \right).$$

Since $\forall j, j_1, j_2 \in \{1, \dots, N\}, j_1 \neq j_2$ and for all $i = 1, \dots, r$

$$\mathbb{P}\{j \in J_i^k\} = \frac{M_i^k}{N}, \quad \mathbb{P}\{j_1, j_2 \in J_i^k\} = \frac{M_i^k(M_i^k - 1)}{N^2},$$

we have

$$\begin{aligned} \mathbb{E}_{\pi^k} \left[\frac{1}{N} \sum_{j=1}^N \|\theta_j^k - \bar{\theta}\|^2 \right] &= \frac{1}{N} \sum_{i=1}^r \frac{1}{M_i^k} \left(\frac{M_i^k}{N} \sum_{j=1}^N \|\theta_j^{k-1} - \bar{\theta}\|^2 + 2 \frac{M_i^k(M_i^k - 1)}{N^2} \sum_{1 \leq j_1 < j_2 \leq N} \langle \theta_{j_1}^{k-1} - \bar{\theta}, \theta_{j_2}^{k-1} - \bar{\theta} \rangle \right) \\ &= \frac{r}{N^2} \sum_{j=1}^N \|\theta_j^{k-1} - \bar{\theta}\|^2 + 2 \frac{N-r}{N^3} \sum_{1 \leq j_1 < j_2 \leq N} \langle \theta_{j_1}^{k-1} - \bar{\theta}, \theta_{j_2}^{k-1} - \bar{\theta} \rangle \\ &= \left(\frac{r}{N^2} - \frac{N-r}{N^3} \right) \sum_{j=1}^N \|\theta_j^{k-1} - \bar{\theta}\|^2 \\ &\quad + \frac{N-r}{N^3} \left(\sum_{j=1}^N \|\theta_j^{k-1} - \bar{\theta}\|^2 + 2 \sum_{1 \leq j_1 < j_2 \leq N} \langle \theta_{j_1}^{k-1} - \bar{\theta}, \theta_{j_2}^{k-1} - \bar{\theta} \rangle \right) \\ &= \frac{N(r-1) + r}{N^3} \sum_{j=1}^N \|\theta_j^{k-1} - \bar{\theta}\|^2 + \frac{N-r}{N^3} \underbrace{\left\| \sum_{j=1}^N (\theta_j^{k-1} - \bar{\theta}) \right\|^2}_{\|N\bar{\theta} - N\bar{\theta}\|^2=0} \\ &= \left(\frac{r-1}{N} + \frac{r}{N^2} \right) \cdot \frac{1}{N} \sum_{j=1}^N \|\theta_j^{k-1} - \bar{\theta}\|^2. \end{aligned}$$

Finally, we take the full expectation from the both sides of the above equation and apply the tower property $\mathbb{E}[\mathbb{E}_{\pi^k}[\cdot]] = \mathbb{E}[\cdot]$:

$$\mathbb{E} \left[\frac{1}{N} \sum_{j=1}^N \|\theta_j^k - \bar{\theta}\|^2 \right] = \left(\frac{r-1}{N} + \frac{r}{N^2} \right) \mathbb{E} \left[\frac{1}{N} \sum_{j=1}^N \|\theta_j^{k-1} - \bar{\theta}\|^2 \right].$$

Unrolling the recurrence for $k = T$, we establish (16). \square

Remark C.1. Our analysis can be easily generalized to the case when number of groups r can depend on k and be a random variable independent from the choice of permutations and the number of groups at previous steps. In this case, (16) transforms into

$$\mathbb{E} \left[\frac{1}{N} \sum_{i=1}^N \|\theta_i^T - \bar{\theta}\|^2 \right] = \frac{1}{N} \sum_{i=1}^N \|\theta_i - \bar{\theta}\|^2 \cdot \prod_{k=1}^T \left(\frac{\mathbb{E}[r_k] - 1}{N} + \frac{\mathbb{E}[r_k]}{N^2} \right), \quad (17)$$

where r_k is the number of groups at iteration k .

C.4. Additional Guarantees For Moshpit Averaging

In this section, we derive the result measuring the rate of variance reduction when averaging random vectors with Algorithm 1. We start with the following technical lemma:

Lemma C.1. Let $\xi \sim \text{Binom}(M, p)$ have a binomial distribution with parameters M (number of trials) and p (probability of success for each trial). Then

$$m_1(M, p) := \mathbb{E} \left[\min \left\{ \frac{1}{\xi}, 1 \right\} \right] = (1-p)^M + \sum_{i=1}^M \frac{1}{i} \left((1-p)^{M-i} - (1-p)^M \right), \quad (18)$$

$$m_2(M, p) := \mathbb{E} \left[\min \left\{ \frac{1}{\xi^2}, 1 \right\} \right] = (1-p)^M + \sum_{i=1}^M \frac{1}{i} \left((1-p)^{M-i} - (1-p)^M \right) \sum_{j=i}^M \frac{1}{j}. \quad (19)$$

Proof. We start with the proof of (18). By definition of the expectation, we have

$$\mathbb{E} \left[\min \left\{ \frac{1}{\xi}, 1 \right\} \right] = (1-p)^M + \sum_{i=1}^M \frac{1}{i} p^i (1-p)^{M-i} \binom{M}{i}.$$

For simplicity of further derivations, we introduce the following notation: $m_1(M, p) = \mathbb{E} \left[\min \left\{ \frac{1}{\xi}, 1 \right\} \right]$ and $m_2(M, p) = \mathbb{E} \left[\min \left\{ \frac{1}{\xi^2}, 1 \right\} \right]$. Taking the derivative of $m_1(M, p)$ by p , we obtain

$$\begin{aligned} m_1'(M, p) &= -M(1-p)^{M-1} + \sum_{i=1}^M p^{i-1} (1-p)^{M-i} \binom{M}{i} - \sum_{i=1}^M \frac{M-i}{i} p^i (1-p)^{M-i-1} \binom{M}{i} \\ &= -M(1-p)^{M-1} + \frac{1}{p} \left(-(1-p)^M + \sum_{i=0}^M p^i (1-p)^{M-i} \binom{M}{i} \right) \\ &\quad - \frac{M}{1-p} \sum_{i=1}^M \frac{1}{i} p^i (1-p)^{M-i} \binom{M}{i} + \frac{1}{1-p} \left(-(1-p)^M + \sum_{i=0}^M p^i (1-p)^{M-i} \binom{M}{i} \right) \\ &= -M(1-p)^{M-1} + \frac{1}{p} (1 - (1-p)^M) - \frac{M}{1-p} (m_1(M, p) - (1-p)^M) + \frac{1}{1-p} (1 - (1-p)^M) \\ &= \frac{1}{p(1-p)} - \frac{(1-p)^{M-1}}{p} - \frac{M}{1-p} m_1(M, p). \end{aligned}$$

Rearranging the terms, we get the following linear first-order ODE

$$m_1'(M, p) + \frac{M}{1-p} m_1(M, p) = \frac{1}{p(1-p)} - \frac{(1-p)^{M-1}}{p}. \quad (20)$$

To solve it, we consider the following homogeneous ODE:

$$m_1'(M, p) + \frac{M}{1-p} m_1(M, p) = 0.$$

The solution of this ODE is $m_1(M, p) = C(1-p)^M$, where $C \in \mathbb{R}$ is an arbitrary real constant. Next, we go back to the initial ODE (20) and try to find a solution of the form $m_1(M, p) = C(p)(1-p)^M$, where $C(p) : \mathbb{R} \rightarrow \mathbb{R}$ is a differentiable function:

$$\begin{aligned} (C(p)(1-p)^M)' + \frac{M}{1-p} C(p)(1-p)^M &= \frac{1}{p(1-p)} - \frac{(1-p)^{M-1}}{p} \\ &\Downarrow \\ C'(p)(1-p)^M &= \frac{1}{p(1-p)} - \frac{(1-p)^{M-1}}{p} \\ &\Downarrow \\ C'(p) &= \frac{1}{p(1-p)^{M+1}} - \frac{1}{p(1-p)}. \end{aligned}$$

Since

$$\frac{1}{x(1-x)^{k+1}} = \frac{1}{x(1-x)^k} + \frac{1}{(1-x)^{k+1}} \quad (21)$$

for all $x \notin \{0, 1\}$ and all non-negative integers k , we have

$$\begin{aligned} C'(p) &= \frac{1}{p} + \frac{1}{1-p} + \frac{1}{(1-p)^2} + \dots + \frac{1}{(1-p)^{M+1}} - \frac{1}{p} - \frac{1}{1-p} \\ &\Downarrow \\ C'(p) &= \sum_{i=1}^M (1-p)^{-i-1}, \end{aligned}$$

hence

$$C(p) = \hat{C} + \sum_{i=1}^M \frac{1}{i} (1-p)^{-i},$$

where \hat{C} is a real constant. Putting all together, we obtain

$$m_1(M, p) = C(p)(1-p)^M = \hat{C}(1-p)^M + \sum_{i=1}^M \frac{1}{i} (1-p)^{M-i}.$$

Taking $m_1(M, 0) = 1$ into account, we conclude that $\hat{C} = 1 - \sum_{i=1}^M \frac{1}{i}$ and obtain (18).

Using a similar technique, we derive (19). By definition of the expectation, we have

$$m_2(M, p) = (1-p)^M + \sum_{i=1}^M \frac{1}{i^2} p^i (1-p)^{M-i} \binom{M}{i}.$$

Taking the derivative of $m_2(M, p)$ by p , we obtain

$$\begin{aligned} m_2'(M, p) &= -M(1-p)^{M-1} + \sum_{i=1}^M \frac{1}{i} p^{i-1} (1-p)^{M-i} \binom{M}{i} - \sum_{i=1}^M \frac{M-i}{i^2} p^i (1-p)^{M-i-1} \binom{M}{i} \\ &= -M(1-p)^{M-1} + \frac{1}{p} \sum_{i=1}^M \frac{1}{i} p^i (1-p)^{M-i} \binom{M}{i} \\ &\quad - \frac{M}{1-p} \sum_{i=1}^M \frac{1}{i^2} p^i (1-p)^{M-i} \binom{M}{i} + \frac{1}{1-p} \sum_{i=1}^M \frac{1}{i} p^i (1-p)^{M-i} \binom{M}{i} \\ &= -M(1-p)^{M-1} + \frac{1}{p} (m_1(M, p) - (1-p)^M) \\ &\quad + \frac{1}{1-p} (-Mm_2(M, p) + M(1-p)^M + m_1(M, p) - (1-p)^M) \\ &= \frac{m_1(M, p)}{p(1-p)} - \frac{(1-p)^{M-1}}{p} - \frac{M}{1-p} m_2(M, p). \end{aligned}$$

Rearranging the terms, we get the following linear first-order ODE

$$m_2'(M, p) + \frac{M}{1-p} m_2(M, p) = \frac{m_1(M, p)}{p(1-p)} - \frac{(1-p)^{M-1}}{p}. \quad (22)$$

To solve this ODE, we consider the homogeneous ODE:

$$m_2'(M, p) + \frac{M}{1-p} m_2(M, p) = 0.$$

The solution of this ODE is $m_2(M, p) = C(1-p)^M$, where $C \in \mathbb{R}$ is an arbitrary real constant. Next, we go back to the initial ODE (22) and try to find a solution of the form $m_2(M, p) = C(p)(1-p)^M$, where $C(p) : \mathbb{R} \rightarrow \mathbb{R}$ is a differentiable function:

$$\begin{aligned} (C(p)(1-p)^M)' + \frac{M}{1-p} C(p)(1-p)^M &= \frac{m_1(M, p)}{p(1-p)} - \frac{(1-p)^{M-1}}{p} \\ &\Downarrow \\ C'(p)(1-p)^M &= \frac{m_1(M, p)}{p(1-p)} - \frac{(1-p)^{M-1}}{p} \\ &\Downarrow \\ C'(p) &= \frac{m_1(M, p)}{p(1-p)^{M+1}} - \frac{1}{p(1-p)}. \end{aligned}$$

Using (21) and (18), we derive

$$\begin{aligned}
 C'(p) &\stackrel{(18)}{=} -\frac{\sum_{i=1}^M \frac{1}{i}}{p(1-p)} + \frac{\sum_{i=1}^M \frac{1}{i}(1-p)^{M-i}}{p(1-p)^{M+1}} \\
 &= -\sum_{i=1}^M \frac{1}{ip(1-p)} + \sum_{i=1}^M \frac{1}{ip(1-p)^{i+1}} \\
 &\stackrel{(21)}{=} -\sum_{i=1}^M \frac{1}{i} \left(\frac{1}{p} + \frac{1}{1-p} \right) + \sum_{i=1}^M \frac{1}{i} \left(\frac{1}{p} + \frac{1}{1-p} + \frac{1}{(1-p)^2} + \dots + \frac{1}{(1-p)^{i+1}} \right) \\
 &= \sum_{i=1}^M \frac{1}{i} \left(\frac{1}{(1-p)^2} + \dots + \frac{1}{(1-p)^{i+1}} \right) = \sum_{i=1}^M \frac{1}{(1-p)^{i+1}} \sum_{j=i}^M \frac{1}{j},
 \end{aligned}$$

hence

$$C(p) = \hat{C} + \sum_{i=1}^M \frac{1}{i} (1-p)^{-i} \sum_{j=i}^M \frac{1}{j},$$

where \hat{C} is a real constant. Putting all together, we obtain

$$m_2(M, p) = C(p)(1-p)^M = \hat{C}(1-p)^M + \sum_{i=1}^M \frac{1}{i} (1-p)^{M-i} \sum_{j=i}^M \frac{1}{j}.$$

Taking $m_2(M, 0) = 1$ into account, we conclude that $\hat{C} = 1 - \sum_{i=1}^M \frac{1}{i} \sum_{j=i}^M \frac{1}{j}$ and obtain (19). \square

Using this lemma, we derive the following result:

Theorem C.4. *Assume that peers participating in Moshpit Averaging have independent random vectors $\theta_1, \dots, \theta_N$ with means $\bar{\theta}_1, \dots, \bar{\theta}_N$ and variances bounded by σ^2 before the averaging. Let $\theta_1^T, \dots, \theta_N^T$ be the outputs of Moshpit Averaging after T iterations. Finally, we assume that each peer from the grid can be dropped out for the whole averaging process before averaging independently from other peers, i.e., $N \sim \text{Binom}(M^d, p)$. Then, for all $i = 1, \dots, N$ we have*

$$\mathbb{E} \left[\|\theta_i^T - \mathbb{E}_\theta [\theta_i^T]\|^2 \right] \leq M^{T-1} \sigma^2 m_1(M-1, p) (m_2(M-1, p))^{T-1}, \quad (23)$$

where functions $m_1(M, p)$ and $m_2(M, p)$ are defined in (18) and (19) respectively, and $\mathbb{E}_\theta [\cdot]$ denotes the expectation w.r.t. the randomness from $\theta_1, \dots, \theta_N$. Moreover, if $p \geq \frac{2}{3}$ and $M \geq 11$, then $m_1(M-1, p) \leq \frac{2}{M}$, $m_2(M-1, p) \leq \frac{3}{M^2}$ and

$$\mathbb{E} \left[\|\theta_i^T - \mathbb{E}_\theta [\theta_i^T]\|^2 \right] \leq \frac{2\sigma^2}{M(M/3)^{T-1}}. \quad (24)$$

Proof. First of all, we recall an equivalent formulation of Moshpit Averaging. Consider a hypercube $\{1, \dots, M\}^d$. One can consider the elements of this hypercube as hyperindices and assign a unique hyperindex to each peer so that peers can be viewed as vertices in the hypercube. Then, during the k -th iteration of Moshpit All-Reduce, each worker computes the average among those peers that have hyperindices with the same values except the k -th index; in other words, peers compute averages along the k -th dimension of the hypercube. Next, if $N = 0$, we assume that $\theta_i^T = \mathbb{E}_\theta [\theta_i^T]$ and (23) holds for free. Therefore, to derive (23), we assume that $N > 0$.

More formally, we use the following notation: $\theta_{C_i} = \theta_i$ for all $i = 1, \dots, N$, where $C_i = (c_1^i, c_2^i, \dots, c_d^i)$, $c_j^i \in \{1, \dots, M\}$ for all $j = 1, \dots, d$, and $C_i \neq C_k$ for $i \neq k$. Let \mathcal{C} be the set of hyperindices corresponding to all peers. Next, we use $\theta_{C_i}^t$ to define the vector stored on i -th peer after t iterations of Moshpit Averaging. Then, for all $i = 1, \dots, N$ we have $\theta_{C_i}^0 = \theta_{C_i}$ and for all $t = 1, \dots, d$

$$\theta_{C_i}^t = \frac{1}{b_{i,t}} \sum_{k \in J_{i,t}} \theta_{C_k}^{t-1},$$

where $J_{i,t} = \{k \in N \mid C_k = (c_1^k, \dots, c_d^k) \in \mathcal{C} \text{ and } c_j^k = c_j^i \forall j \neq t\}$ and $b_{i,t} = |J_{i,t}|$. Using this, we derive the following formula for $\theta_{C_i}^t$:

$$\theta_i^T \equiv \theta_{C_i}^T = \frac{1}{b_{i,T}} \sum_{i_1 \in J_{i,T}} \frac{1}{b_{i_1, T-1}} \sum_{i_2 \in J_{i_1, T-1}} \frac{1}{b_{i_2, T-2}} \sum_{i_3 \in J_{i_2, T-1}} \dots \frac{1}{b_{i_{T-1}, 1}} \sum_{i_T \in J_{i_{T-1}, 1}} \theta_{i_T}.$$

Taking the expectation w.r.t. $\theta_1, \dots, \theta_N$, we get

$$\mathbb{E}_\theta [\theta_i^T] = \frac{1}{b_{i,T}} \sum_{i_1 \in J_{i,T}} \frac{1}{b_{i_1, T-1}} \sum_{i_2 \in J_{i_1, T-1}} \frac{1}{b_{i_2, T-2}} \sum_{i_3 \in J_{i_2, T-1}} \dots \frac{1}{b_{i_{T-1}, 1}} \sum_{i_T \in J_{i_{T-1}, 1}} \bar{\theta}_{i_T}.$$

Using the independence of $\theta_1, \dots, \theta_N$, we derive

$$\begin{aligned} \mathbb{E}_\theta \left[\left\| \theta_i^T - \mathbb{E}_\theta [\theta_i^T] \right\|^2 \right] &= \mathbb{E}_\theta \left[\left\| \sum_{i_1 \in J_{i,T}} \sum_{i_2 \in J_{i_1, T-1}} \dots \sum_{i_T \in J_{i_{T-1}, 1}} \frac{\theta_{i_T} - \bar{\theta}_{i_T}}{b_{i,T} b_{i_1, T-1} \dots b_{i_{T-1}, 1}} \right\|^2 \right] \\ &= \sum_{i_1 \in J_{i,T}} \sum_{i_2 \in J_{i_1, T-1}} \dots \sum_{i_T \in J_{i_{T-1}, 1}} \frac{\mathbb{E}_\theta [\|\theta_{i_T} - \bar{\theta}_{i_T}\|^2]}{b_{i,T}^2 b_{i_1, T-1}^2 \dots b_{i_{T-1}, 1}^2} \\ &\leq \sum_{i_1 \in J_{i,T}} \sum_{i_2 \in J_{i_1, T-1}} \dots \sum_{i_T \in J_{i_{T-1}, 1}} \frac{\sigma^2}{b_{i,T}^2 b_{i_1, T-1}^2 \dots b_{i_{T-1}, 1}^2} \\ &= \sum_{i_1 \in J_{i,T}} \sum_{i_2 \in J_{i_1, T-1}} \dots \sum_{i_{T-1} \in J_{i_{T-2}, 2}} \frac{\sigma^2}{b_{i,T}^2 b_{i_1, T-1}^2 \dots b_{i_{T-2}, 2}^2 b_{i_{T-1}, 1}}. \end{aligned}$$

Next, taking the full expectation from the both sides of the previous inequality and using the tower property, we obtain

$$\mathbb{E} \left[\left\| \theta_i^T - \mathbb{E}_\theta [\theta_i^T] \right\|^2 \right] \leq \mathbb{E} \left[\sum_{i_1 \in J_{i,T}} \sum_{i_2 \in J_{i_1, T-1}} \dots \sum_{i_{T-1} \in J_{i_{T-2}, 2}} \frac{\sigma^2}{b_{i,T}^2 b_{i_1, T-1}^2 \dots b_{i_{T-2}, 2}^2 b_{i_{T-1}, 1}} \right]. \quad (25)$$

Notice that $J_{i_k, T-k} \cap J_{i_{k+1}, T-k-1} = \{i_{k+1}\}$ for all $k = 0, \dots, T-1$, where $i_0 = i$. Moreover, for $k_1, k_2 \in \{0, 1, \dots, T\}$, $k_1 < k_2$ either $J_{i_{k_1}, T-k_1} \cap J_{i_{k_2}, T-k_2} = \{k_2\}$ or $J_{i_{k_1}, T-k_1} \cap J_{i_{k_2}, T-k_2} = \emptyset$. The first situation is possible iff $i_{k_1} = i_{k_1+1} = \dots = i_{k_2-1}$.

Taking these observations about sets $J_{i_k, T-k}$ into account, we consider the sets $J'_{i_k, T-k} = J_{i_k, T-k} \setminus \{i_k\}$ for $k = 0, 1, \dots, T-1$. These sets are pairwise disjoint and their cardinalities $b'_{i_k, T-k} = |J'_{i_k, T-k}|$ satisfy the following relations: $b_{i_k, T-k} = 1 + b'_{i_k, T-k} \geq \max\{1, b'_{i_k, T-k}\} =: \hat{b}_{i_k, T-k}$ for $k = 1, 2, \dots, T-1$. Moreover, $b'_{i_1, T}, b'_{i_1, T-1}, \dots, b'_{i_{T-1}, 1}$ are independent random variables from the binomial distribution $\text{Binom}(M-1, p)$. Finally, we notice that the number of terms in (25) is upper-bounded by M^{T-1} , since $|J_{i,t}| \leq M$ for all $i = 1, \dots, N$ and $t = 0, \dots, T$.

Putting all together, we obtain

$$\begin{aligned} \mathbb{E} \left[\left\| \theta_i^T - \mathbb{E}_\theta [\theta_i^T] \right\|^2 \right] &\leq \mathbb{E} \left[\sum_{i_1 \in J_{i,T}} \sum_{i_2 \in J_{i_1, T-1}} \dots \sum_{i_{T-1} \in J_{i_{T-2}, 2}} \frac{\sigma^2}{\hat{b}_{i,T}^2 \hat{b}_{i_1, T-1}^2 \dots \hat{b}_{i_{T-2}, 2}^2 \hat{b}_{i_{T-1}, 1}} \right] \\ &\leq M^{T-1} \sigma^2 \mathbb{E} \left[\frac{1}{\hat{\xi}_1^2 \hat{\xi}_2^2 \dots \hat{\xi}_{T-1}^2 \hat{\xi}_T} \right] \\ &= M^{T-1} \sigma^2 \mathbb{E} \left[\frac{1}{\hat{\xi}_1^2} \right] \mathbb{E} \left[\frac{1}{\hat{\xi}_2^2} \right] \dots \mathbb{E} \left[\frac{1}{\hat{\xi}_{T-1}^2} \right] \mathbb{E} \left[\frac{1}{\hat{\xi}_T} \right], \end{aligned}$$

where $\hat{\xi}_k^2 = \max\{1, \xi_1^2\}$ for $k = 1, \dots, T$ and ξ_1, \dots, ξ_T are i.i.d. random variables having the binomial distribution $\text{Binom}(M-1, p)$. Then one can simplify the inequality above using Lemma C.1 and get

$$\mathbb{E} \left[\left\| \theta_i^T - \mathbb{E}_\theta [\theta_i^T] \right\|^2 \right] \leq M^{T-1} \sigma^2 m_1(M-1, p) (m_2(M-1, p))^{T-1},$$

where functions $m_1(M, p)$ and $m_2(M, p)$ are defined in (18) and (19) respectively.

Next, we simplify the obtained upper bound under the assumption that M and p are not too small; specifically, $M \geq 11$ and $p \geq 2/3$. From (18), we have

$$\begin{aligned} m_1(M-1, p) &= (1-p)^{M-1} + \sum_{i=1}^{M-1} \frac{1}{i} \left((1-p)^{M-1-i} - (1-p)^{M-1} \right) \\ &\leq (1-p)^{M-1} \sum_{i=1}^{M-1} \frac{1}{i(1-p)^i}. \end{aligned}$$

Since

$$\frac{1}{(k+1)(1-p)^{k+1}} \cdot \frac{k(1-p)^k}{1} = \frac{k}{(k+1)(1-p)} \xrightarrow{k \rightarrow \infty} \frac{1}{1-p} \geq 3,$$

we have

$$(1-p)^{M-1} \sum_{i=1}^{M-1} \frac{1}{i(1-p)^i} = \Theta \left((1-p)^M \cdot \frac{1}{M(1-p)^M} \right) = \Theta \left(\frac{1}{M} \right).$$

Using simple algebra, one can prove that for $M \geq 11$ and $p \geq 2/3$ the following inequality holds:

$$m_1(M-1, p) \leq (1-p)^{M-1} \sum_{i=1}^{M-1} \frac{1}{i(1-p)^i} \leq \frac{2}{M}.$$

Similarly, we analyze $m_2(M-1, p)$:

$$\begin{aligned} m_2(M-1, p) &= (1-p)^{M-1} + \sum_{i=1}^{M-1} \frac{1}{i} \left((1-p)^{M-1-i} - (1-p)^{M-1} \right) \sum_{j=i}^{M-1} \frac{1}{j} \\ &\leq (1-p)^{M-1} \sum_{i=1}^{M-1} \frac{1}{i(1-p)^i} \sum_{j=i}^{M-1} \frac{1}{j}. \end{aligned}$$

Since

$$\frac{\frac{1}{k(1-p)^k} \sum_{j=k}^{M-1} \frac{1}{j}}{\frac{1}{(k-1)(1-p)^{k-1}} \sum_{j=k-1}^{M-1} \frac{1}{j}} = \frac{(k-1) \sum_{j=k}^{M-1} \frac{1}{j}}{k(1-p) \left(\frac{1}{k-1} + \sum_{j=k}^{M-1} \frac{1}{j} \right)} \geq \frac{3(k-1) \cdot \frac{1}{k}}{k \left(\frac{1}{k-1} + \frac{1}{k} \right)} = \frac{3(k-1)^2}{k(2k-1)} \xrightarrow{k \rightarrow \infty} \frac{3}{2},$$

we have

$$(1-p)^{M-1} \sum_{i=1}^{M-1} \frac{1}{i(1-p)^i} \sum_{j=i}^{M-1} \frac{1}{j} = \Theta \left((1-p)^M \cdot \frac{1}{M^2(1-p)^M} \right) = \Theta \left(\frac{1}{M^2} \right).$$

Next, one can prove with simple algebra that for $M \geq 11$ and $p \geq 2/3$ the following inequality holds:

$$m_2(M-1, p) \leq (1-p)^{M-1} \sum_{i=1}^{M-1} \frac{1}{i(1-p)^i} \sum_{j=i}^{M-1} \frac{1}{j} \leq \frac{3}{M^2}.$$

Plugging the obtained upper bounds for $m_1(M-1, p)$ and $m_2(M-1, p)$ in (23), we obtain (24). □

D. Convergence Proofs of Moshpit SGD

In this section, we provide the complete statements of the theorems establishing the convergence of Moshpit SGD together with the full proofs. First, we introduce all necessary definitions, basic inequalities and auxiliary lemmas; then we prove the convergence in strongly convex and convex cases; lastly, we provide the proofs for the non-convex case.

D.1. Definitions, Basic Facts and Auxiliary Results

Below we provide several classical definitions and results which are used in our proofs.

D.1.1. STANDARD DEFINITIONS FROM OPTIMIZATION THEORY

Definition D.1 (*L-smoothness*). A function $f : \mathbb{R}^n \rightarrow \mathbb{R}$ is called *L-smooth* if for all $x, y \in \mathbb{R}^n$, the following inequality holds:

$$\|\nabla f(x) - \nabla f(y)\| \leq L\|x - y\|. \quad (26)$$

If the function f is *L-smooth*, then for all $x, y \in \mathbb{R}^n$

$$f(y) \leq f(x) + \langle \nabla f(x), y - x \rangle + \frac{L}{2}\|y - x\|^2. \quad (27)$$

Next, if f is additionally convex and x^* is its minimizer, then for all $x \in \mathbb{R}^d$

$$\|\nabla f(x)\|^2 \leq 2L(f(x) - f(x^*)). \quad (28)$$

Definition D.2 (*μ -strong convexity*). A differentiable function $f : \mathbb{R}^n \rightarrow \mathbb{R}$ is called *μ -strongly convex* if there exists a constant $\mu \geq 0$ such that for all $x, y \in \mathbb{R}^n$

$$f(y) \geq f(x) + \langle \nabla f(x), y - x \rangle + \frac{\mu}{2}\|y - x\|^2. \quad (29)$$

D.1.2. BASIC FACTS

For all $a, b, \theta_1, \dots, \theta_N \in \mathbb{R}^n$ and $\alpha > 0$, the following inequalities hold:

$$\|a + b\|^2 \leq 2\|a\|^2 + 2\|b\|^2, \quad (30)$$

$$\left\| \frac{1}{N} \sum_{i=1}^N \theta_i \right\|^2 \leq \frac{1}{N} \sum_{i=1}^N \|\theta_i\|^2, \quad (31)$$

$$\langle a, b \rangle \leq \frac{\|a\|^2}{2\alpha} + \frac{\alpha\|b\|^2}{2}. \quad (32)$$

D.1.3. PROPERTIES OF EXPECTATION

Variance decomposition. For a random vector $\eta \in \mathbb{R}^d$ and any deterministic vector $x \in \mathbb{R}^d$, the variance satisfies

$$\mathbb{E} \left[\|\eta - \mathbb{E}\eta\|^2 \right] = \mathbb{E} \left[\|\eta - x\|^2 \right] - \|\mathbb{E}\eta - x\|^2 \quad (33)$$

Tower property of expectation. For any random variables $\xi, \eta \in \mathbb{R}^d$ we have

$$\mathbb{E}[\xi] = \mathbb{E}[\mathbb{E}[\xi \mid \eta]] \quad (34)$$

under the assumption that $\mathbb{E}[\xi]$ and $\mathbb{E}[\mathbb{E}[\xi \mid \eta]]$ are well-defined.

D.1.4. AUXILIARY RESULTS

For the readers' convenience, we list all auxiliary results that we use in our proofs below. The first result is classical and establishes that the gradient descent step is a contractive operator.

Lemma D.1 (Lemma 6 from [Karimireddy et al., 2020](#)). For any *L-smooth* and *μ -strongly convex* function $f : \mathbb{R}^n \rightarrow \mathbb{R}$, points $x, y \in \mathbb{R}^n$, and stepsize $\gamma \in (0, 1/L]$, the following inequality holds:

$$\|x - \gamma \nabla f(x) - y + \gamma \nabla f(y)\|^2 \leq (1 - \gamma\mu)\|x - y\|^2. \quad (35)$$

The next two lemmas are useful for analyzing typical recurrences appearing in the convergence analysis.

Lemma D.2 (Lemma I.2 from Gorbunov et al., 2020a). *Let $\{r_k\}_{k \geq 0}$ satisfy*

$$r_K \leq \frac{a}{\gamma W_K} + c_1 \gamma + c_2 \gamma^2$$

for all $K \geq 0$ with some constants $a, c_2 \geq 0, c_1 \geq 0$, where $w_k = (1 - \gamma\mu(1 - \delta_{pv,1}))^{-(k+1)}$, $W_K = \sum_{k=0}^K w_k$, $\mu > 0$, $\delta_{pv,1} \in [0, 1)$ and $\gamma \leq \gamma_0$ for some $\gamma_0 > 0$, $\gamma_0 \leq 1/\mu(1 - \delta_{pv,1})$. Then, for all K such that

$$\begin{aligned} & \text{either } \frac{\ln(\max\{2, \min\{a\mu^2(1 - \delta_{pv,1})^2 K^2/c_1, a\mu^3(1 - \delta_{pv,1})^3 K^3/c_2\}\})}{K} \leq 1 \\ & \text{or } \gamma_0 \leq \frac{\ln(\max\{2, \min\{a\mu^2(1 - \delta_{pv,1})^2 K^2/c_1, a\mu^3(1 - \delta_{pv,1})^3 K^3/c_2\}\})}{(1 - \delta_{pv,1})\mu K} \end{aligned}$$

and

$$\gamma = \min \left\{ \gamma_0, \frac{\ln(\max\{2, \min\{a\mu^2(1 - \delta_{pv,1})^2 K^2/c_1, a\mu^3(1 - \delta_{pv,1})^3 K^3/c_2\}\})}{(1 - \delta_{pv,1})\mu K} \right\}$$

we have that

$$r_K = \tilde{\mathcal{O}} \left(\frac{a}{\gamma_0} \exp(-\gamma_0 \mu (1 - \delta_{pv,1}) K) + \frac{c_1}{(1 - \delta_{pv,1})\mu K} + \frac{c_2}{(1 - \delta_{pv,1})^2 \mu^2 K^2} \right).$$

Lemma D.3 (Lemma I.3 from Gorbunov et al., 2020a). *Let $\{r_k\}_{k \geq 0}$ satisfy*

$$r_K \leq \frac{a}{\gamma K} + c_1 \gamma + c_2 \gamma^2$$

for all $K \geq 0$ with some constants $a, c_2 \geq 0, c_1 \geq 0$ where $\gamma \leq \gamma_0$ for some $\gamma_0 > 0$. Then for all K and

$$\gamma = \min \left\{ \gamma_0, \sqrt{\frac{a}{c_1 K}}, \sqrt[3]{\frac{a}{c_2 K}} \right\}$$

we have that

$$r_K = \mathcal{O} \left(\frac{a}{\gamma_0 K} + \sqrt{\frac{ac_1}{K}} + \frac{\sqrt[3]{a^2 c_2}}{K^{2/3}} \right).$$

Finally, the lemma below is useful for our convergence analysis in the non-convex case.

Lemma D.4 (Lemma I.1 from Gorbunov et al., 2020a). *For any τ random vectors $\xi_1, \dots, \xi_\tau \in \mathbb{R}^d$ such that $\forall t = 2, \dots, \tau$ the random vector ξ_t depends on ξ_1, \dots, ξ_{t-1} and does not depend on $\xi_{t+1}, \dots, \xi_\tau$ the following inequality holds*

$$\mathbb{E} \left[\left\| \sum_{t=1}^{\tau} \xi_t \right\|^2 \right] \leq e\tau \sum_{t=1}^{\tau} \mathbb{E} \left[\|\mathbb{E}_t[\xi_t]\|^2 \right] + e \sum_{t=1}^{\tau} \mathbb{E} \left[\|\xi_t - \mathbb{E}_t[\xi_t]\|^2 \right], \quad (36)$$

where $\mathbb{E}_t[\cdot]$ denotes the conditional expectation $\mathbb{E}[\cdot \mid \xi_{t-1}, \dots, \xi_1]$.

D.2. Convex Case

In this section, we give the full proof of Theorem 3.3 about the convergence of Moshpit SGD for convex and strongly convex problems. The scheme of the proof follows the similar steps as in the state-of-the-art analysis of Local-SGD (Khaled et al., 2020; Woodworth et al., 2020b; Gorbunov et al., 2020a). We start with the following lemma:

Lemma D.5. *Let $f_1 = \dots = f_N = f$, function f be μ -strongly convex (Def. D.2) and L -smooth (see Def. D.1), and Assumptions 3.1 and 3.2 hold with $\Delta_{pv}^k = \delta_{pv,1} \gamma \mu \mathbb{E}[\|\theta^k - \theta^*\|^2] + \gamma^2 \delta_{pv,2}^2$ and $\tilde{\theta} = \theta^*$, where $\theta^* \in \operatorname{argmin}_{\theta \in \mathbb{R}^n} f(\theta)$ and $\delta_{pv,1} \in [0, 1)$, $\delta_{pv,2} \geq 0$. Then, for any $k \geq 0$ the iterates produced by Moshpit SGD with $\gamma \leq 1/4L$ satisfy*

$$\begin{aligned} \gamma \mathbb{E} [f(\theta^k) - f(\theta^*)] & \leq (1 - \gamma\mu(1 - \delta_{pv,1})) \mathbb{E} [\|\theta^k - \theta^*\|^2] - \mathbb{E} [\|\theta^{k+1} - \theta^*\|^2] \\ & \quad + \frac{3L\gamma}{2} \mathbb{E}[V_k] + \gamma^2 \left(\frac{\sigma^2}{N_{\min}} + \delta_{pv,2}^2 \right), \end{aligned} \quad (37)$$

where $V_k = \frac{1}{N_k} \sum_{i \in P_k} \|\theta_i^k - \theta^k\|^2$ and $\theta^k = \frac{1}{N_k} \sum_{i \in P_k} \theta_i^k$.

Proof. Recall that Assumption 3.2 with $\Delta_{pv}^k = \delta_{pv,1}\gamma\mu\mathbb{E}[\|\theta^k - \theta^*\|^2] + \gamma^2\delta_{pv,2}^2$ and $\tilde{\theta} = \theta^*$ states

$$\mathbb{E} \left[\langle \theta^{k+1} - \hat{\theta}^{k+1}, \theta^{k+1} + \hat{\theta}^{k+1} - 2\theta^* \rangle \right] \leq \delta_{pv,1}\gamma\mu\mathbb{E}[\|\theta^k - \theta^*\|^2] + \gamma^2\delta_{pv,2}^2, \quad (38)$$

where $\hat{\theta}^{k+1} = \frac{1}{N_k} \sum_{i \in P_k} (\theta_i^k - \gamma g_i^k)$. Next, the definition of $\hat{\theta}^{k+1}$ implies

$$\hat{\theta}^{k+1} = \frac{1}{N_k} \sum_{i \in P_k} \theta_i^k - \frac{\gamma}{N_k} \sum_{i \in P_k} g_i^k = \theta^k - \gamma g^k,$$

where $g^k = \frac{1}{N_k} \sum_{i \in P_k} g_i^k$. Using this, we derive

$$\begin{aligned} \|\theta^{k+1} - \theta^*\|^2 &= \|\hat{\theta}^{k+1} - \theta^*\|^2 + 2\langle \theta^{k+1} - \hat{\theta}^{k+1}, \hat{\theta}^{k+1} - \theta^* \rangle + \|\theta^{k+1} - \hat{\theta}^{k+1}\|^2 \\ &= \|\theta^k - \theta^* - \gamma g^k\|^2 + \langle \theta^{k+1} - \hat{\theta}^{k+1}, \theta^{k+1} + \hat{\theta}^{k+1} - 2\theta^* \rangle \\ &= \|\theta^k - \theta^*\|^2 - 2\gamma\langle \theta^k - \theta^*, g^k \rangle + \gamma^2\|g^k\|^2 + \langle \theta^{k+1} - \hat{\theta}^{k+1}, \theta^{k+1} + \hat{\theta}^{k+1} - 2\theta^* \rangle. \end{aligned}$$

Taking the conditional expectation $\mathbb{E}[\cdot | \theta^k] := \mathbb{E}[\cdot | P_k, \theta_i^k, i \in P_k]$ from the both sides of the previous equation and using Assumption 3.1, we obtain

$$\begin{aligned} \mathbb{E}[\|\theta^{k+1} - \theta^*\|^2 | \theta^k] &= \|\theta^k - \theta^*\|^2 - 2\gamma \left\langle \theta^k - \theta^*, \frac{1}{N_k} \sum_{i \in P_k} \nabla f(\theta_i^k) \right\rangle + \gamma^2 \mathbb{E} \left[\left\| \frac{1}{N_k} \sum_{i \in P_k} g_i^k \right\|^2 \middle| \theta^k \right] \\ &\quad + \mathbb{E} \left[\langle \theta^{k+1} - \hat{\theta}^{k+1}, \theta^{k+1} + \hat{\theta}^{k+1} - 2\theta^* \rangle \middle| \theta^k \right]. \end{aligned} \quad (39)$$

Next, we estimate the second and the third terms in the right-hand side of (39). First,

$$\begin{aligned} -2\gamma \left\langle \theta^k - \theta^*, \frac{1}{N_k} \sum_{i \in P_k} \nabla f(\theta_i^k) \right\rangle &= \frac{2\gamma}{N_k} \sum_{i \in P_k} (\langle \theta^* - \theta_i^k, \nabla f(\theta_i^k) \rangle + \langle \theta_i^k - \theta^k, \nabla f(\theta_i^k) \rangle) \\ &\stackrel{(29),(27)}{\leq} \frac{2\gamma}{N_k} \sum_{i \in P_k} \left(f(\theta^*) - f(\theta_i^k) - \frac{\mu}{2} \|\theta_i^k - \theta^*\|^2 \right) \\ &\quad + \frac{2\gamma}{N_k} \sum_{i \in P_k} \left(f(\theta_i^k) - f(\theta^k) + \frac{L}{2} \|\theta_i^k - \theta^k\|^2 \right) \\ &\stackrel{(31)}{\leq} 2\gamma (f(\theta^*) - f(\theta^k)) - \gamma\mu\|\theta^k - \theta^*\|^2 + L\gamma V_k, \end{aligned} \quad (40)$$

where $V_k = \frac{1}{N_k} \sum_{i \in P_k} \|\theta_i^k - \theta^k\|^2$. Secondly, since stochastic gradients $\{g_i^k\}_{i \in P_k}$ are computed independently, we get

$$\begin{aligned} \gamma^2 \mathbb{E} \left[\left\| \frac{1}{N_k} \sum_{i \in P_k} g_i^k \right\|^2 \middle| \theta^k \right] &\stackrel{(33)}{=} \gamma^2 \left\| \frac{1}{N_k} \sum_{i \in P_k} \nabla f(\theta_i^k) \right\|^2 + \gamma^2 \mathbb{E} \left[\left\| \frac{1}{N_k} \sum_{i \in P_k} (g_i^k - \nabla f(\theta_i^k)) \right\|^2 \middle| \theta^k \right] \\ &\stackrel{(31)}{\leq} 2\gamma^2 \left\| \frac{1}{N_k} \sum_{i \in P_k} (\nabla f(\theta_i^k) - \nabla f(\theta^k)) \right\|^2 + 2\gamma^2 \|\nabla f(\theta^k)\|^2 \\ &\quad + \frac{\gamma^2}{N_k^2} \sum_{i \in P_k} \mathbb{E} [\|g_i^k - \nabla f(\theta_i^k)\|^2 | \theta^k] \\ &\stackrel{(31),(28),(7)}{\leq} \frac{2\gamma^2}{N_k} \sum_{i \in P_k} \|\nabla f(\theta_i^k) - \nabla f(\theta^k)\|^2 + 4L\gamma^2 (f(\theta^k) - f(\theta^*)) + \frac{\gamma^2\sigma^2}{N_k} \\ &\stackrel{(26)}{\leq} \underbrace{\frac{2L^2\gamma^2}{N_k} \sum_{i \in P_k} \|\theta_i^k - \theta^k\|^2}_{2L^2\gamma^2 V_k} + 4L\gamma^2 (f(\theta^k) - f(\theta^*)) + \frac{\gamma^2\sigma^2}{N_{\min}}. \end{aligned} \quad (41)$$

Plugging (40) and (41) in (39), we obtain

$$\begin{aligned} \mathbb{E} [\|\theta^{k+1} - \theta^*\|^2 \mid \theta^k] &\leq (1 - \gamma\mu)\|\theta^k - \theta^*\|^2 - 2\gamma(1 - 2L\gamma)(f(\theta^k) - f(\theta^*)) + L\gamma(1 + 2L\gamma)V_k + \frac{\gamma^2\sigma^2}{N_{\min}} \\ &\quad + \mathbb{E} [\langle \theta^{k+1} - \widehat{\theta}^{k+1}, \theta^{k+1} + \widehat{\theta}^{k+1} - 2\theta^* \rangle \mid \theta^k], \end{aligned}$$

and

$$\begin{aligned} \mathbb{E} [\|\theta^{k+1} - \theta^*\|^2] &\stackrel{(38)}{\leq} (1 - \gamma\mu(1 - \delta_{pv,1}))\mathbb{E} [\|\theta^k - \theta^*\|^2] - 2\gamma(1 - 2L\gamma)\mathbb{E} [f(\theta^k) - f(\theta^*)] \\ &\quad + L\gamma(1 + 2L\gamma)\mathbb{E}[V_k] + \gamma^2 \left(\frac{\sigma^2}{N_{\min}} + \delta_{pv,2}^2 \right) \\ &\leq (1 - \gamma\mu(1 - \delta_{pv,1}))\mathbb{E} [\|\theta^k - \theta^*\|^2] - \gamma\mathbb{E} [f(\theta^k) - f(\theta^*)] \\ &\quad + \frac{3L\gamma}{2}\mathbb{E}[V_k] + \gamma^2 \left(\frac{\sigma^2}{N_{\min}} + \delta_{pv,2}^2 \right), \end{aligned}$$

where in the last inequality we use $\gamma \leq 1/4L$. \square

Next, we estimate the term $\mathbb{E}[V_k]$ measuring the expected dissimilarity between local iterates and their global average at iteration k .

Lemma D.6. *Let $f_1 = \dots = f_N = f$, function f be μ -strongly convex (Def. D.2) and L -smooth (see Def. D.1), and Assumptions 3.1 and 3.2 hold with $\Delta_{pv}^k = \delta_{pv,1}\gamma\mu\mathbb{E}[\|\theta^k - \theta^*\|^2] + \gamma^2\delta_{pv,2}^2$ and $\widetilde{\theta} = \theta^*$, where $\theta^* \in \operatorname{argmin}_{\theta \in \mathbb{R}^n} f(\theta)$ and $\delta_{pv,1} \in [0, 1)$, $\delta_{pv,2} \geq 0$. Then, for any $k \geq 0$ the iterates produced by Moshpit SGD with $\gamma \leq 1/4L$ satisfy*

$$\mathbb{E}[V_k] \leq 2\gamma^2 (4\delta_{aq}^2 + (\tau - 1)\sigma^2), \quad (42)$$

where $V_k = \frac{1}{N_k} \sum_{i \in P_k} \|\theta_i^k - \theta^k\|^2$ and $\theta^k = \frac{1}{N_k} \sum_{i \in P_k} \theta_i^k$.

Proof. First of all, if $k = a\tau$ for some integer $a \geq 0$, then (42) follows from Assumption 3.2 (eq. (10)). Therefore, we consider such k that $k = a\tau + t'$ for some $t' \in (0, \tau)$. Then, for any $i, j \in P_k$, $i \neq j$

$$\begin{aligned} \mathbb{E} [\|\theta_i^k - \theta_j^k\|^2 \mid \theta^{k-1}] &= \mathbb{E} [\|\theta_i^{k-1} - \gamma g_i^{k-1} - \theta_j^{k-1} + \gamma g_j^{k-1}\|^2 \mid \theta^{k-1}] \\ &\stackrel{(33)}{=} \mathbb{E} [\|\theta_i^{k-1} - \gamma \nabla f(\theta_i^{k-1}) - \theta_j^{k-1} + \gamma \nabla f(\theta_j^{k-1})\|^2 \\ &\quad + \gamma^2 \mathbb{E} [\|g_i^{k-1} - \nabla f(\theta_i^{k-1}) + g_j^{k-1} - \nabla f(\theta_j^{k-1})\|^2 \mid \theta^{k-1}]]. \end{aligned}$$

Using Lemma D.1 and independence of g_i^{k-1} and g_j^{k-1} for given $\theta_i^{k-1}, \theta_j^{k-1}$, $i \neq j$ we derive

$$\begin{aligned} \mathbb{E} [\|\theta_i^k - \theta_j^k\|^2 \mid \theta^{k-1}] &\stackrel{(35)}{\leq} (1 - \gamma\mu)\|\theta_i^{k-1} - \theta_j^{k-1}\|^2 + \gamma^2 \mathbb{E} [\|g_i^{k-1} - \nabla f(\theta_i^{k-1})\|^2 \mid \theta^{k-1}] \\ &\quad + \gamma^2 \mathbb{E} [\|g_j^{k-1} - \nabla f(\theta_j^{k-1})\|^2 \mid \theta^{k-1}] \\ &\stackrel{(7)}{\leq} (1 - \gamma\mu)\|\theta_i^{k-1} - \theta_j^{k-1}\|^2 + 2\gamma^2\sigma^2, \end{aligned}$$

from which we get the following:

$$\mathbb{E}_g [\|\theta_i^k - \theta_j^k\|^2] \leq (1 - \gamma\mu)\mathbb{E}_g [\|\theta_i^{k-1} - \theta_j^{k-1}\|^2] + 2\gamma^2\sigma^2 \leq \mathbb{E}_g [\|\theta_i^{k-1} - \theta_j^{k-1}\|^2] + 2\gamma^2\sigma^2.$$

Here, $\mathbb{E}_g[\cdot]$ denotes the expectation conditioned on $\{P_k\}_{k=a\tau}^{(a+1)\tau-1}$. Unrolling the recurrence, we get

$$\mathbb{E}_g [\|\theta_i^k - \theta_j^k\|^2] \leq \mathbb{E}_g [\|\theta_i^{a\tau} - \theta_j^{a\tau}\|^2] + 2(k - a\tau)\gamma^2\sigma^2 \leq \mathbb{E}_g [\|\theta_i^{a\tau} - \theta_j^{a\tau}\|^2] + 2(\tau - 1)\gamma^2\sigma^2. \quad (43)$$

Using this, we estimate $\mathbb{E}_g[V_k]$:

$$\begin{aligned}
 \mathbb{E}_g[V_k] &= \frac{1}{N_k} \sum_{i \in P_k} \mathbb{E}_g \left[\left\| \theta_i^k - \frac{1}{N_k} \sum_{j \in P_k} \theta_j^k \right\|^2 \right] \stackrel{(31)}{\leq} \frac{1}{N_k} \sum_{i,j \in P_k} \mathbb{E}_g [\|\theta_i^k - \theta_j^k\|^2] \\
 &\stackrel{(43)}{\leq} \frac{1}{N_k^2} \sum_{i,j \in P_k} \mathbb{E}_g [\|\theta_i^{a\tau} - \theta_j^{a\tau}\|^2] + 2(\tau-1)\gamma^2\sigma^2 \\
 &\stackrel{(30)}{\leq} \frac{2}{N_k^2} \sum_{i,j \in P_k} (\mathbb{E}_g [\|\theta_i^{a\tau} - \theta^{a\tau}\|^2] + \mathbb{E}_g [\|\theta_j^{a\tau} - \theta^{a\tau}\|^2]) + 2(\tau-1)\gamma^2\sigma^2 \\
 &= \frac{4}{N_k} \sum_{i \in P_k} \mathbb{E}_g [\|\theta_i^{a\tau} - \theta^{a\tau}\|^2] + 2(\tau-1)\gamma^2\sigma^2 \\
 &\leq \frac{4}{N_{a\tau}} \cdot \frac{N_{a\tau}}{N_k} \sum_{i \in P_{a\tau}} \mathbb{E}_g [\|\theta_i^{a\tau} - \theta^{a\tau}\|^2] + 2(\tau-1)\gamma^2\sigma^2 \\
 &\leq \mathbb{E}_g \left[\frac{8}{N_{a\tau}} \sum_{i \in P_{a\tau}} \|\theta_i^{a\tau} - \theta^{a\tau}\|^2 \right] + 2(\tau-1)\gamma^2\sigma^2,
 \end{aligned}$$

where in the last inequality we use $2N_{(a+1)\tau} = 2|P_{(a+1)\tau}| \geq |P_{a\tau}| = N_{a\tau}$ and $|N_k| \leq |N_{k-1}|$ following from Assumption 3.2. Finally, we take the full expectation from the previous inequality and derive

$$\mathbb{E}[V_k] \stackrel{(34)}{\leq} 8\mathbb{E} \left[\frac{1}{N_{a\tau}} \sum_{i \in P_{a\tau}} \|\theta_i^{a\tau} - \theta^{a\tau}\|^2 \right] + 2(\tau-1)\gamma^2\sigma^2 \stackrel{(10)}{\leq} 2\gamma^2 (4\delta_{aq}^2 + (\tau-1)\sigma^2),$$

which finishes the proof. \square

Combining Lemmas D.5 and D.6, we get the following result:

Theorem D.1 (Theorem 3.3, convergence in the convex case). *Let $f_1 = \dots = f_N = f$ be μ -strongly convex (Def. D.2) and L -smooth (see Def. D.1), and Assumptions 3.1 and 3.2 hold with $\Delta_{pv}^k = \delta_{pv,1}\gamma\mu\mathbb{E}[\|\theta^k - \theta^*\|^2] + \gamma^2\delta_{pv,2}^2$ and $\theta = \theta^*$, where $\theta^* \in \operatorname{argmin}_{\theta \in \mathbb{R}^n} f(\theta)$ and $\delta_{pv,1} \in [0, 1)$, $\delta_{pv,2} \geq 0$. Then, for any $K \geq 0$, the iterates produced by Moshpit SGD with $\gamma \leq 1/4L$ satisfy*

$$\mathbb{E} [f(\bar{\theta}^K) - f(\theta^*)] \leq (1 - \gamma\mu(1 - \delta_{pv,1}))^K \frac{R_0^2}{\gamma} + \gamma \left(\frac{\sigma^2}{N_{\min}} + \delta_{pv,2}^2 + 3L\gamma (4\delta_{aq}^2 + (\tau-1)\sigma^2) \right), \quad (44)$$

when $\mu > 0$, and

$$\mathbb{E} [f(\bar{\theta}^K) - f(\theta^*)] \leq \frac{R_0^2}{\gamma K} + \gamma \left(\frac{\sigma^2}{N_{\min}} + \delta_{pv,2}^2 + 3L\gamma (4\delta_{aq}^2 + (\tau-1)\sigma^2) \right), \quad (45)$$

when $\mu = 0$, where $R_0 = \|\theta^0 - \theta^*\|$, $\bar{\theta}^K = \frac{1}{W_K} \sum_{k=0}^K w_k \theta^k = \frac{1}{W_K} \sum_{k=0}^K \frac{w_k}{N_k} \sum_{i \in P_k} \theta_i^k$, $w_k = (1 - \gamma\mu(1 - \delta_{pv,1}))^{-(k+1)}$, and $W_K = \sum_{k=0}^K w_k$. That is, Moshpit SGD achieves $\mathbb{E}[f(\bar{\theta}^K) - f(\theta^*)] \leq \varepsilon$ after

$$K = \tilde{\mathcal{O}} \left(\frac{L}{(1 - \delta_{pv,1})\mu} + \frac{\sigma^2}{N_{\min}(1 - \delta_{pv,1})\mu\varepsilon} + \frac{\delta_{pv,2}^2}{(1 - \delta_{pv,1})\mu\varepsilon} + \sqrt{\frac{L((\tau-1)\sigma^2 + \delta_{aq}^2)}{(1 - \delta_{pv,1})^2\mu^2\varepsilon}} \right) \quad (46)$$

iterations with

$$\gamma = \min \left\{ \frac{1}{4L}, \frac{\ln \left(\max \left\{ 2, \min \left\{ \frac{R_0^2\mu^2(1 - \delta_{pv,1})^2 K^2}{(\delta_{pv,2}^2 + \sigma^2/N_{\min})}, \frac{R_0^2\mu^3(1 - \delta_{pv,1})^3 K^3}{3L(4\delta_{aq}^2 + (\tau-1)\sigma^2)} \right\} \right) \right)}{(1 - \delta_{pv,1})\mu K} \right\}$$

when $\mu > 0$, and after

$$K = \mathcal{O} \left(\frac{LR_0^2}{\varepsilon} + \frac{R_0^2\sigma^2}{N_{\min}\varepsilon^2} + \frac{R_0^2\delta_{pv,2}^2}{\varepsilon^2} + \frac{R_0^2\sqrt{L((\tau-1)\sigma^2 + \delta_{aq}^2)}}{\varepsilon^{3/2}} \right) \quad (47)$$

iterations with

$$\gamma = \min \left\{ \frac{1}{4L} \sqrt{\frac{R_0}{(\delta_{pv,2}^2 + \sigma^2/N_{\min})K}}, \sqrt[3]{\frac{R_0^2}{3L(4\delta_{aq}^2 + (\tau-1)\sigma^2)K}} \right\}$$

when $\mu = 0$.

Proof. Plugging the result of Lemma D.6 in inequality (37) from Lemma D.5, we obtain

$$\begin{aligned} \gamma \mathbb{E} [f(\theta^k) - f(\theta^*)] &\leq (1 - \gamma\mu(1 - \delta_{pv,1})) \mathbb{E} [\|\theta^k - \theta^*\|^2] - \mathbb{E} [\|\theta^{k+1} - \theta^*\|^2] \\ &\quad + 3L\gamma^3 (4\delta_{aq}^2 + (\tau-1)\sigma^2) + \gamma^2 \left(\frac{\sigma^2}{N_{\min}} + \delta_{pv,2}^2 \right). \end{aligned}$$

Next, we sum up these inequalities for $k = 0, \dots, K$ with weights $w_k = (1 - \gamma\mu(1 - \delta_{pv,1}))^{-(k+1)}$ and divide both sides by γW_K , where $W_K = \sum_{k=0}^K w_k$:

$$\begin{aligned} \frac{1}{W_K} \sum_{k=0}^K w_k \mathbb{E} [f(\theta^k) - f(\theta^*)] &\leq \frac{1}{\gamma W_K} \sum_{k=0}^K ((1 - \gamma\mu(1 - \delta_{pv,1})) w_k \mathbb{E} [\|\theta^k - \theta^*\|^2] - w_k \mathbb{E} [\|\theta^{k+1} - \theta^*\|^2]) \\ &\quad + \gamma \left(\frac{\sigma^2}{N_{\min}} + \delta_{pv,2}^2 + 3L\gamma (4\delta_{aq}^2 + (\tau-1)\sigma^2) \right) \frac{1}{W_K} \sum_{k=0}^K w_k \\ &= \frac{1}{\gamma W_K} \sum_{k=0}^K (w_{k-1} \mathbb{E} [\|\theta^k - \theta^*\|^2] - w_k \mathbb{E} [\|\theta^{k+1} - \theta^*\|^2]) \\ &\quad + \gamma \left(\frac{\sigma^2}{N_{\min}} + \delta_{pv,2}^2 + 3L\gamma (4\delta_{aq}^2 + (\tau-1)\sigma^2) \right) \\ &= \frac{w_{-1} \|\theta^0 - \theta^*\|^2 - w_K \mathbb{E} [\|\theta^{K+1} - \theta^*\|^2]}{\gamma W_K} \\ &\quad + \gamma \left(\frac{\sigma^2}{N_{\min}} + \delta_{pv,2}^2 + 3L\gamma (4\delta_{aq}^2 + (\tau-1)\sigma^2) \right) \\ &\leq \frac{\|\theta^0 - \theta^*\|^2}{\gamma W_K} + \gamma \left(\frac{\sigma^2}{N_{\min}} + \delta_{pv,2}^2 + 3L\gamma (4\delta_{aq}^2 + (\tau-1)\sigma^2) \right). \end{aligned}$$

Since f is convex, we apply the Jensen's inequality

$$f \left(\frac{1}{W_K} \sum_{k=0}^K w_k \theta^k \right) \leq \frac{1}{W_K} \sum_{k=0}^K w_k f(\theta^k)$$

to the previous result and get

$$\mathbb{E} [f(\bar{\theta}^K) - f(\theta^*)] \leq \frac{R_0^2}{\gamma W_K} + \gamma \left(\frac{\sigma^2}{N_{\min}} + \delta_{pv,2}^2 + 3L\gamma (4\delta_{aq}^2 + (\tau-1)\sigma^2) \right),$$

where $R_0 = \|\theta^0 - \theta^*\|$ and $\bar{\theta}^K = \frac{1}{W_K} \sum_{k=0}^K w_k \theta^k = \frac{1}{W_K} \sum_{k=0}^K \frac{w_k}{N_k} \sum_{i \in P_k} \theta_i^k$. If $\mu > 0$, then $W_K \geq w_K \geq (1 - \gamma\mu(1 - \delta_{pv,1}))^{-K}$, implying (44). Next, $w_k = 1$ and $W_K = K$ when $\mu = 0$ gives (45). It remains to estimate the total number of iterations K required by Moshpit SGD to find an ε -solution, i.e., to achieve $\mathbb{E}[f(\bar{\theta}^K) - f(\theta^*)] \leq \varepsilon$. Applying Lemma D.2

to (44), we get the following result: if $\mu > 0$ and

$$\gamma = \min \left\{ \frac{1}{4L}, \frac{\ln \left(\max \left\{ 2, \min \left\{ \frac{R_0^2 \mu^2 (1 - \delta_{pv,1})^2 K^2}{\delta_{pv,2}^2 + \sigma^2 / N_{\min}}, \frac{R_0^2 \mu^3 (1 - \delta_{pv,1})^3 K^3}{3L(4\delta_{aq}^2 + (\tau - 1)\sigma^2)} \right\} \right) \right)}{(1 - \delta_{pv,1})\mu K} \right\},$$

then

$$\mathbb{E} \left[f(\bar{\theta}^K) - f(\theta^*) \right] = \tilde{\mathcal{O}} \left(LR_0^2 \exp \left(-\frac{\mu}{L} (1 - \delta_{pv,1}) K \right) + \frac{\delta_{pv,2}^2 + \sigma^2 / N_{\min}}{(1 - \delta_{pv,1})\mu K} + \frac{L(\delta_{aq}^2 + (\tau - 1)\sigma^2)}{(1 - \delta_{pv,1})^2 \mu^2 K^2} \right),$$

implying (46). Similarly, we apply Lemma D.3 to (45) and get that for $\mu = 0$ and

$$\gamma = \min \left\{ \frac{1}{4L} \sqrt{\frac{R_0}{(\delta_{pv,2}^2 + \sigma^2 / N_{\min})K}}, \sqrt[3]{\frac{R_0^2}{3L(4\delta_{aq}^2 + (\tau - 1)\sigma^2)K}} \right\},$$

$$\mathbb{E} \left[f(\bar{\theta}^K) - f(\theta^*) \right] = \mathcal{O} \left(\frac{LR_0^2}{K} + \sqrt{\frac{R_0^2(\delta_{pv,2}^2 + \sigma^2 / N_{\min})}{K}} + \frac{\sqrt[3]{R_0^4 L(\delta_{aq}^2 + (\tau - 1)\sigma^2)}}{K^{2/3}} \right),$$

implying (47). □

D.3. Non-Convex Case

In this section, we give the full proof of Theorem 3.4 about convergence of Moshpit SGD for general non-convex problems. The proof follows the similar steps as in the state-of-the-art analysis of Local-SGD in non-convex case (Li et al., 2019b; Koloskova et al., 2020b). We start with the following lemma:

Lemma D.7. *Let $f_1 = \dots = f_N = f$, function f be L -smooth and bounded from below by f_* , and Assumptions 3.1 and 3.2 hold with $\Delta_{pv}^k = \delta_{pv,1}\gamma\mathbb{E}[\|\nabla f(\theta^k)\|^2] + L\gamma^2\delta_{pv,2}^2$, $\delta_{pv,1} \in [0, 1/2)$, $\delta_{pv,2} \geq 0$. Then, for any $K \geq 0$ the iterates produced by Moshpit SGD with $\gamma \leq (1 - 2\delta_{pv,1})/8L$ satisfy*

$$\frac{(1 - 2\delta_{pv,1})\gamma}{4} \sum_{k=0}^{K-1} \mathbb{E} [\|\nabla f(\theta^k)\|^2] \leq f(\theta^0) - f_* + \gamma L^2 \sum_{k=0}^{K-1} \mathbb{E}[V_k] + KL\gamma^2 \left(\frac{\sigma^2}{N_{\min}} + \delta_{pv,2}^2 \right), \quad (48)$$

where $V_k = \frac{1}{N_k} \sum_{i \in P_k} \|\theta_i^k - \theta^k\|^2$ and $\theta^k = \frac{1}{N_k} \sum_{i \in P_k} \theta_i^k$.

Proof. Recall that Assumption 3.2 with $\Delta_{pv}^k = \delta_{pv,1}\gamma\mathbb{E}[\|\nabla f(\theta^k)\|^2] + L\gamma^2\delta_{pv,2}^2$ states

$$\mathbb{E} \left[\langle \nabla f(\theta^k), \theta^{k+1} - \hat{\theta}^{k+1} \rangle + L\|\hat{\theta}^{k+1} - \theta^{k+1}\|^2 \right] \leq \delta_{pv,1}\gamma\mathbb{E}[\|\nabla f(\theta^k)\|^2] + L\gamma^2\delta_{pv,2}^2, \quad (49)$$

where $\hat{\theta}^{k+1} = \frac{1}{N_k} \sum_{i \in P_k} (\theta_i^k - \gamma g_i^k)$. As for the convex case, we notice that the definition of $\hat{\theta}^{k+1}$ implies

$$\hat{\theta}^{k+1} = \frac{1}{N_k} \sum_{i \in P_k} \theta_i^k - \frac{\gamma}{N_k} \sum_{i \in P_k} g_i^k = \theta^k - \gamma g^k,$$

where $g^k = \frac{1}{N_k} \sum_{i \in P_k} g_i^k$. Using this and L -smoothness of f , we derive

$$\begin{aligned} f(\theta^{k+1}) - f(\theta^k) &\stackrel{(27)}{\leq} \langle \nabla f(\theta^k), \theta^{k+1} - \theta^k \rangle + \frac{L}{2} \|\theta^{k+1} - \theta^k\|^2 \\ &\stackrel{(30)}{\leq} \langle \nabla f(\theta^k), \hat{\theta}^{k+1} - \theta^k \rangle + \langle \nabla f(\theta^k), \theta^{k+1} - \hat{\theta}^{k+1} \rangle + L\|\hat{\theta}^{k+1} - \theta^k\|^2 + L\|\theta^{k+1} - \hat{\theta}^{k+1}\|^2 \\ &= -\gamma \langle \nabla f(\theta^k), g^k \rangle + L\gamma^2 \|g^k\|^2 + \langle \nabla f(\theta^k), \theta^{k+1} - \hat{\theta}^{k+1} \rangle + L\|\theta^{k+1} - \hat{\theta}^{k+1}\|^2, \end{aligned}$$

from which it follows that

$$\begin{aligned} \mathbb{E} [f(\theta^{k+1}) - f(\theta^k) \mid \theta^k] &\leq -\gamma \left\langle \nabla f(\theta^k), \frac{1}{N_k} \sum_{i \in P_k} \nabla f(\theta_i^k) \right\rangle + L\gamma^2 \mathbb{E} \left[\left\| \frac{1}{N_k} \sum_{i \in P_k} g_i^k \right\|^2 \mid \theta^k \right] \\ &\quad + \mathbb{E} \left[\langle \nabla f(\theta^k), \theta^{k+1} - \widehat{\theta}^{k+1} \rangle + L \|\theta^{k+1} - \widehat{\theta}^{k+1}\|^2 \mid \theta^k \right], \end{aligned} \quad (50)$$

where $\mathbb{E} [\cdot \mid \theta^k] := \mathbb{E} [\cdot \mid P_k, \theta_i^k, i \in P_k]$. Next, we estimate the second and third terms in the right-hand side of (50). First of all,

$$\begin{aligned} -\gamma \left\langle \nabla f(\theta^k), \frac{1}{N_k} \sum_{i \in P_k} \nabla f(\theta_i^k) \right\rangle &= -\gamma \|\nabla f(\theta^k)\|^2 - \gamma \left\langle \nabla f(\theta^k), \frac{1}{N_k} \sum_{i \in P_k} \nabla f(\theta_i^k) - \nabla f(\theta^k) \right\rangle \\ &\stackrel{(32)}{\leq} -\gamma \|\nabla f(\theta^k)\|^2 + \frac{\gamma}{2} \|\nabla f(\theta^k)\|^2 + \frac{\gamma}{2} \left\| \frac{1}{N_k} \sum_{i \in P_k} (\nabla f(\theta_i^k) - \nabla f(\theta^k)) \right\|^2 \\ &\stackrel{(31)}{\leq} -\frac{\gamma}{2} \|\nabla f(\theta^k)\|^2 + \frac{\gamma}{2N_k} \sum_{i \in P_k} \|\nabla f(\theta_i^k) - \nabla f(\theta^k)\|^2 \\ &\stackrel{(26)}{\leq} -\frac{\gamma}{2} \|\nabla f(\theta^k)\|^2 + \frac{\gamma L^2}{2} V_k, \end{aligned} \quad (51)$$

where $V_k = \frac{1}{N_k} \sum_{i \in P_k} \|\theta_i^k - \theta^k\|^2$. Secondly, since the stochastic gradients $\{g_i^k\}_{i \in P_k}$ are computed independently, we derive

$$\begin{aligned} L\gamma^2 \mathbb{E} \left[\left\| \frac{1}{N_k} \sum_{i \in P_k} g_i^k \right\|^2 \mid \theta^k \right] &\stackrel{(33)}{=} L\gamma^2 \left\| \frac{1}{N_k} \sum_{i \in P_k} \nabla f(\theta_i^k) \right\|^2 + L\gamma^2 \mathbb{E} \left[\left\| \frac{1}{N_k} \sum_{i \in P_k} (g_i^k - \nabla f(\theta_i^k)) \right\|^2 \mid \theta^k \right] \\ &\stackrel{(31)}{\leq} 2L\gamma^2 \left\| \frac{1}{N_k} \sum_{i \in P_k} (\nabla f(\theta_i^k) - \nabla f(\theta^k)) \right\|^2 + 2L\gamma^2 \|\nabla f(\theta^k)\|^2 \\ &\quad + \frac{\gamma^2 L}{N_k^2} \sum_{i \in P_k} \mathbb{E} [\|g_i^k - \nabla f(\theta_i^k)\|^2 \mid \theta^k] \\ &\stackrel{(31),(7)}{\leq} \frac{2\gamma^2 L}{N_k} \sum_{i \in P_k} \|\nabla f(\theta_i^k) - \nabla f(\theta^k)\|^2 + 2L\gamma^2 \|\nabla f(\theta^k)\|^2 + \frac{\gamma^2 L \sigma^2}{N_k} \\ &\stackrel{(26)}{\leq} \underbrace{\frac{2L^3 \gamma^2}{N_k} \sum_{i \in P_k} \|\theta_i^k - \theta^k\|^2}_{2L^3 \gamma^2 V_k} + 2L\gamma^2 \|\nabla f(\theta^k)\|^2 + \frac{\gamma^2 L \sigma^2}{N_{\min}}. \end{aligned} \quad (52)$$

Plugging (51) and (52) in (50), we obtain

$$\begin{aligned} \mathbb{E} [f(\theta^{k+1}) - f(\theta^k) \mid \theta^k] &\leq -\frac{\gamma}{2} (1 - 4L\gamma) \|\nabla f(\theta^k)\|^2 + \frac{\gamma L^2}{2} (1 + 4L\gamma) V_k + \frac{L\gamma^2 \sigma^2}{N_{\min}} \\ &\quad + \mathbb{E} \left[\langle \nabla f(\theta^k), \theta^{k+1} - \widehat{\theta}^{k+1} \rangle + L \|\theta^{k+1} - \widehat{\theta}^{k+1}\|^2 \mid \theta^k \right]. \end{aligned}$$

Next, we take the full expectation from the both sides of the above inequality, apply the tower property (34) and take into

account that $\gamma \leq (1-2\delta_{pv,1})/8L$:

$$\begin{aligned}
 \mathbb{E} [f(\theta^{k+1}) - f(\theta^k)] &\leq -\frac{\gamma}{2} (1 - 4L\gamma) \mathbb{E} [\|\nabla f(\theta^k)\|^2] + \frac{\gamma L^2}{2} (1 + 4L\gamma) \mathbb{E}[V_k] + \frac{L\gamma^2 \sigma^2}{N_{\min}} \\
 &\quad + \mathbb{E} \left[\langle \nabla f(\theta^k), \theta^{k+1} - \hat{\theta}^{k+1} \rangle + L \|\theta^{k+1} - \hat{\theta}^{k+1}\|^2 \right] \\
 &\stackrel{(49)}{\leq} -\frac{\gamma}{2} (1 - 2\delta_{pv,1} - 4L\gamma) \mathbb{E} [\|\nabla f(\theta^k)\|^2] + \frac{\gamma L^2}{2} (1 + 4L\gamma) \mathbb{E}[V_k] + L\gamma^2 \left(\frac{\sigma^2}{N_{\min}} + \delta_{pv,2}^2 \right) \\
 &\leq -\frac{(1 - 2\delta_{pv,1})\gamma}{4} \mathbb{E} [\|\nabla f(\theta^k)\|^2] + \gamma L^2 \mathbb{E}[V_k] + L\gamma^2 \left(\frac{\sigma^2}{N_{\min}} + \delta_{pv,2}^2 \right).
 \end{aligned}$$

Summing up the obtained inequalities for $k = 0, \dots, K-1$ and rearranging the terms, we derive

$$\begin{aligned}
 \frac{(1 - 2\delta_{pv,1})\gamma}{4} \sum_{k=0}^{K-1} \mathbb{E} [\|\nabla f(\theta^k)\|^2] &\leq \sum_{k=0}^{K-1} \mathbb{E} [f(\theta^k) - f(\theta^{k+1})] + \gamma L^2 \sum_{k=0}^{K-1} \mathbb{E}[V_k] + KL\gamma^2 \left(\frac{\sigma^2}{N_{\min}} + \delta_{pv,2}^2 \right) \\
 &= f(\theta^0) - \mathbb{E}[f(\theta^K)] + \gamma L^2 \sum_{k=0}^{K-1} \mathbb{E}[V_k] + KL\gamma^2 \left(\frac{\sigma^2}{N_{\min}} + \delta_{pv,2}^2 \right) \\
 &\leq f(\theta^0) - f_* + \gamma L^2 \sum_{k=0}^{K-1} \mathbb{E}[V_k] + KL\gamma^2 \left(\frac{\sigma^2}{N_{\min}} + \delta_{pv,2}^2 \right),
 \end{aligned}$$

where f_* is a uniform lower bound for f . □

The next step towards completing the proof of Theorem 3.4 gives the upper bound for $\sum_{k=0}^{K-1} \mathbb{E}[V_k]$ that appeared in (48).

Lemma D.8. *Let $f_1 = \dots = f_N = f$ be L -smooth and bounded from below by f_* , and Assumptions 3.1 and 3.2 hold with $\Delta_{pv}^k = \delta_{pv,1}\gamma\mathbb{E}[\|\nabla f(\theta^k)\|^2] + L\gamma^2\delta_{pv,2}^2$, $\delta_{pv,1} \in [0, 1/2]$, $\delta_{pv,2} \geq 0$. Then, for any $K \geq 0$ the iterates produced by Moshpit SGD with $\gamma \leq 1/(4\sqrt{e}L(\tau-1))$ satisfy*

$$\sum_{k=0}^{K-1} \mathbb{E}[V_k] \leq 8e\gamma^2(\tau-1)^2 \sum_{k=0}^{K-1} \mathbb{E}[\|\nabla f(\theta^k)\|^2] + 4\gamma^2 K (2\delta_{aq}^2 + e(\tau-1)\sigma^2), \quad (53)$$

where $V_k = \frac{1}{N_k} \sum_{i \in P_k} \|\theta_i^k - \theta^k\|^2$ and $\theta^k = \frac{1}{N_k} \sum_{i \in P_k} \theta_i^k$.

Proof. First of all, consider k such that $k = a\tau + t'$ for some $t' \in [0, \tau)$. Let $\mathbb{E}_g[\cdot]$ denote the expectation conditioned on $\{P_t\}_{t=a\tau}^{(a+1)\tau-1}$. Then

$$\begin{aligned}
 \mathbb{E}_g[V_k] &= \frac{1}{N_k} \sum_{i \in P_k} \mathbb{E}_g [\|\theta_i^k - \theta^k\|^2] \stackrel{(33)}{\leq} \frac{1}{N_k} \sum_{i \in P_k} \mathbb{E}_g [\|\theta_i^k - \theta^{a\tau}\|^2] \\
 &= \frac{1}{N_k} \sum_{i \in P_k} \mathbb{E}_g \left[\left\| \theta_i^{a\tau} - \theta^{a\tau} - \gamma \sum_{t=a\tau}^{k-1} g_i^t \right\|^2 \right] \\
 &\stackrel{(30)}{\leq} \frac{2}{N_k} \sum_{i \in P_k} \mathbb{E}_g [\|\theta_i^{a\tau} - \theta^{a\tau}\|^2] + \frac{2\gamma^2}{N_k} \sum_{i \in P_k} \mathbb{E}_g \left[\left\| \sum_{t=a\tau}^{k-1} g_i^t \right\|^2 \right]. \quad (54)
 \end{aligned}$$

Next, we estimate the second term in the right-hand side of (54) using Lemma D.4:

$$\begin{aligned}
 \frac{2\gamma^2}{N_k} \sum_{i \in P_k} \mathbb{E}_g \left[\left\| \sum_{t=a\tau}^{k-1} g_i^t \right\|^2 \right] &\stackrel{(36)}{\leq} \frac{2e\gamma^2(k-a\tau)}{N_k} \sum_{i \in P_k} \sum_{t=a\tau}^{k-1} \mathbb{E}_g [\|\nabla f(\theta_i^t)\|^2] \\
 &\quad + \frac{2e\gamma^2}{N_k} \sum_{i \in P_k} \sum_{t=a\tau}^{k-1} \mathbb{E}_g [\|g_i^t - \nabla f(\theta_i^t)\|^2] \\
 &\stackrel{(30),(7)}{\leq} 4e\gamma^2(\tau-1) \sum_{t=a\tau}^{k-1} \mathbb{E}_g [\|\nabla f(\theta^t)\|^2] \\
 &\quad + 4e\gamma^2(\tau-1) \sum_{t=a\tau}^{k-1} \frac{1}{N_k} \sum_{i \in P_k} \mathbb{E}_g [\|\nabla f(\theta_i^t) - \nabla f(\theta^t)\|^2] + 2e\gamma^2(k-a\tau)\sigma^2 \\
 &\stackrel{(26)}{\leq} 4e\gamma^2(\tau-1) \sum_{t=a\tau}^{k-1} \mathbb{E}_g [\|\nabla f(\theta^t)\|^2] \\
 &\quad + 4e\gamma^2 L^2(\tau-1) \sum_{t=a\tau}^{k-1} \frac{N_t}{N_k} \cdot \frac{1}{N_t} \sum_{i \in P_t} \mathbb{E}_g [\|\theta_i^t - \theta^t\|^2] + 2e\gamma^2(\tau-1)\sigma^2 \\
 &\leq 4e\gamma^2(\tau-1) \sum_{t=a\tau}^{k-1} \mathbb{E}_g [\|\nabla f(\theta^t)\|^2] + 8e\gamma^2 L^2(\tau-1) \sum_{t=a\tau}^{k-1} \mathbb{E}_g [V_t] \\
 &\quad + 2e\gamma^2(\tau-1)\sigma^2,
 \end{aligned}$$

where in the last two inequalities we use $N_k = |P_k| \leq |P_{k-1}| = N_{k-1}$ for all $k \geq 1$ and $N_{a\tau} \leq 2N_{(a+1)\tau}$ for all integer $a \geq 0$. Plugging this inequality in (54) and taking the full expectation from the result, we get

$$\begin{aligned}
 \mathbb{E}[V_k] &\leq 2\mathbb{E} \left[\frac{1}{N_k} \sum_{i \in P_k} \|\theta_i^{a\tau} - \theta^{a\tau}\|^2 \right] + 4e\gamma^2(\tau-1) \sum_{t=a\tau}^{k-1} \mathbb{E} [\|\nabla f(\theta^t)\|^2] + 8e\gamma^2 L^2(\tau-1) \sum_{t=a\tau}^{k-1} \mathbb{E}[V_t] \\
 &\quad + 2e\gamma^2(\tau-1)\sigma^2 \\
 &\leq 4\mathbb{E} \left[\frac{1}{N_{a\tau}} \sum_{i \in P_{a\tau}} \|\theta_i^{a\tau} - \theta^{a\tau}\|^2 \right] + 4e\gamma^2(\tau-1) \sum_{t=a\tau}^{k-1} \mathbb{E} [\|\nabla f(\theta^t)\|^2] + 8e\gamma^2 L^2(\tau-1) \sum_{t=a\tau}^{k-1} \mathbb{E}[V_t] \\
 &\quad + 2e\gamma^2(\tau-1)\sigma^2 \\
 &\stackrel{(10)}{\leq} 4e\gamma^2(\tau-1) \sum_{t=a\tau}^{k-1} \mathbb{E} [\|\nabla f(\theta^t)\|^2] + 8e\gamma^2 L^2(\tau-1) \sum_{t=a\tau}^{k-1} \mathbb{E}[V_t] + 2\gamma^2 (2\delta_{aq}^2 + e(\tau-1)\sigma^2),
 \end{aligned}$$

where in the second inequality we also use $N_k = |P_k| \leq |P_{k-1}| = N_{k-1}$ for all $k \geq 1$ and $N_{a\tau} \leq 2N_{(a+1)\tau}$ for all integer $a \geq 0$. Summing up the obtained inequalities for $k = a\tau, a\tau + 1, \dots, K'$ for some $K' \in [a\tau, (a+1)\tau - 1]$ we derive

$$\begin{aligned}
 \sum_{k=a\tau}^{K'} \mathbb{E}[V_k] &\leq 4e\gamma^2(\tau-1) \sum_{k=a\tau}^{K'} \sum_{t=a\tau}^{k-1} \mathbb{E} [\|\nabla f(\theta^t)\|^2] + 8e\gamma^2 L^2(\tau-1) \sum_{k=a\tau}^{K'} \sum_{t=a\tau}^{k-1} \mathbb{E}[V_t] \\
 &\quad + 2\gamma^2(K' - a\tau + 1) (2\delta_{aq}^2 + e(\tau-1)\sigma^2) \\
 &\leq 4e\gamma^2(\tau-1)^2 \sum_{k=a\tau}^{K'} \mathbb{E} [\|\nabla f(\theta^k)\|^2] + 8e\gamma^2 L^2(\tau-1)^2 \sum_{k=a\tau}^{K'} \mathbb{E}[V_k] \\
 &\quad + 2\gamma^2(K' - a\tau + 1) (2\delta_{aq}^2 + e(\tau-1)\sigma^2) \\
 &\leq 4e\gamma^2(\tau-1)^2 \sum_{k=a\tau}^{K'} \mathbb{E} [\|\nabla f(\theta^k)\|^2] + \frac{1}{2} \sum_{k=a\tau}^{K'} \mathbb{E}[V_k] + 2\gamma^2(K' - a\tau + 1) (2\delta_{aq}^2 + e(\tau-1)\sigma^2),
 \end{aligned}$$

where in the last inequality we use $\gamma \leq 1/(4\sqrt{e}L(\tau-1))$. Rearranging the terms, we get that for $K' \geq 0$

$$\sum_{k=a\tau}^{K'} \mathbb{E}[V_k] \leq 8e\gamma^2(\tau-1)^2 \sum_{k=a\tau}^{K'} \mathbb{E}[\|\nabla f(\theta^k)\|^2] + 4\gamma^2(K' - a\tau + 1) (2\delta_{aq}^2 + e(\tau-1)\sigma^2),$$

where $a \geq 0$ is an integer such that $a\tau \leq K' \leq (a+1)\tau - 1$. Summing up the obtained inequalities for $K' = \tau - 1, 2\tau - 1, \dots, \tau \lfloor (K-1)/\tau \rfloor - 1, K - 1$, we derive (53). \square

Combining Lemmas D.7 and D.8, we get the following result:

Theorem D.2 (Theorem 3.4). *Let $f_1 = \dots = f_N = f$, function f be L -smooth and bounded from below by f_* , and Assumptions 3.1 and 3.2 hold with $\Delta_{pv}^k = \delta_{pv,1}\gamma\mathbb{E}[\|\nabla f(\theta^k)\|^2] + L\gamma^2\delta_{pv,2}^2$, $\delta_{pv,1} \in [0, 1/2)$, $\delta_{pv,2} \geq 0$. Then, for any $K \geq 0$ the iterates produced by Moshpit SGD with*

$$\gamma \leq \min \left\{ \frac{1 - 2\delta_{pv,1}}{8L}, \frac{\sqrt{1 - 2\delta_{pv,1}}}{8\sqrt{e}L(\tau-1)} \right\}$$

satisfy

$$\mathbb{E} [\|\nabla f(\theta_{rand}^K)\|^2] \leq \frac{8\Delta_0}{(1 - 2\delta_{pv,1})K\gamma} + \frac{8L\gamma}{1 - 2\delta_{pv,1}} \left(\frac{\sigma^2}{N_{\min}} + \delta_{pv,2}^2 + 4\gamma L (2\delta_{aq}^2 + e(\tau-1)\sigma^2) \right), \quad (55)$$

where $\Delta_0 = f(\theta^0) - f_*$ and θ_{rand}^K is chosen uniformly at random from $\{\theta^0, \theta^1, \dots, \theta^{K-1}\}$. That is, Moshpit SGD achieves $\mathbb{E} [\|\nabla f(\theta_{rand}^K)\|^2] \leq \varepsilon^2$ after

$$K = \mathcal{O} \left(\frac{L\Delta_0}{(1 - 2\delta_{pv,1})^2\varepsilon^2} \left[1 + (\tau-1)\sqrt{1 - 2\delta_{pv,1}} + \frac{\delta_{pv,2}^2 + \sigma^2/N_{\min}}{\varepsilon^2} + \frac{\sqrt{(1 - 2\delta_{pv,1})(\delta_{aq}^2 + (\tau-1)\sigma^2)}}{\varepsilon} \right] \right) \quad (56)$$

iterations with

$$\gamma = \min \left\{ \frac{1 - 2\delta_{pv,1}}{8L}, \frac{\sqrt{1 - 2\delta_{pv,1}}}{8\sqrt{e}L(\tau-1)}, \sqrt{\frac{\Delta_0}{LK(\delta_{pv,2}^2 + \sigma^2/N_{\min})}}, \sqrt[3]{\frac{\Delta_0}{4L^2(2\delta_{aq}^2 + e(\tau-1)\sigma^2)}} \right\}.$$

Proof of Theorem 3.4. Plugging the result of Lemma D.8 in the inequality (48) from Lemma D.7, we obtain

$$\begin{aligned} \frac{(1 - 2\delta_{pv,1})\gamma}{4} \sum_{k=0}^{K-1} \mathbb{E} [\|\nabla f(\theta^k)\|^2] &\leq f(\theta^0) - f_* + 8e\gamma^3 L^2 \tau (\tau-1) \sum_{k=0}^{K-1} \mathbb{E} [\|\nabla f(\theta^k)\|^2] \\ &\quad + KL\gamma^2 \left(\frac{\sigma^2}{N_{\min}} + \delta_{pv,2}^2 + 4\gamma L (2\delta_{aq}^2 + e(\tau-1)\sigma^2) \right) \\ &\leq f(\theta^0) - f_* + \frac{(1 - 2\delta_{pv,1})\gamma}{8} \sum_{k=0}^{K-1} \mathbb{E} [\|\nabla f(\theta^k)\|^2] \\ &\quad + KL\gamma^2 \left(\frac{\sigma^2}{N_{\min}} + \delta_{pv,2}^2 + 4\gamma L (2\delta_{aq}^2 + e(\tau-1)\sigma^2) \right). \end{aligned}$$

Next,

$$\frac{1}{K} \sum_{k=0}^K \mathbb{E} [\|\nabla f(\theta^k)\|^2] \leq \frac{8\Delta_0}{(1 - 2\delta_{pv,1})K\gamma} + \frac{8L\gamma}{1 - 2\delta_{pv,1}} \left(\frac{\sigma^2}{N_{\min}} + \delta_{pv,2}^2 + 4\gamma L (2\delta_{aq}^2 + e(\tau-1)\sigma^2) \right),$$

where $\Delta_0 = f(\theta^0) - f_*$. Since θ_{rand}^K is chosen uniformly at random from $\{\theta^0, \theta^1, \dots, \theta^{K-1}\}$, we have

$$\mathbb{E} [\|\nabla f(\theta_{rand}^K)\|^2] \stackrel{(34)}{=} \frac{1}{K} \sum_{k=0}^K \mathbb{E} [\|\nabla f(\theta^k)\|^2]$$

and (55) holds. Applying Lemma D.3 to (55), we get the following result: if

$$\gamma = \min \left\{ \frac{1 - 2\delta_{pv,1}}{8L}, \frac{\sqrt{1 - 2\delta_{pv,1}}}{8\sqrt{\epsilon}L(\tau - 1)}, \sqrt{\frac{\Delta_0}{LK(\delta_{pv,2}^2 + \sigma^2/N_{\min})}}, \sqrt[3]{\frac{\Delta_0}{4L^2(2\delta_{aq}^2 + \epsilon(\tau - 1)\sigma^2)}} \right\},$$

then

$$\mathbb{E} [\|\nabla f(\theta_{\text{rand}}^K)\|^2] = \mathcal{O} \left(\frac{L\Delta_0(1 + (\tau - 1)\sqrt{1 - 2\delta_{pv,1}})}{(1 - 2\delta_{pv,1})^2 K} + \sqrt{\frac{L\Delta_0(\delta_{pv,2}^2 + \sigma^2/N_{\min})}{(1 - 2\delta_{pv,1})^2 K}} + \frac{\sqrt[3]{L^2\Delta_0^2(\delta_{aq}^2 + (\tau - 1)\sigma^2)}}{(1 - 2\delta_{pv,1})K^{2/3}} \right),$$

which implies the desired convergence result from (56). \square

E. Load balancing via linear programming

When running Moshpit Averaging on heterogeneous devices, one must regularly perform Butterfly All-Reduce among peers with uneven network bandwidth. In order to speed up the protocol, we can make low-throughput peers receive, average, and send smaller partitions of the averaged vector; conversely, the high-throughput peers can process greater fractions of the input vector. To compute the optimal partitioning, peers must solve an optimization problem that minimizes the total time spent on communication during all-reduce.

Consider a group of M peers with network bandwidths b_1, \dots, b_M , defined for simplicity as the minimum of the upload and download speed for each peer. Our objective is to find w_i — a fraction of all input vectors to be processed by the i -th peer.

In Butterfly All-Reduce, each peer i splits its vector into parts and sends these parts to corresponding peers. Since there is no need to send w_i to itself, i -th peer will upload a total of $1 - w_i$ of the vector to its peers. On the receiving side, peer i will average w_i of the vector from all peers in its group. To do so, it must download $M - 1$ vector parts of size w_i from all other peers. After that, peers distribute the averaged parts by running the same procedure in reverse (see Figure 1).

Thus, the communication time for each peer is proportional to $t_i = (1 - w_i + (M - 1)w_i) \cdot \frac{1}{b_i}$ and the total runtime of Butterfly All-Reduce is the maximum communication time over all peers: $T = \max_i t_i = \max_i (1 - w_i + (M - 1)w_i) \cdot \frac{1}{b_i}$. Formally, we minimize T with respect to w_i with two constraints on the fraction weights:

$$\begin{aligned} \min_w \quad & \max_i (1 - w_i + (M - 1)w_i) \cdot \frac{1}{b_i} \\ \text{subject to} \quad & \sum_{i=1}^M w_i = 1 \\ & w_i \geq 0 \quad \forall i = 1, \dots, M \end{aligned}$$

Because the functions being maximized and the constraints are linear in w_i , this problem can be reduced to linear programming (Kaplan, 1974). Namely, we can minimize a surrogate variable ξ such that $\forall i, \xi \geq (1 - w_i + (M - 1)w_i) \cdot \frac{1}{b_i}$. The resulting linear program is formulated as follows:

$$\begin{aligned} \min_{w, \xi} \quad & \xi \\ \text{subject to} \quad & \sum_{i=1}^M w_i = 1 \\ & w_i \geq 0 \quad \forall i = 1, \dots, M \\ & \xi \geq (1 - w_i + (M - 1)w_i) \cdot \frac{1}{b_i} \quad \forall i = 1, \dots, M \end{aligned}$$

We solve this problem using the interior point method (Andersen & Andersen, 2000) implemented as part of the SciPy package (`scipy.optimize.linprog`). Note that depending on the conditions given by participant bandwidth, optimal

weights of specific peers might be equal to 0 in some cases. In essence, this allows our method to smoothly interpolate between data parallelism (Valiant, 1990), parameter server (Li, 2014) and sharded parameter server (Dean et al., 2012) in manner similar to BytePS (Jiang et al., 2020).

F. Detailed experimental setup

In this section, we provide the detailed hardware configuration of servers used for each of our distributed training experiments.

F.1. ImageNet training

Both homogeneous and heterogeneous training setups for ImageNet are provisioned in our on-premise infrastructure across multiple data centers and an office space (for the heterogeneous setup only).

Homogeneous. For the homogeneous setup, we use 16 identical instances with the following specifications:

- **GPU:** V100-PCIe,
- **CPU:** 6 vCPUs (Xeon E5-2650v4),
- **RAM:** 64GB.

Heterogeneous. In turn, the heterogeneous setup contains multiple instance types listed in Table 2:

Instances	GPUs	GPU type	Cores	RAM, GB	CPU type
4	1	V100-PCIe	6	64	E5-2650v4
17	2	GTX 1080Ti	8	64	E5-2650v4
7	1	GTX 1080Ti	4	32	E5-2650v4
16	1	P40	4	32	E5-2667v2
20	1	M40-24GB	4	32	E5-2667v2

Table 2. **Heterogeneous** setup for ImageNet training.

F.2. ALBERT training

Homogeneous. For the homogeneous setup, we use a single virtual machine with the following specifications:

- **GPU:** $8 \times$ V100-PCIe,
- **CPU:** 48 vCPUs (Xeon E5-2650v4),
- **RAM:** 488GB.

At the time of writing, the cloud rent cost for this instance is **\$24.48** per hour.

Heterogeneous. Our heterogeneous setup is composed of two parts: AWS EC2 Spot instances and crowdsourced machines from the `Vast.ai` marketplace. For spot instances, we picked the smallest suitable instance size available from the cloud provider and further limited their bandwidth to 1Gb/s⁸. As for marketplace instances, we report the hardware specifications for each worker gathered 1 hour after the start of ALBERT training.

Since both cloud and marketplace instances are preemptible, the actual cost of the server fleet will vary based on the current price. For simplicity, we report the maximum hourly price we ended up paying for this instance (enforced via maximum bid). Finally, some marketplace instances have missing specifications, such as unknown CPU type. This is likely caused by non-standard virtualization configured by the device owner. The resulting fleet configuration, shown in Table 3, costs up to \$15.43/hour, depending on the number of active instances.

⁸We use `tc qdisc` Linux utility to artificially limit the network throughput, similarly to Jayarajan et al. (2019)

Moshpit SGD

GPU	Cores	RAM, GB	CPU type	Download, Mb/s	Upload, Mb/s	Cost, \$/hour
Preemptible g4dn.xlarge instances (32×)						
T4	4	16	Xeon Platinum 8259CL	1000	1000	0.1578
Marketplace instances						
GTX 1070Ti	6	16	E5-2640	425	255	0.036
GTX 1070Ti	6	16	i3-6100T	121	36	0.06
GTX 1080Ti	4	20	i3-6096P	817	308	0.101
GTX 1080Ti	20	129	E5-2630v4	660	475	0.182
GTX 1080Ti	1	16	i7-7700K	245	210	0.302
GTX 1080Ti	48	97	Xeon Platinum 8124	583	539	0.217
GTX 1080Ti	10	16	Unknown	n/a	n/a	0.15
GTX 1080Ti	4	16	Xeon Gold 6149	98	100	0.2
GTX 1080Ti	4	16	Xeon Gold 6149	99	98	0.2
GTX 1080Ti	4	16	Xeon Gold 6149	99	99	0.2
GTX 1080Ti	4	16	Xeon Gold 6149	99	99	0.2
RTX 2070S	24	32	E5-2620v2	199	25	0.199
RTX 2070S	32	97	E5-2650	162	64	0.285
RTX 2080	6	16	E5-2620v3	271	287	0.25
RTX 2080	24	32	E5-2630v3	199	25	0.302
RTX 2080S	4	32	E5-2697v4	101	99	0.292
RTX 2080S	4	32	E5-2697v4	93	99	0.292
RTX 2080S	4	32	E5-2697v4	94	98	0.292
RTX 2080S	4	32	E5-2697v4	94	98	0.292
RTX 2080S	4	32	E5-2697v4	100	99	0.292
RTX 2080Ti	4	16	Ryzen Threadripper 3960x	279	271	0.35
RTX 2080Ti	8	129	E5-2670v3	616	672	0.201
RTX 2080Ti	6	32	E5-2620v3	217	61	0.22
RTX 2080Ti	8	16	E5-2697v2	100	58	0.3
RTX 2080Ti	8	21	E5-2697v2	145	49	0.243
RTX 2080Ti	12	32	Unknown	111	92	0.326
RTX 2080Ti	12	64	E5-2690v3	205	61	0.549
RTX 3080	16	16	i7-10700K	69	49	0.462
RTX 3090	14	32	E5-2695v3	93	37	0.498
RTX 3090	16	32	Ryzen 9 3950X	338	38	0.511
Titan RTX	4	32	Xeon W-3223	321	115	1
Titan RTX	4	32	Xeon Gold 6149	99	100	0.702
Titan V	8	32	i7-7700K	97	50	0.282
V100-FHHL	8	60	Xeon Gold 6148	544	584	0.39
Total hourly cost (as listed):						15.43

Table 3. Heterogeneous setup for ALBERT training.

G. Additional averaging experiments

In this section, we evaluate the averaging precision with the same methodology as in 4.1, but for different worker configurations. In Figure 5, plots 1–5 explore several combinations of grid sizes and failure rates, whereas plot 6 (bottom right) demonstrates a setup with the same number of peers (10^6) arranged into several different grid sizes and its relation to convergence. Note that $M=32$ outperforms the alternatives only for the specific failure rate of 0.001.

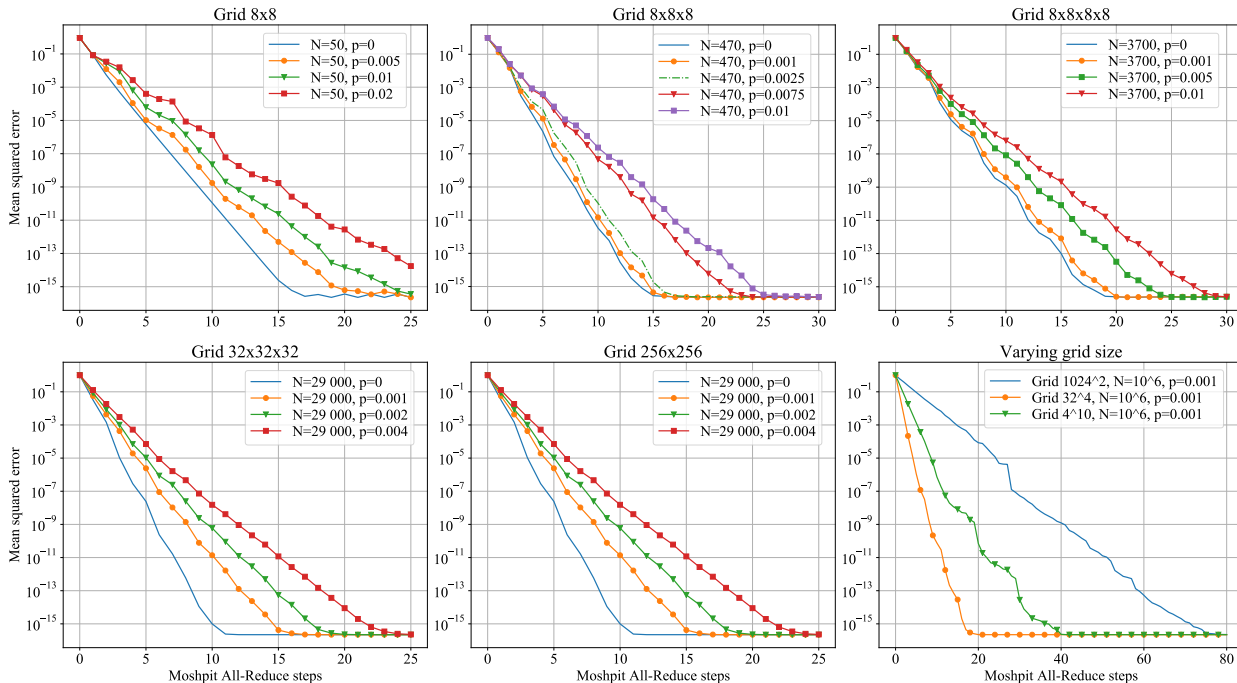


Figure 5. Averaging error of Moshpit All-Reduce as a function of the iteration number for different configurations and failure rates.

H. Additional image classification experiments

Aside from the two evaluation scenarios provided in 4.2, we also measure the performance of Moshpit-SGD in a non-distributed setup, i.e. on a single server with multiple GPUs. We conduct this experiment on the same $8 \times V100$ machine that was used in the **homogeneous** setup for training ALBERT (see Appendix F.2).

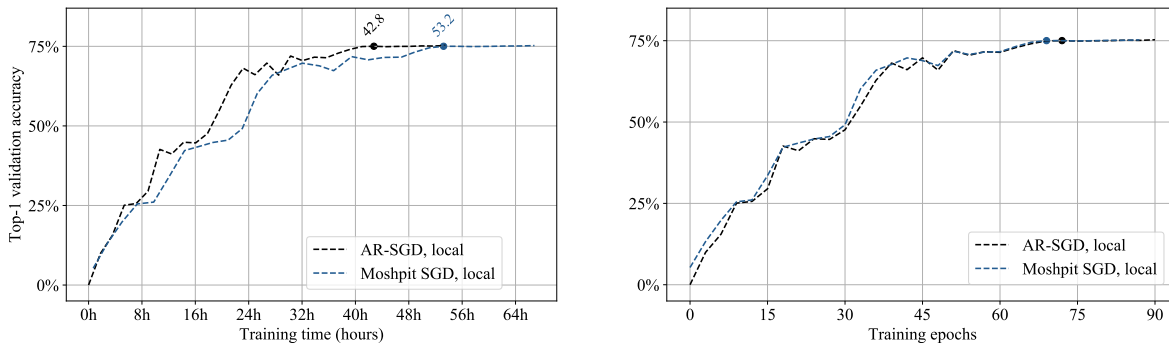


Figure 6. ResNet-50 top-1 validation accuracy on ImageNet when training on a single node with $8 \times V100$ -PCIe GPUs. **(Left)** Convergence in terms of training time, **(Right)** Convergence in terms of training epochs

As Figure 6 demonstrates, Moshpit SGD is slower than AR-SGD by approximately 25%. This result is expected, since our implementation of Moshpit All-Reduce is more general and communicates over a TCP connection, whereas AR-SGD uses direct peer-to-peer GPU communication over PCIe. On average, this incurs a slowdown of 27% in terms of training time.